CHEMISTRY AND CATALYSIS OF COAL LIQUEFACTION: CATALYTIC AND THERMAL UPGRADING OF COAL LIQUID AND HYDROGENATION OF CO TO PRODUCE FUELS. QUARTERLY PROGRESS REPORT, JULY-SEPTEMBER 1982

UTAH UNIV., SALT LAKE CITY. DEPT. OF FUELS ENGIEERING

SEP 1982

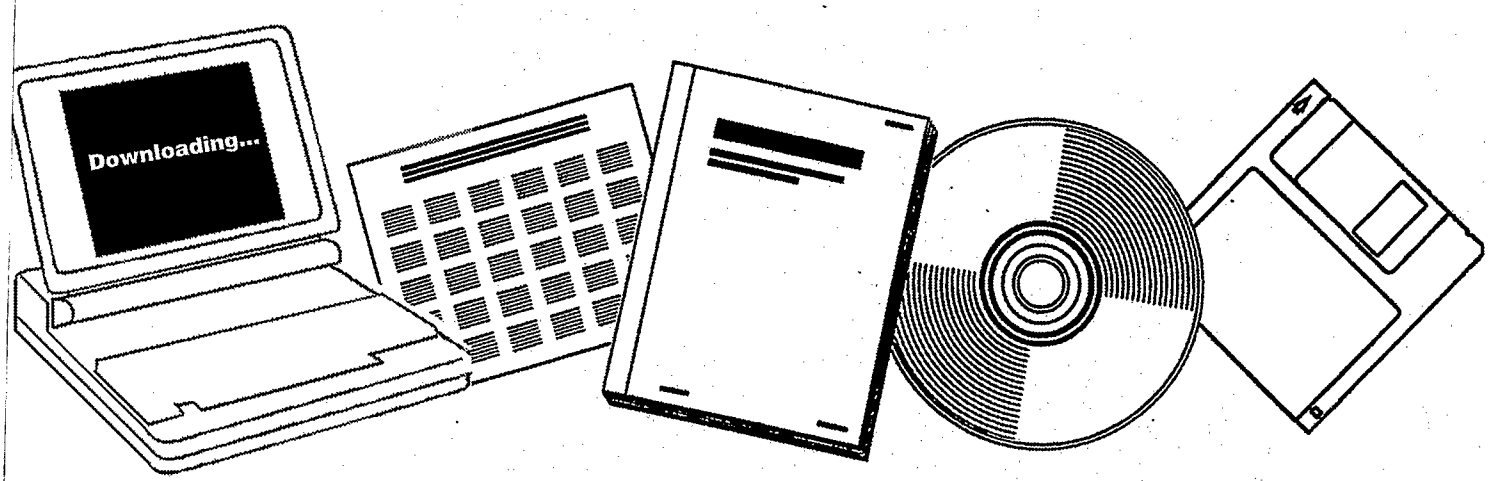

DOE/ET/14700-12
(DE83001403)
Distribution Category UC-90d

Chemistry and Catalysis of Coal Liquefaction Catalytic and Thermal Upgrading of Coal Liquid and Hydrogenation of CO to Produce Fuels

Quarterly Progress Report
for the Period July-Sept 1982

Dr. Wendell H. Wiser

University of Utah - Department of
Fuels Engineering
Salt Lake City, Utah 84112

Date Published - September 1982

Prepared for the United States Department
of Energy
Under Contract No. DE-AC01-79ET14700

CONTENTS

OBJECTIVE AND SCOPE OF WORK

I. The chemistry and Catalysis of Coal Liquefaction

Task 1 Chemical-Catalytic Studies

Coal will be reacted at subsoftening temperatures with selective reagents to break bridging linkages between clusters with minimal effect on residual organic clusters. The coal will be pretreated to increase surface area and then reacted at 25 to 350°C. Reagents and catalysts will be used which are selective so that the coal clusters are solubilized with as little further reaction as possible.

Task 2 Carbon-13 NMR Investigation of CDL and Coal

Carbon-13 NMR spectroscopy will be used to examine coal, coal derived liquids (CDL) and residues which have undergone subsoftening reactions in Task 1 and extraction. Improvements in NMR techniques, such as crosspolarization and magic angle spinning, will be applied. Model compounds will be included which are representative of structural units thought to be present in coal. Comparisons of spectra from native coals, CDL and residues will provide evidence for bondings which are broken by mild conditions.

Task 3 Catalysis and Mechanism of Coal Liquefaction

This fundamental study will gain an understanding of metal salt chemistry and catalysis in coal liquefaction through study of reactions known in organic chemistry. Zinc chloride and other catalytic materials will be tested as Friedel-Crafts catalysts and as redox catalysts using coals and selected model compounds. Zinc chloride, a weak Friedel-Crafts catalyst, will be used at conditions common to coal liquefaction to participate in well defined hydrogen transfer reactions. These experiments will be augmented by mechanistic studies of coal hydrogenation using high pressure thermogravimetric analysis and structural analysis. The results of these studies will be used to develop concepts of catalysis involved in coal liquefaction.

Task 4 Momentum Heat and Mass Transfer in CoCurrent Flow of Particle-Gas Systems for Coal Hydrogenation

A continuation of ongoing studies of heat and transport phenomena in cocurrent, co-gravity flow is planned for a one-year period. As time and development of existing work permits, the extension of this study to include a coiled reactor model will be undertaken. Mathematical models of coal hydrogenation systems will utilize correlations from these straight and coiled reactor configurations.

Task 5 The Fundamental Chemistry and Mechanism of Pyrolysis of Bituminous Coal

Previous work at the University of Utah indicates that coal pyrolysis, dissolution (in H-donor) and catalytic hydrogenation all have similar rates and activation energies. A few model compounds will be pyrolyzed in the range of 375 to 475°C. Activation energies, entropies and pro-

duct distributions will be determined. The reactions will assist in formulating the thermal reaction routes which also can occur during hydro-liquefaction.

II. Catalytic and Thermal Upgrading of Coal Liquids

Task 6 Catalytic Hydrogenation of CD Liquids and Related Polycyclic Aromatic Hydrocarbons

A variety of coal derived (CD) liquids will be hydrogenated with sulfided catalysts prepared in Task 10 from large pore, commercially available supports. The hydrogenation of these liquids will be systematically investigated as a function of catalyst structure and operating conditions. The effect of extent of hydrogenation will be the subject of study in subsequent tasks in which crackability and hydropyrolysis of the hydrogenated product will be determined. To provide an understanding of the chemistry involved, model polycyclic arenes will be utilized in hydrogenation studies. These studies and related model studies in Task 7 will be utilized to elucidate relationships between organic reactants and the structural-topographic characteristics of hydrogenation catalysts used in this work.

Task 7 Denitrogenation and Deoxygenation of CD Liquids and Related Nitrogen- and Oxygen-Containing Compounds

Removal of nitrogen and oxygen heteroatoms from CD liquids is an important upgrading step which must be accomplished to obtain fuels corresponding to those from petroleum sources. Using CD liquids as described in Task 6, exhaustive HDN and HDO will be sought through study of catalyst systems and operating conditions. As in Task 6, catalysts will be prepared in Task 10 and specificity for N- and O-removal will be optimized for the catalyst systems investigated. Model compounds will also be systematically hydrogenated using effective HDN/HDO catalysts. Kinetics and reaction pathways will be determined. A nonreductive denitrogenation system will be investigated using materials which undergo reversible nitridation. Conditions will be sought to cause minimal hydrogen consumption and little reaction of other reducible groups.

Task 8 Catalytic Cracking of Hydrogenated CD Liquids and Related Polycyclic Naphthenes and Naphthenoaromatics

Catalytic cracking of hydrogenated CD liquid feedstocks will be studied to evaluate this scheme as a means of upgrading CD liquids. Cracking kinetics and product distribution as a function of preceding hydrogenation will be evaluated to define upgrading combinations which require the minimal level of CD liquid aromatic saturation to achieve substantial heteroatom removal and high yields of cracked liquid products. Cracking catalysts to be considered for use in this task shall include conventional zeolite-containing catalysts and large-pore molecular sieve, CLS (cross-linked smectites) types under study at the University of Utah. Model compounds will be subjected to tests to develop a mechanistic understanding of the reactions of hydro CD liquids under catalytic cracking conditions.

Task 9 Hydropyrolysis (Thermal Hydrocracking) of CD Liquids

Heavy petroleum fractions can be thermally hydrocracked over a specific range of conditions to produce light liquid products without excessive hydrogenation occurring. This noncatalytic method will be applied to a variety of CD liquids and model compounds, as mentioned in Task 6, to determine the conditions necessary and the reactibility of these CD feedstocks with and without prior hydrogenation and to derive mechanism and reaction pathway information needed to gain an understanding of the hydropyrolysis reactions. Kinetics, coking tendencies and product compositions will be studied as a function of operating conditions.

Task 10 Systematic Structural-Activity Study of Supported Sulfide Catalysts for Coal Liquids Upgrading

This task will undertake catalyst preparation, characterization and measurement of activity and selectivity. The work proposed is a fundamental study of the relationship between the surface-structural properties of supported sulfide catalysts and their catalytic activities for various reactions desired. Catalysts will be prepared from commercially available. Supports composed of alumina, silica-alumina, silica-magnesia and silica-titania, modification of these supports to change acidity and to promote interaction with active catalytic components is planned. The active constituents will be selected from those which are effective in a sulfided state, including but not restricted to Mo, W, Ni and Co. The catalysts will be presulfided before testing. Catalyst characterization will consist of physico-chemical property measurements and surface property measurements. Activity and selectivity tests will also be conducted using model compounds singly and in combination.

Task 11 Basic Study of the Effects of Coke and Poisons on the Activity of Upgrading Catalysts

This task will begin in the second year of the contract after suitable catalysts have been identified from Tasks 6, 7 and/or 10. Two commercial catalysts or one commercial catalyst and one catalyst prepared in Task 10 will be selected for a two-part study, (1) simulated laboratory poisoning/coking and (2) testing of realistically aged catalysts. Kinetics of hydrogenation, hydrodesulfurization, hydrodenitrogenation and hydrocracking will be determined before and after one or more stages of simulated coking. Selected model compounds will be used to measure detailed kinetics of the above reactions and to determine quantitatively how kinetic parameters change with the extent and type of poisoning/coking simulated. Realistically aged catalysts will be obtained from coal liquids upgrading experiments from other tasks in this program or from other laboratories conducting long-term upgrading studies. Deactivation will be assessed based on specific kinetics determined and selective poisoning studies will be made to determine characteristics of active sites remaining.

Task 12 Diffusion of Polyaromatic Compounds in Amorphous Catalyst Supports

If diffusion of a reactant species to the active sites of the catalyst is slow in comparison to the intrinsic rate of the surface reaction, then only sites near the exterior of the catalyst particles will be utilized effectively. A systematic study of the effect of molecular size on the sorptive diffusion kinetics relative to pore geometry will

be made using specific, large diameter aromatic molecules. Diffusion studies with narrow boiling range fractions of representative coal liquid will also be included. Experimental parameters for diffusion kinetic runs shall include aromatic diffusion model compounds, solvent effects, catalyst sorption properties, temperature and pressure.

III. Hydrogenation of CO to Produce Fuels

Task 13 Catalyst Research and Development

Studies with iron catalysts will concentrate on promoters, the use of supports and the effects of carbiding and nitriding. Promising promoters fall into two classes: (1) nonreducible metal oxides, such as CaO, K_2O, Al_2O_3 and MgO, and (2) partially reducible metal oxides which can be classified as co-catalysts, such as oxides of Mn, Mo, Ce, La, V, Re and rare earths. Possible catalyst supports include zeolites, alumina, silica, magnesia and high area carbons. Methods of producing active supported iron catalysts for CO hydrogenation will be investigated, such as development of shape selective catalysts which can provide control of product distribution. In view of the importance of temperature, alternative reactor systems (to fixed bed) will be investigated to attain better temperature control. Conditions will be used which give predominately lower molecular weight liquids and gaseous products.

Task 14 Characterization of Catalysts and Mechanistic Studies

Catalysts which show large differences in selectivity in Task 13 will be characterized as to surface and bulk properties. Differences in properties may provide the key to understanding why one catalyst is superior to another and identify critical properties, essential in selective catalysts. Factors relating to the surface mechanism of CO hydrogenation will also be investigated. Experiments are proposed to determine which catalysts form "surface" (reactive) carbon and the ability of these catalysts to exchange C and O of isotopically labelled CO. Reactions of CO and H_2 at temperatures below that required for CO dissociation are of particular interest.

Task 15 Completion of Previously Funded Studies and Exploratory Investigations

This task is included to provide for the orderly completion of coal liquefaction research underway in the expiring University of Utah contract, EX-76-C-01-2006.

III Highlights to Date

A series of Co and Ni promoted 8% Mo/Al_2O_3 catalysts was evaluated for HDS, hydrogenation and HDN of model compounds in a high pressure reactor. At low promoter level, the Co-containing catalyst was better for HDS, but at high levels, the Ni catalyst was superior for hydrogenation and HDN.

Pressures of He or H_2 up to 70 atm had no effect on effective (pore) diffusivities of aromatic compounds in activated alumina supports.

Papers and Presentations

"Hydrodesulfurization Catalysis," F.E. Massoth and G. Muralidhar, plenary lecture presented at Fourth Climax International Conference on Chemistry and Uses of Molybdenum, Golden, Colorado, August 1982.

"Catalytic Functionalities of Supported Catalysts. Effect of Support on Mo Dispersion," G. Muralidhar, F.E. Massoth and J. Shabtai, presented at ACS meeting, Kansas City, Missouri, September 1982.

Task 1

Comparison of Catalysts for Coal Conversion at Subsoftening Conditions

Faculty Advisor: L.L. Anderson
Graduate Student: Tiee-Chyau Miin

Introduction

Research on the direct catalytic liquefaction of coal has included many catalysts of various types from those employed by the Germans such as Luxmasse and molybdenum oxide to expensive compounds such as germanium chloride. Some of the catalysts are actually poor hydrogenation or hydrogenolysis catalysts but give good yield in coal conversion reactions. To understand the catalytic conversion of coal, the chemical characteristics and reactivity of the catalytic materials used are important considerations.

Project Status

Recent work on these properties has led to the application of the HSAB (Hard and Soft Acids and Bases) principle. Catalytic compounds in the categories of Hard, Borderline, and Soft were tested as catalysts under the same hydrotreatment conditions. These conditions were a pressure of 2000 psi hydrogen and temperatures less than 300°C. About thirty single inorganic, salts were tested as conversion catalyts. The results show that salts which have "borderline" acidic sites are better catalyts than either hard or soft compounds. The conversion to gases and liquids (mostly liquids at these mild conditions) ranged from 20 to 99 percent for borderline cation salts while those for hard and soft were less than 20 percent (see Table 1).

Future Work

The liquids produced by different catalytic reactions will be analyzed and compared. The reason for the activity of borderline catalysts will be explained and more catalysts will be studied. The results could lead to a better understanding of the catalysis of the conversion of coal and other solid fuels as well as an indication of the chemical structures participating in the catalytic conversion reactions.

Table 1. Conversion of high volatile bituminous coal (Hiawatha, Utah) with treatment by H_2 at 2000 psi and 290°C for 3 hours. Yields in weight per cent of THF extracted coal.[a]

Catalysts	Liquid	Gas	Total
$GeCl_4$	81	4.3	85
$SnCl_4$	71	1.5	72
$SnCl_2 \cdot 2H_2O$	77	9	86
SnF_2	10	3	13
$SnBr_2$	80	13	93
SnI_2	80	13	93
SnO	5	3	8
$PbCl_2$	15	1.3	16
$CuCl_2 \cdot 2H_2O$	10	3	13
$RhCl_3 \cdot nH_2O$	14	13	27
$CoCl_2 \cdot 6H_2O$	18	0.6	19
FeF_2	11	1.5	12
$FeCl_2 \cdot 4H_2O$	21	2.5	23
$FeBr_2$	4	1	5
FeI_2	3	2	5
FeS	10	1.4	11
$FeCl_3$	3.5	1.5	5
$ZnSO_3$	27	2	29
ZnF_2	9	1	10
$ZnCl_2$	70	8	78
$ZnBr_2$	82	12	94
ZnI_2	77	7	84
$CdCl_2 \cdot 2\ 1/2H_2O$	8	1	9
$HgCl_2$	18	1.0	19
$SbCl_3$	20	2	22
$NiCl_2 \cdot 6H_2O$	7	10	17
$CeCl_3 \cdot 7H_2O$	4	1	5

[a]Raw coal was pre-extracted as completely as possible with tetrahydrofuran in a soxhlet extractor before catalytic treatment.

Task 3

Catalysis and Mechanism of Coal Liquefaction

Faculty Advisor: D.M. Bodily
Graduate Student: Tsejing Ray

Introduction

Metal halides such as $ZnCl_2$ are well-known to be active catalysts for coal hydrogenation. Zinc chloride has been shown to be a very effective catalyst for coal hydrogenation in the entrained-flow reactor developed at the University of Utah.[1,2] Bell and co-workers[3-5] have studied the reactions of model compounds with $ZnCl_2$ under conditions similar to those employed in coal hydrogenation. They observed cleavage of C-O and C-C bonds in the model compound and proposed that the active catalytic species is a Bronsted acid formed $ZnCl_2$.

Shibaoka, Russell and Bodily[6] proposed a model to explain the liquefaction of coal, based on microscopic examination of the solid products from metal halide catalyzed coal hydrogenation. The model involves a competition between hydrogenation and carbonization reactions. The hydrogenation process starts at the surface of vitrinite particles and progresses toward the center. The vitrinite is converted to a plastic material of lower reflectance, which is the source of oils, asphaltenes and preasphaltenes. Concurrently, carbonization occurs in the center of the particles, resulting in vesiculation and a higher reflectance material. The partially carbonized material can be hydrogenated at later stages, but at a lower rate than the original coal.

Thermal and/or catalytic bond rupture occurs during the liquefaction process. The initial products of the bond cleavage reactions may be stabilized by hydrogen addition, resulting in cleavage of bridges between aromatic ring systems and in dealkylation of aromatic rings. If the initial products of the reaction are not stabilized, they may polymerize to form semicoke-like material. This primary semicoke may be isotropic or exhibit a fine-grained anisotropic mosiac texture, depending on the rank of coal. The plastic material formed by stabilization of the initial products may be further hydrogenated or, under hydrogen deficient conditions, may form secondary semicoke. The secondary semicoke is of medium to coarse-grained anisotropic mosiac texture. Bodily and Shibaoka[7] used this model to explain the nature of the residues from hydrogenation in the short-residence, entrained-flow hydrogenation reactor. The role of the $ZnCl_2$ catalyst is examined in this study.

Project Status

Samples of Clear Creek, Utah coal have been reacted in a short-residence time, tubing-bomb reactor. The nominal reaction time is 5 minutes, with two minutes required for heat up. The temperature varied from 350 to 500°C and the initial hydrogen pressure at room temperature was 1000 psi. Zinc chloride catalyst was impregnated on the coal from aqueous solution by the method of Lee et al.[8]

Hydrogenolysis products were extracted in soxhlet apparatus with THF. A separate set of samples was examined by optical microscopy, using reflectance techniques. The optical microscope observations are reported in Table 1.

The optical microscope observations indicate that in the presence of $ZnCl_2$, the softening temperature of the coal is lower. Under the conditions of these experiments, anisotropic semi-coke is formed when the coal is rapidly heated to the region of 450°C or above. At a given temperature, the anisotropic regions are more developed when $ZnCl_2$ is present.

Future Work

The hydrogenolysis residues will be further characterized. Additional samples will be reacted. Samples will be reacted in a nitrogen atmosphere for comparison with the samples reacted under hydrogenolysis conditions.

References

1. R.E. Wood and W.H. Wiser, Ind. Eng. Chem., Proc. Design Devel., 15, 144 (1976).
2. J.M. Lytle, R.E. Wood and W.H. Wiser, Fuel, 59, 471 (1980).
3. D.P. Mobley and A.T. Bell, Fuel, 58, 661 (1979).
4. N.D. Taylor and A.T. Bell, Fuel, 59, 499 (1980).
5. D.P. Mobley and A.T. Bell, Fuel, 59, 507 (1980).
6. M. Shibaoka, N.J. Russell and D.M. Bodily, Fuel, 61, 201 (1982).
7. D.M. Bodily and M. Shibaoka, Fuel, submitted.
8. H.D. Lee, Technical Report to Dept of Interior, Office of Coal Research, Contract No. 14-32-0001-1200, University of Utah, Dept. of Mining, Metallurgical and Fuels Engineering, Salt Lake City, Utah, June 1974.

Table 1. Hydrogenolysis residues from Clear Creek, Utah coal.

Reaction Temperature, °C	Catalyst	Agglomeration	Appearance in Optical Microscope
384	None	Free flowing	No evidence of softening. Small pockets of oil form interference colors when dissolved in immersion oil.
405	None	Free flowing	Edges uneven. No pockets of oil. No evidence of softening.
464	None	Some agglomeration	Edges of grains are rounded. Mostly composed of small agglomerates. Apparent lower reflectance. Small anisotropic spots.
526	None	Caking	Anisotropic. Apparent higher reflectance. Edges reacted.
362	10% $ZnCl_2$	Free flowing	Edges of grains are fragmented and there is much fine material. No evidence of softening.
389	10% $ZnCl_2$	Some agglomeration	Very much fine material that tends to weakly agglomerate.
445	10% $ZnCl_2$	Caking	Edges reacted. Apparent lower reflectance. Large agglomerates with many cavities. Some vesiculation. Some anisotropic regions.
483	10% $ZnCl_2$	Highly agglomerating	Large agglomerates with many cavities and vesicules. Anisotropic.

Task 5

The Mechanism of Pyrolysis of Bituminous Coal

Faculty Advisor: W.H. Wiser
Graduate Student: J.K. Shigley

Introduction

In the present state of knowledge concerning the fundamental chemistry of coal liquefaction in the temperature range 375-550°C, the liquefaction reactions are initiated by thermal rupture of bonds in the brides joining configurations in the coal, yielding free radicals. The different approaches to liquefaction, except for Fischer-Tropsch variations, represent ways of stabilizing the free radicals to produce molecules. The stabilization involving abstraction by the free radicals of hydrogen from the hydro-aromatic structures of the coal is believed to be the predominant means of yielding liquid size molecules in the early stages of all coal liquefaction processes, except Fischer-Tropsch variations. The objective of this research is to understand the chemistry of this pyrolytic operation using model compounds which contain structures believed to be prominant in bituminous coals.

Project Status

The variation in experimental technique alluded to in the previous quarterly report has been further refined to improve material balances and analyses consistency. Improvements in solvent delivery, reaction temperature control, reaction time measurement and reaction quenching have been incorporated into the technique.

Five experiments were conducted at 350°C with 9-benzyl-1,2,3,4-tetrahydrocarbazole for times of one, three and five minutes. The low conversions encountered at this temperature made initial analysis of the technique difficult. Material balances ranged from 83 to 99%, but the conversions were consistently between 16 to 19% of the starting material. It was decided to continue experiments at a higher temperature to determine the feasibility of the experimental technique.

Experiments were conducted at 400°C for times ranging from one to thirty minutes. The data for these experiments are shown in Table 1. Material balances ranged from 82 to 105% of starting material, with conversions from 21 to 75% of starting material (9-BTHC). This signifies a tremendous improvement in the consistency and accuracy of the experimental data utilizing this technique. A majority of the experiments had material balances from 88 to 95%. It must be remembered that the kinetics data presented in this report are for one temperature only, and therefore, limit the conclusions. The conclusions made are speculative and must remain as such until further data can be gathered for comparison.

Kinetic analysis of these data was performed initially with the integral technique[1] for zero, first and second order kinetics. Zero order kinetics does not model the data well at all and can be discarded as a possible description

of the reactions occurring. The results of the first and second order kinetics analyses are shown in Table 2. A linear regression analysis was performed on the first and second order kinetics data and the results are shown at the bottom of Table 2.

The first and second order kinetic data are plotted in Figures 1 and 2, respectively. The line drawn on each plot is the result of the linear regression analysis of the data.

The data was also analyzed utilizing the differential technique.[1] This technique involves the determination of the rate of change of the concentration of the starting material (dC_A/dt) from a concentration versus time curve. The concentration (C_A) versus time curve is shown in Figure 3. The results of this analysis are shown in Table 3, with the plot of $Ln(-dC_A/dt)$ versus $Ln\ (C_A)$ in Figure 4. The differential analysis strongly suggests that the reaction(s) occurring at 400°C can be modeled more effectively by second order kinetics. If Figures 1 and 2 are compared, visually and by linear regression analysis, it can be seen that the data fit the second order plot better. Experimental error makes the comparison a little more difficult than necessary. Utilizing the differential and integral analyses, it can be concluded (for this temperature, 400°C) that the reactions occurring can be modeled most effectively by second order kinetics.

Pyrolysis experiments for 9-BTHC have also been conducted at 425°C. Problems have been encountered with the formation, due to side reactions, of what appears to be condensation reaction products. Material balances above 90% have not been consistently attainable, with the recovery decreasing as reaction time and heavy products formation increases. The side reaction products are similar in appearance to coke and tars from coal or petroleum reactions. They are very resistant to dissolution in standard solvents and complicate product analyses considerably. The data gathered thus far at 425°C are shown in Table 4.

Future Work

In an attempt to identify unknown pyrolysis reaction products occurring at 400 and 425°C, gas chromatographic/mass spectrometric analyses will be performed in an attempt to understand the pyrolysis mechanism better and to verify previous analyses. It is also hoped that some information will be obtained to confirm or refute the production of the apparent condensation reaction(s) products.

GC/MS analysis will also be performed on the three model compounds to be utilized in this study.[2] These analyses will be performed to verify composition and structure of the model compounds.

Improvements in sample preparation to prevent the retention of any oxygen and/or water in the sealed tubes will be studied and implemented if deemed necessary. Certain means to prevent this retention are currently utilized but refinements may be necessary.

Also, work will continue to improve the experimental technique and in doing so improve data consistency, especially at higher pyrolysis temperatures ($T > 425°C$).

References

1. Levenspiel, Octave, "Chemical Reaction Engineering," 2nd Ed., John Wiley & Sons, New York, New York, 1972.

2. W.H. Wiser et al., DOE Contract No. E(49-18) - 2006, Quarterly Progress Report, Salt Lake City, Utah, Jan - Mar 1979.

Table 1. PYROLYSIS OF 9-BENZYL-1,2,3,4-TETRAHYDROCARBAZOLE

Temperature: 400°C

Reaction Time, min.	Initial m moles of 9BTHC	Tube Volume, cc	Material Balance, %	Conversion of 9BTHC
1.0	.01515	.5629	89.12	.2103
3.0	.01611	.6582	90.47	.2839
5.0	.01531	.7354	98.40	.3574
5.0	.01580	.6719	88.44	.3662
8.0	.01286	.6537	96.07	.3784
10.0	.01718	.6083	82.02	.5718
15.0	.01332	.8199	105.61	.5333
20.0	.01194	.5175	87.60	.6406
30.0	.01358	.6355	97.35	.7539

NOTES: 1. Tube Volume = $\frac{\pi D^2 L}{4}$

2. % Material Balance = $\left[\frac{N(THC) + N(Carb) + N(Unk) + N(9BTHC) + N(9BC)}{N_0\ (9BTHC)} \right]$ X 100

3. Conversion = $1 - \frac{N_A}{N_{AO}} = 1 - \frac{N\ (9BTHC)}{N_0\ (9BTHC)}$

where,

N(A) = millimoles of A

N_0(A) = initial millimoles of A

Table 2. Pyrolysis of 9-benzyl-1,2,3,4-tetrahydrocarbazole overall reaction(s) order determination via the integral technique. Temp: 400°C.

Reaction Time, Minutes	Kinetic Plots' Ordinates: First Order $-Ln(1-X_A)$	Second Order $X_A/[C_{AO}(1-X_A)]$
1	0.2361	9.894
3	0.3340	16.20
5	0.4423	26.73
5	0.4560	24.57
8	0.4755	30.96
10	0.8481	47.28
15	0.7620	70.36
20	1.0234	77.29
30	1.402	143.36

Linear Regression Analysis

	Y-Intcpt	Slope	r^2
First Order $-Ln(1-X_A) = k_1 t$	0.2427	0.0391	0.9471
Second Order $\frac{X_A}{C_{AO}(1-X_A)} = k_2 t$	1.774	4.44	0.9778

where,

k_1[=] min^{-1}, k_2[=] $\frac{cc}{mmole\text{-}min}$, r^2 = correlation coefficient

Table 3. Pyrolysis of 9-benzyl-1,2,3,4-tetrahydrocarbazole overall reaction(s) order determination differential method. Temp: 400°C.

Reaction Time, Minutes	C_A	$-(\frac{dC_A}{dt})$	$Ln[C_A]$	$Ln[-(\frac{dC_A}{dt})]$
1	0.02125	2.499×10^{-3}	-3.851	-5.992
3	0.01753	1.999×10^{-3}	-4.044	-6.215
5	0.01495	1.201×10^{-3}	-4.203	-6.725
5	0.01491		-4.206	
8	0.01223	8.334×10^{-4}	-4.404	-7.090
10	0.01209	7.145×10^{-4}	-4.415	-7.244
15	0.00758	3.748×10^{-4}	-4.882	-7.889
20	0.00829	3.335×10^{-4}	-4.793	-8.006
30	0.00526	1.666×10^{-4}	-5.248	-8.700

Linear Regression Analysis

$Ln[-(\frac{dC_A}{dt})] = Ln(k) + nLn[C_A]$, where $C_A = \frac{N_{A0}(1-X_A)}{V_T}$

Y-intercept = 1.623 = Ln(k)

Slope = 1.98 = n

r^2 = 0.9849 = correlation coefficient

Table 4. Pyrolysis of 9-BTHC at 425°C.

Reaction Time, Minutes	Initial mmoles of 9-BTHC	Tube Volume, cubic cm	Material Balance, Percent	Conversion of 9-BTHC (fractional)
1	0.01309	0.7654	96.90	0.1647
3	0.01527	0.7654	100.76	0.5130
5	0.01569	0.7418	86.81	0.6347
8	0.01496	0.7422	75.16	0.8519
8	0.01420	0.7699	81.73	0.8534
10	0.01986	0.8235	72.88	0.8897
15	0.01148	0.8253	69.40	0.9611
20	0.01936	0.8317	75.59	0.9707

Tube Volume = $\frac{\pi D^2 L}{4}$

Percent Material Balance = $\left[\frac{N(THC) + N(CARB) + N(UNK) + N(9BTHC) + N(9BC)}{N_0\ (9BTHC)}\right] \times 100$

Conversion = $1 - \frac{N(9BTHC)}{N_0(9BTHC)}$

where, THC = 1,2,3,4-tetrahydrocarbazole, CARB = carbazole, 9BC = 9-benzylcarbazole, UNK = N-containing unknowns.

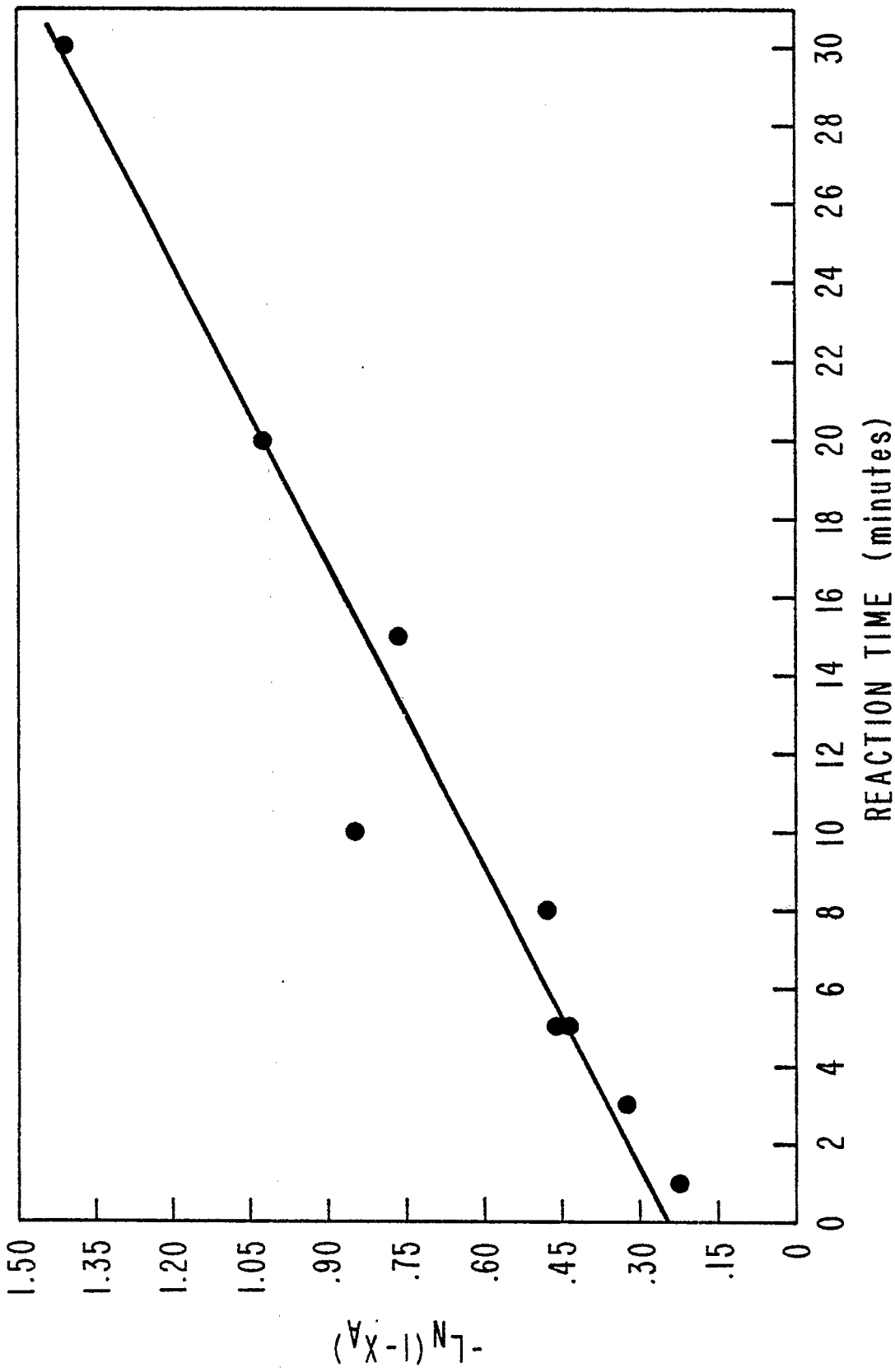

Figure 1.. First order kinetics plot.

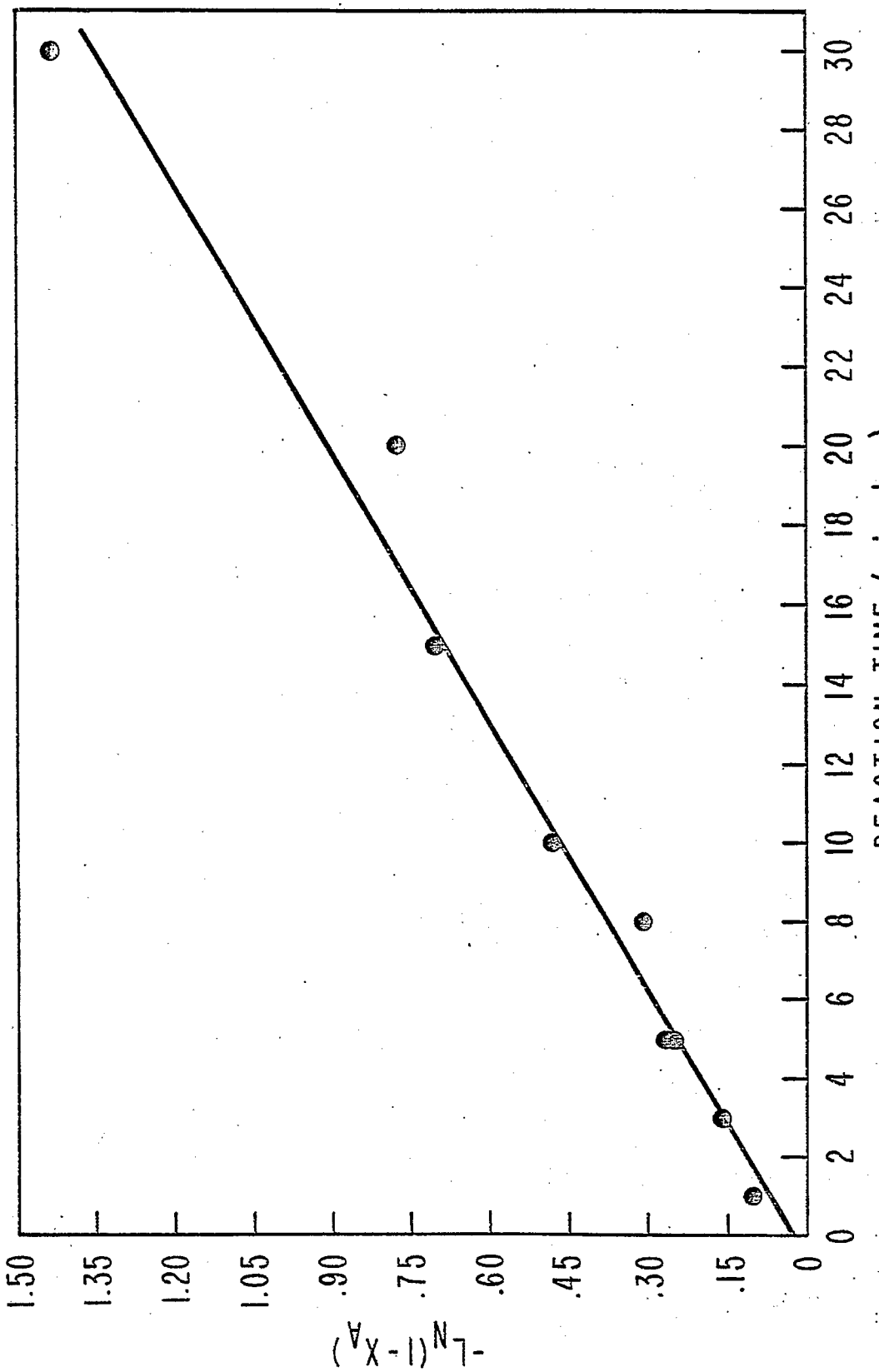

Figure 2. Second order kinetics plot.

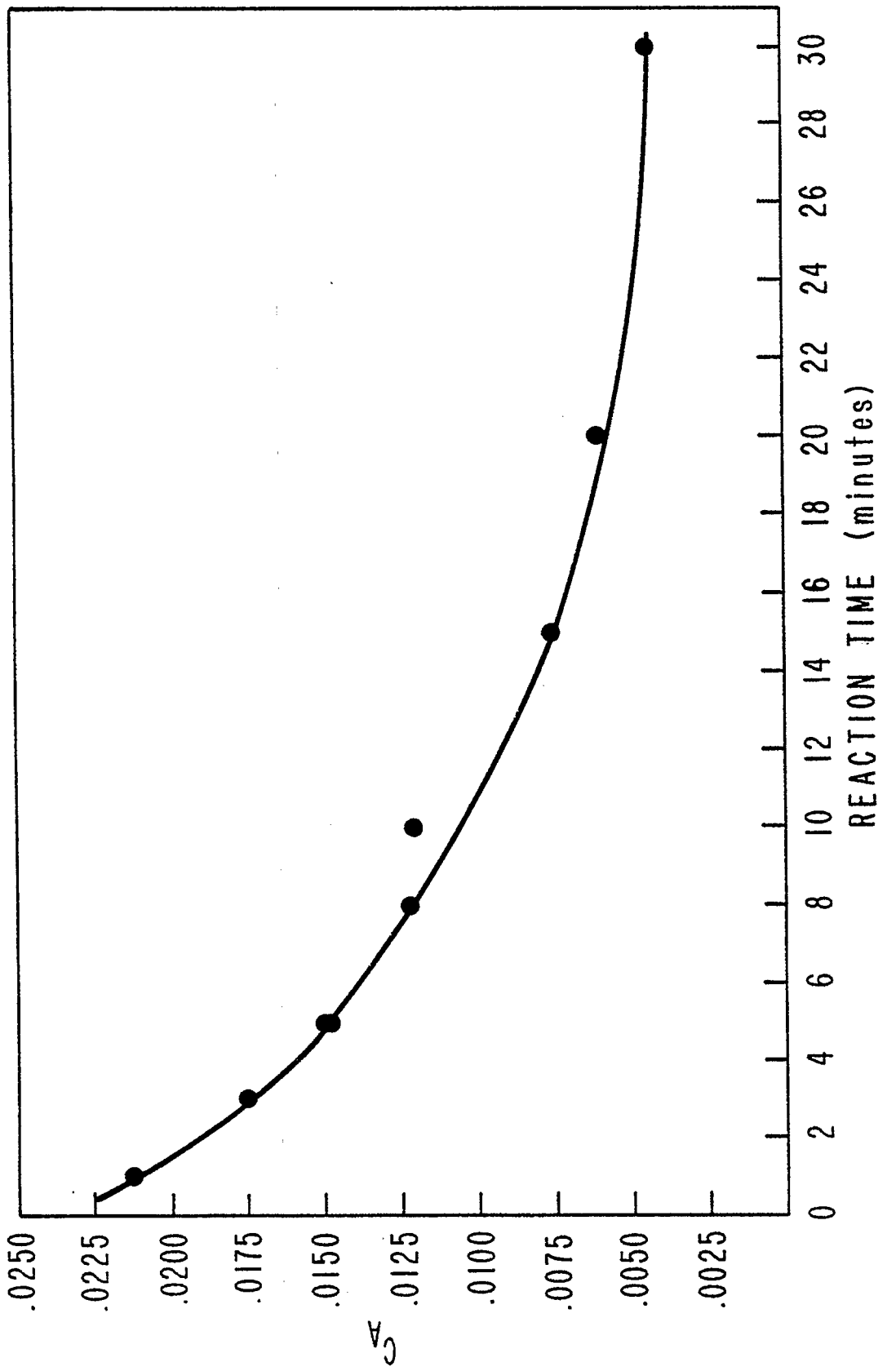

Figure 3. Concentration of 9-BTHC vs. time.

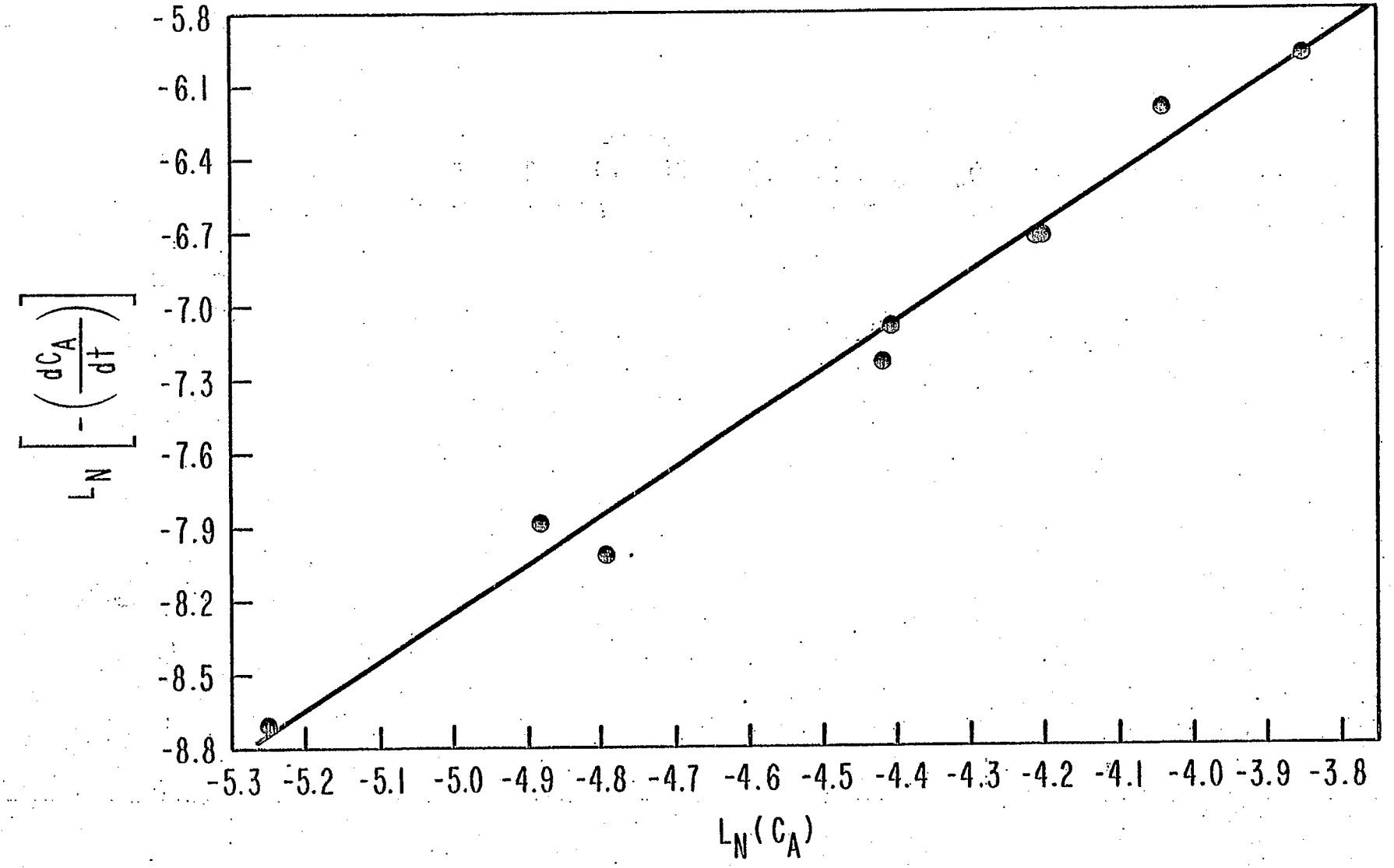

Figure 4. Differential kinetic order analysis.

Task 6

Catalytic Hydrogenation of CD Liquids and Related Polycyclic Aromatic Hydrocarbons

Faculty Advisor: J. Shabtai
Research Associate: C. Russell

Introduction

The main objective of this research project is to develop a versatile process for controllable hydrotreating of highly aromatic coal liquids, viz., a process permitting production of naphthenic-aromatic feedstocks containing variable relative concentrations of hydroaromatic vs. aromatic ring structures. Such feedstocks, including the extreme case of a fully hydrogenated coal liquid, are suitable starting materials for catalytic cracking, as applied for preferential production of light liquid fuels. The overall objective of this project and of a parallel catalytic cracking study is, therefore, to develop and optimize a hydrotreating-catalytic cracking process sequence for conversion of coal liquids into conventional fuels.

The present project includes also a study of metal sulfide-catalyzed hydrogenation of model polycyclic arenes present in coal liquids, e.g., phenanthrene, pyrene, anthracene and triphenylene, as a function of catalyst type and experimental variables.[1] This part of the study provides basic information on the rate, mechanism and stereochemistry of hydrogenation of structurally distinct aromatic systems in the presence of sulfided catalysts.

Project Status

The systematic studies of the hydrogenation reactions of chrysene and of an SRC-II distillate (b.p. range 230 - 455^{o}) are being continued.

Future Work

The study of the hydrogenation kinetics of a typical coal liquid (SRC-II middle-heavy distillate) and of a tetracyclic model compound, i.e., chrysene, will be continued and completed.

Reference

1. J. Shabtai, C. Russell, L. Veluswamy and A.G. Oblad, to be published.

Task 7

Denitrogenation and Deoxygenation of CD Liquids and Related N- and O- Compounds

Catalytic Hydrodeoxygenation of Coal-Derived Liquids and Related Oxygen-Containing Compounds

Faculty Advisor: J. Shabtai
Graduate Student: Y. Shukla

Introduction

Coal-derived liquids are characterized by the presence of a considerable concentration of oxygen-containing components. Therefore, a systematic catalytic hydrodeoxygenation (HDO) study of coal-derived liquids and related model compounds is being carried out. The study provides information not only on the mechanism of HDO as related to catalytic upgrading of coal liquids, but also on the role of oxygen-containing compounds in primary coal liquefaction processes.

Project Status

Systematic HDO studies of representative diaryl ethers and dibenzofurans are in progress. These two types of compounds are found as components of coal-derived oils, asphaltenes and asphaltols and show considerable resistance to hydrodeoxygenation.[1] Ongoing kinetic studies indicate that HDO rates for dibenzofurans are markedly lower as compared with those of diaryl ethers. In effect, evidence is being accumulated to indicate that dibenzofuran type of components in coal liquids show highest resistance to HDO in upgrading reactions catalyzed by sulfided Co-Mo and Ni-Mo catalysts.

Future Work

The above indicated studies will be continued.

Reference

1. H.B. Oblad, Ph.D. Thesis, University of Utah, Salt Lake City, Utah, 1982.

Task 8

Catalytic Cracking of Hydrogenated Coal-Derived Liquids and Related Compounds

Faculty Advisors: J. Shabtai
A.G. Oblad
Graduate Student: John McCauley

Introduction

Hydrogenation followed by catalytic cracking provides a feasible process sequence for conversion of coal liquids into conventional fuels. Such a sequence has certain advantages in comparison with a hydrodcracking-catalytic reforming scheme.

The present project is concerned with the following interrelated subjects: (1) systematic catalytic cracking studies of polycyclic naphthenes and naphthenoaromatics found in hydrogenated coal liquids and (2) systematic catalytic cracking studies of hydrotreated coal-derived liquids.

Project Status

Systematic catalytic cracking studies, using newly synthesized cross-linked smectite (CLS) molecular sieves[1,2] are being continued. One type of newly prepared catalyst systems, i.e., cross-linked fluorhectorites (CLFH molecular sieves) show much higher cracking activities as compared to those of conventional, zeolite-containing cracking catalysts in model reactions with a variety of alkylsubstituted arenes (see previous report, DE/ET/14700-10). Data will be provided in the next report.

Future Work

The above indicated studies will be continued.

References

1. J. Shabtai, U.S. Patent 4,238,364 (1980).

2. J. Shabtai, R. Lazar and A.G. Oblad, Proc. 7th International Congress on Catalysis, Tokyo, Japan, 1980, pp 828-840.

Task 9

Hydropyrolysis (Thermal Hydrocracking) of CD Liquids

Faculty Advisors: J. Shabtai
A.G. Oblad
Graduate Student: Y. Wen

Introduction

This project is concerned with a systematic investigation of hydropyrolysis (thermal hydrocracking) as an alternative processing concept for upgrading of heavy coal-derived liquids into light liquid products. The high efficiency and versatility of hydropyrolysis has been indicated in previous studies with heavy CDL feedstocks and with model compounds.[1-3] The present project is an extension of this previous work for the purpose of (a) further developing and enlarging the scope of the hydropyrolytic reaction, and (b) optimizing the operating conditions for different types of feedstocks, e.g., coal liquids from different liquefaction processes, partially hydrotreated coal liquids, and relevant model compounds. The project includes systematic studies of reaction kinetics, product composition, and coking tendencies, as a function of operating variables. The work with model compounds provides necessary data for further elucidation of mechanistic aspects of the hydropyrolysis process.

Project Status

The systematic hydropyrolysis studies of representative naphthenoaromatic hydrocarbons and of an SRC-II middle-heavy distillate (b.p. range, 230 - 455°C) are being continued. In addition to tetralin (see preceding progress report DE/ET/14700-10) a study of the hydropyrolytic reactions of 9, 10-dihydroanthracene was initiated.

Future Work

Hydropyrolysis studies with (a) partially hydrogenated coal liquids, and (b) polycyclic naphthenoaromatics as feeds will be continued.

References

1. J. Shabtai, R. Ramakrishnan and A.G. Oblad, Advances in Chemistry, No. 183, Thermal Hydrocarbon Chemistry, Amer. Chem. Soc., 1979, pp 297-328.

2. R. Ramakrishnan, Ph.D. Thesis, University of Utah, Salt Lake City, Utah, 1978.

3. A.G. Oblad, J. Shabtai and R. Ramakrishnan, U.S. Patent 4,298,457 (1981).

Task 10

Systematic Structural Activity Study of Supported Sulfided Catalysts for Coal Liquids Upgrading

Faculty Advisors: F.E. Massoth
J. Shabtai
Post-Doctoral Fellow: Y. Liu
Graduate Student: K. Baluswamy

Introduction

The objective of this research is to develop an insight into the basic properties of supported sulfide catalysts and to determine how these relate to coal liquids upgrading. The proposed program involves a fundamental study of the relationship between the surface-structural properties of various supported sulfide catalysts and their catalytic activities for various types of reactions. Thus, there are two clearly defined and closely related areas of investigation, viz., (1) catalyst characterization, especially of the sulfided and reaction states and (2) elucidation of the mode of interaction between catalyst surfaces and organic substrates of different types. The study of subject (1) will provide basic data on sulfided catalyst structure and functionality, and would allow the development of catalyst surface models. Subject (2), on the other hand, involves systematic studies of model reactions on sulfide catalysts, and the utilization of data obtained for development of molecular level surface reaction models correlating the geometry (and topography) of catalyst surfaces with the steric-conformational structure of adsorbed organic reactants. The overall objective of the project is to provide fundamental data needed for design of specific and more effective catalysts for upgrading of coal liquids.

Atmospheric activity tests using model compounds representative of hydrodesulfurization (thiophene), hydrogenation (hexene) and cracking (isooctene) have been developed. These were employed to assay changes in the catalytic functions of various supported CoMo catalysts. It was found that hydrodesulfurization (HDS) and hydrogenation (HYD) activities were generally unaffected by the type of alumina used or by the cobalt salt used in the preparation; whereas, cracking activity varied considerably, being highest for γ-Al_2O_3 and cobalt sulfate addition. Addition of acidic, basic or neutral ions to the standard γ-alumina catalyst at 0.5 wt % level showed interesting changes in catalytic activities for the various functions. In a series of catalysts employing silica-alumina as the support, the HDS and hydrogenation functions decreased with increasing silica content, while cracking went through a maximum in activity. Catalysts prepared by supporting CoMo on TiO_2, SiO_2·MgO and carbon showed low activities, except for high cracking activity for the two former catalysts.

Oxide precursors of CoMo and Mo catalysts supported on various silica-aluminas evaluated by ESCA showed that support-active component interaction decreased with increase of silica in the support. It was also found that cobalt did not influence the Mo dispersion. On alumina, the Mo phase was found to be dispersed in essentially a monoatomic form.

Several catalysts, which were evaluated in the atmospheric pressure test unit, were subsequently tested at high pressure (34 atm) using dibenzothiophene (HDS), naphthalene (HYD) and indole (HDN). Results showed poor correlation of HDS and HYD activities between the two test conditions. The high pressure runs are carried out sequentially in the order indicated to assess the separate catalytic functionalities. Repeat runs of HDS and HYD after HDN gave appreciably lower activities for HDS and HYD which was found to be due to strongly adsorbed residues containing nitrogen.

Project Status

In this period several NiW catalysts were prepared and tested in the low pressure reactor. High pressure tests on a $CoMo/Al_2O_3$ and $NiMo/Al_2O_3$ series of catalysts were carried out. Also, the effect of H_2S on HDS, HYD and HDN was evaluated.

Catalysts containing 3% Ni and 16% W were prepared by impregnation on the following supports: γ-Al_2O_3, 10% SiO_2-Al_2O_3 and 25% SiO_2-Al_2O_3. The levels of Ni and W were chosen to give equimolar concentrations to those previously used in CoMo and NiMo catalysts. The catalysts were tested for thiophene HDS, hexene HYD and isooctene CKG in the low pressure reactor, as described previously.[1] The results, in terms of rate constants, are given in Table 1, together with comparable results for CoMo and NiMo catalysts. On Al_2O_3, the NiW catalyst is only about 2/3 as active for HDS and HYD as the CoMo catalyst, and as active for HDS but slightly less active for HYD as the NiMo catalyst. However, on the SiO_2-containing supports, NiW is more active for HDS but less active for HYD than the comparable CoMo catalysts. This interesting reversal gives significantly higher HDS/HYD selectivities for these catalysts. Also, the presence of W has markedly increased the cracking function on these catalysts, complete conversion even being obtained on the Al_2O_3 catalyst. Thus, WS_2 has appreciably more protonic acidity than MoS_2.

High pressure tests were carried out on a series of $CoMo/Al_2O_3$ and $NiMo/Al_2O_3$ catalysts which had been previously screened in the low pressure reactor.[2] In these tests, made at 500 psi, dibenzothiophene is used for HDS, naphthalene for HYD and indole for HDN.[3] Results are presented in Table 2. Several interesting differences are observed for Co versus Ni promotion. At 1% level, Co promoted HDS more than Ni while HYD and HDN promotions were about the same. However, at 3% and 6% levels, Ni promoted all reactions more than Co. Generally, Ni promoted HYD and HDN relatively more than HDS compared to Co. These results are in general agreement with the low pressure data on these same catalysts,[2] except for lower HDS for the Ni compared to the Co catalysts obtained at low pressure. Apparently, the Ni catalysts become more active with increased H_2 pressure than the comparable Co catalysts.

The effect of H_2S on promoting HDN was reported previously.[2] Similar tests were made on HDS and HYD, and repeated on HDN. In these, the amount of CS_2 (converted to H_2S in the reactor) in the liquid feed was increased fourfold over the standard amount used. Table 3 presents the results obtained for the 6% Co 8% Mo/Al_2O_3 catalyst. Increase in H_2S partial pressure resulted in a large loss in HDS activity and a moderate loss in HYD activity. The increase in HDN confirms our earlier result. The different responses to H_2S indicate different sites are involved for these three reactions. Evidence for different sites for these reactions has recently been reviewed.[4]

Future Work

Several additional NiW catalysts will be prepared and tested. A high pressure test for HDO will be developed and a number of different catalysts will be evaluated for HDO activity. Reactivity tests will be instigated on selected reactants expected to give information on the stereochemistry of HYD, HDN and HDO reactions in order to obtain insight into the nature of the active sites present.

References

1. W.H. Wiser, F.E. Massoth, J. Shabtai and G. Muralidhar, DOE Contract No.DE-AC01-79ET14700, Quarterly Progress Report, Salt Lake City, Utah, April-June 1980.

2. ibid, April-June 1982.

3. ibid, April- June 1981.

4. F.E. Massoth and G. Muralidhar, paper presented at Fourth Climax Intern. Conf. Chemistry and Uses of Molybdenum, Golden, Colorado, 1982.

Table 1. Activities of NiW, CoMo and NiMo catalysts.

Support	NiW				CoMo				NiMo			
	k_T	k_H	k_c[a]	HDS/HYD	k_T	k_H	k_c[a]	HDS/HYD	k_T	k_H	k_c	HDS/HYD
Al_2O_3	19.9	46.4	c	0.43	32.5	64.2	156	0.51	20.0	58.6	208	0.34
10% SiO_2-Al_2O_3	28.7	43.4	c	0.66	18.8	58.2	319	0.32	--	--	--	--
25% SiO_2-Al_2O_3	20.2	38.5	c	0.52	15.6	46.3	c	0.34	--	--	--	--

[a]c stands for complete conversion.

Table 2. Activities of $CoMo/Al_2O_3$ and $NiMo/Al_2O_3$ catalysts at high pressure. Values are % conversion at a liquid feed rate of 10 cm^3/hr.

% Co or Ni[a]	CoMo			NiMo		
	HDS	HYD	HDN	HDS	HYD	HDN
0	2	15	12	2	15	12
1	28	46	41	11	47	39
3	45	48	44	76	96	67
6	64	57	53	78	97	87

[a]All catalysts contained 8% Mo.

Table 3. Effect of H_2S on reactions at high pressure. Values are % conversions at a liquid feed rate of 7 cm^3/hr.

CS_2, %	HDS	HYD	HDN
1.2	87.3	68.5	62.5
4.8	44.5	55.5	77.8
% Change	-49	-19	+25

Task 11

Basic Study of the Effects of Poisons on the Activity of Upgrading Catalysts

Faculty Advisor: F.E. Massoth
Post-Doctoral Fellow: J. Miciukiewicz

Introduction

The importance of cobalt-molybdena catalysts for hydrotreating and hydrodesulfurization of petroleum feedstocks is well-known. These catalysts are also being studied for hydrodesulfurization and liquefaction of coal slurries and coal-derived liquids. However, such complex feedstocks result in rapid deactivation of the catalysts. To gain an insight into the deactivation mechanism, the detailed kinetics of reactions of model compounds representative of heteratom hydrogenolysis and hydrogenation are compared before and after addition of various poisons and coke precursors. The studies are carried out using a constant stirred microbalance reactor, which enables simultaneous measurement of catalyst weight change and activity. Supplementary studies are made to gain additional insight into the effect of poisons on the active catalyst sites. Finally, catalysts aged in an actual coal pilot plant run are studied to compare with laboratory studies.

Previous work on this project has shown that catalyst poisoning by pyridine or coke results in loss of active sites for benzothiophene HDS, but that the remaining unpoisoned sites retain their original activity. Pyridine appeared to be site selective in poisoning effect whereas coke was nonspecific. Furthermore, at least two HDS sites were indicated from the pyridine poisoning studies.

Poisoning of a $CoMo/Al_2O_3$ catalyst with several nitrogen-containing compounds gave the following order of deactivation of hexene hydrogenation: quinoline > pyridine > indole > aniline. Thiophene hydrodesulfurization was deactivated more than hexene hydrogenation, but was less sensitive to the type of poison adsorbed. Poisoning with 2,5-pyridine gave opposite results, hydrogenation being deactivated more than hydrodesulfurization, showing that steric and inductive effects are important in the effect of specific poisons on catalyst deactivation.

Project Status

Work has continued on the effects of N-compound poisoning on thiophene HDS and hexene hydrogenation (HYD) activities of a $CoMo/Al_2O_3$ catalyst. The experimental technique has been described in the last progress report.[1]

Figure 1 presents results of relative catalyst deactivation of HDS and HYD for piperidine and pyridine. Relative activity is the ratio of the activity of the poisoned to the unpoisoned catalyst. Piperidine had a greater deactivating effect on HDS than pyridine, probably due to the greater basic character of piperidine. However, there was no difference in HYD deactivation between the two compounds, somewhat surprising in view of the greater effect of basicity on HYD poisoning found previously for other N-compounds.

Comparisons of deactivations with N,N-dimethylaniline and aniline are shown in Figure 2. Both HDS and HYD activities were more deactivated with the methyl-substituted compound. This may be due to the partial overlap of a methyl group on an adjacent active site, rendering that site less active. Interestingly, a steric hindrance effect was not present (moderating adsorption) as had been observed for 2,6-dimethylpyridine on HDS activity.[1] Apparently, the N atom in N,N-dimethylaniline is able to bond to the HDS site without hindrance, whereas the N atom in 2,6-dimethylpyridine encounters some hindrance due to the methyl groups.

The effect of excess H_2S on the poisoning effects of aniline, pyridine and 2,6-dimethylpryidine was studied. In excess H_2S, the HDS activity was lower than in its absence, but the HYD activity was unaffected. Relative activity deactivations for both reactions with the three poisons were essentially the same with or without added H_2S. Thus, the presence of H_2S, while depressing HDS activity, had no effect on the relative deactivating effect of these poisons.

Four general findings come from these poisoning studies: (1) for the same total amount of a given poison adsorbed, HDS activity is deactivated more than the HYD; (2) deactivation-uptake plots of both show concave curvature; (3) stronger bases give greater deactivation of HYD, but little difference for HDS; and (4) steric hindrance affects HDS deactivation but not HYD. Interpretation of these results is complicated by the fact that total adsorption of the poison is measured rather than the specific amount on active sites, while activity data is related to only active sites, whose number may be relatively small compared to the total adsorption sites (catalytically active plus inactive sites). For a given poison, this complication is of no importance in evaluating its effect on HDS vs. HYD activity. Thus, the greater deactivation effect on HDS compared to HYD for all unhindered poisons means that relatively more poison adsorbs on HDS sites than HYD sites, and indicates that HDS sites are stronger Lewis acid sites. That the deactivation-uptake plots show curvature implies a distribution of strengths (acidity) of both HDS and HYD sites is present.

When comparing the effect of different poisons on activities, differences in adsorption on inactive sites may come into play. However, it can be shown that this cannot account for differences in deactivation of HYD while HDS deactivation is essentially unaffected for different poisons. Therefore, we assume that adsorption on active sites is proportional to total adsorption. Then, the greater deactivation on HYD for stronger bases may be rationalized by an electron inductive effect on a neighboring uncovered site, lowering its Lewis acidity and catalytic activity (e.g. pyridine vs. aniline). That HDS deactivation is not similarly affected may be due to the stronger acidity of HDS sites, neighboring inductive effects having less effect on its strong acidity than on the weaker acidity of HYD sites.

The effect of 2,6-dimethylpyridine on greater deactivation of HYD compared to pyridine may be similarly explained as the former is a stronger base. However, the greater deactivation of HDS is not observed; in fact, HDS is less deactivated with dimethylpyridine. This may be explained by a steric effect, the methyl groups preventing close approach of the molecule to the active adsorption site, rendering it effectively less basic in this case; thus, its inductive effect on a neighboring HDS site will be weakened and less deactivation will occur. If this explanation is correct, it indicates

that the geometry of HDS and HYD sites is different, the former being susceptible to steric hindrance effects and the lattter not. Finally, it should be noted that no steric effects on either HDS or HYD were obtained with N,N-dimethylaniline compared to aniline. Orientation of the adsorbed molecule on the HDS site must be different in this case than for pyridine to account for differences in steric effects.

Future Work

Additional poisoning studies will be made with several O-compounds to compare results with the N-compounds. Kinetic studies of HDS and HYD on a fresh and aged catalyst which had been used in an H-coal pilot plant run will be initiated.

Reference

1. W.H. Wiser and F.E. Massoth, DOE Contract No. DE-AC01-79ET14700, Quarterly Progress Report, Salt Lake City, Utah, April-June 1982.

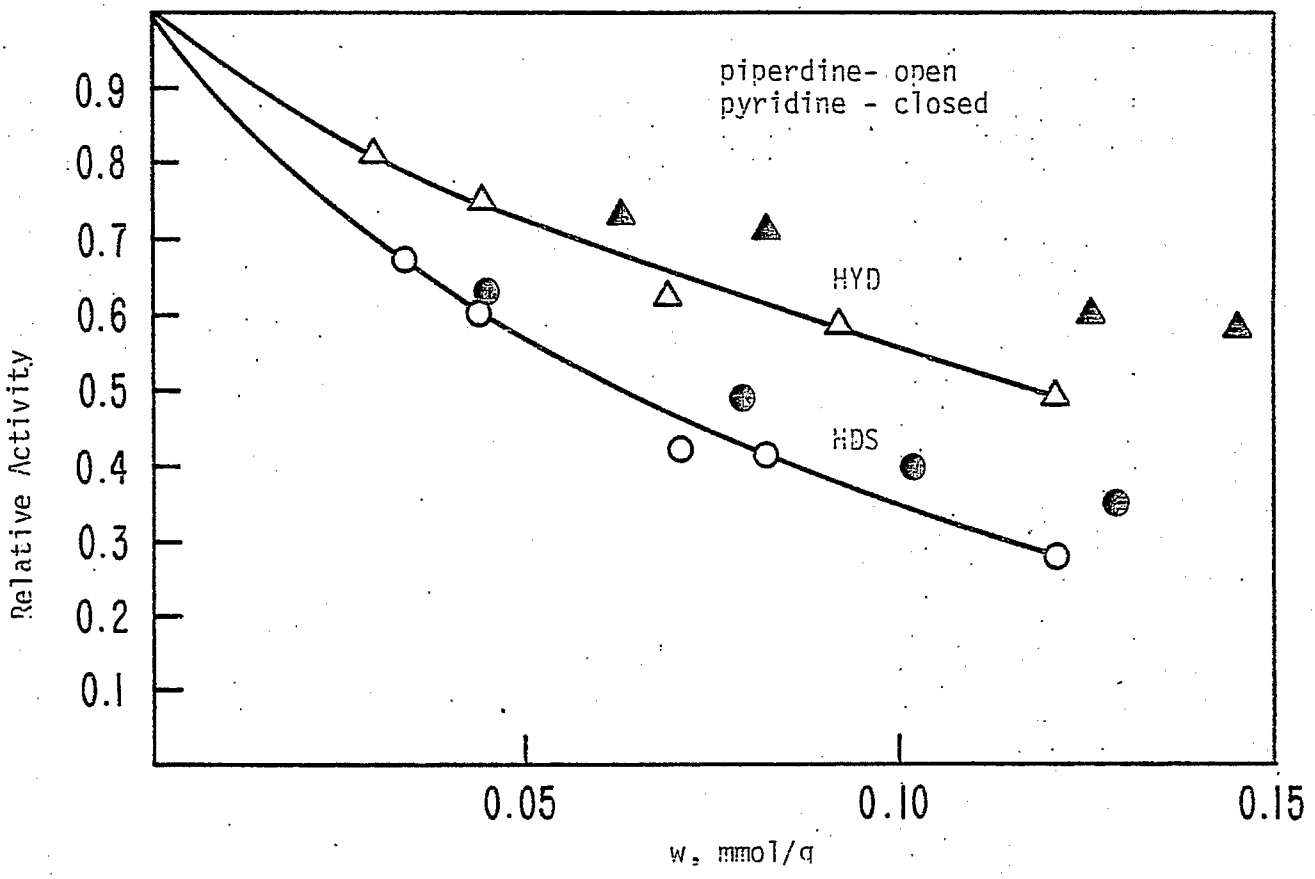

Figure 1. Poisoning effect of piperidine vs. pyridine.

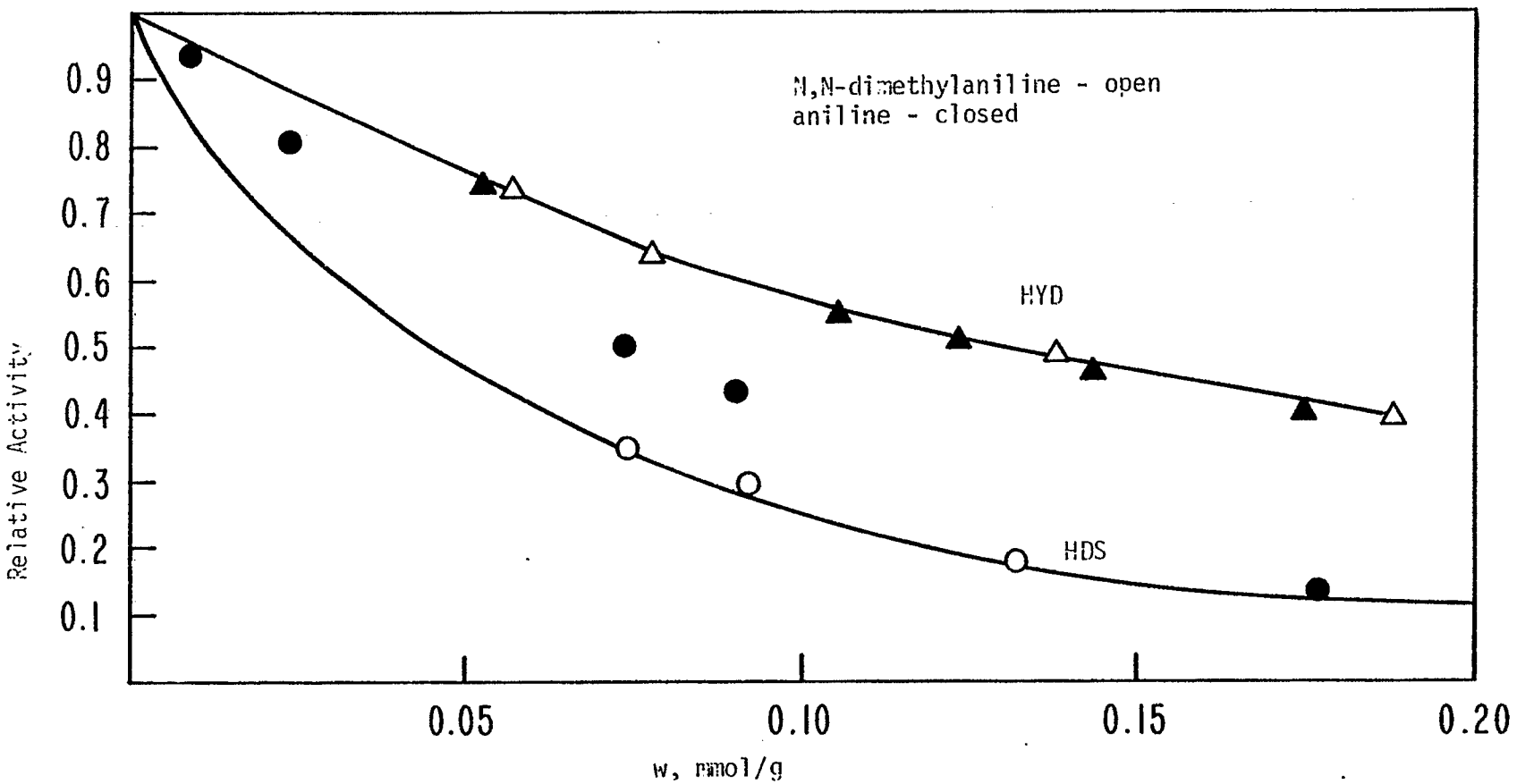

Figure 2. Poisoning effect of N,N-dimethylaniline vs. aniline.

Task 12

Diffusion of Polyaromatic Compounds in Amorphous Catalysts Supports

Faculty Advisor: F.E. Massoth
Post-Doctoral Fellow: G. Seo

Introduction

This project involves assessing diffusional resistances within amorphous-type catalysts. Of primary concern is the question of whether the larger, multiring hydro-aromatics found in coal-derived liquids will have adequate accessibility to the active sites within the pores of typical processing catalysts. When molecular dimensions approach pore size diameters, the effectiveness of a particular catalyst is reduced owing to significant mass transport resistance. An extreme case occurs when molecular and pore size are equivalent, and pores below this size are physically inaccessible.

The project objective can be achieved through a systematic study of the effect of molecular size on sorptive diffusion rates relative to pore geometry. Conceptually, the diffusion of model aromatic compounds is carried out using a stirred batch reactor. The preferential uptake of the aromatic from the aliphatic solvent is measured using a UV spectrometer. Adsorption isotherms are determined to supplement the diffusion studies.

Studies to date have been confined to ambient temperature and pressure. Four aromatic solutes ranging from 7 to 19 Å and four aluminas (representative of catalyst supports) having average pore sizes of 50 to 150 m^2/g have been studied. The solutes were dissolved in cyclohexane solvent. Equilibrium adsorption isotherms of the various solutes for the different aluminas were all nonlinear and well represented by Freundlich equations. Uptake experiments demonstrated that the slow step in the adsorption process was intraparticle diffusion. Effective diffusivities were determined from the uptake data by applying a pore diffusion model incorporating a Freundlich isotherm. The effective diffusivities were found to be less than those for free pore diffusion, the ratio giving a measure of the restrictive effect due to the pores. This restrictive factor was shown to decrease with increasing ratio of solute molecular diameter to alumina pore diameter. Empirical correlations between the restrictive factor and the ratio of molecular to pore diameter were obtained, which agreed well with literature results for other systems.

The effect of temperature on diffusivity was studied for alumina M using tetraphenylporphine as solute. Because of the relatively high vapor pressure of the cyclohexane solvent used previously, dodecane was employed as solvent for higher temperature studies. But difficulties were encountered due to the impurities in dodecane which adsorbed on the alumina. Though reproducible adsorption isotherms were not obtained, effective diffusivities could be calculated from the uptake data assuming a linear isotherm.

Project Status

The effect of pressure and temperature on effective diffusivity was studied during this period. Diffusion experiments were carried out with aluminas M, C and L using tetraphenylporphine and coronene as solute under different pressures in the autoclave stirred reactor. Because of impurities, dodecane and decane solvents were treated with molecular sieve 13x and an activated alumina. Removal of impurities in the solvents was still not complete after this treatment, but reproducible effective diffusivities could be calculated from uptake data. As the adsorption isotherms at elevated temperature and pressure were not obtained, effective diffusivities were calculated under the assumption of linear isotherms.

No significant effect of helium pressure on effective diffusivities of solutes was observed up to 70 atm, as shown in Table 1. Although hydrogen dissolved slightly in the cyclohexane, there was no difference in effective diffusivities to 70 atm of hydrogen, as shown in Table 2. The same results were observed regardless of the alumina or solute used. Although liquid viscosity increases with pressure and liquid bulk diffusivity decreases with increase in viscosity, this effect is very small, and diffusivities were not noticeably affected by pressure.

A question arises on the effect of solvent on the effective diffusivity. Caro et al. observed a surface blocking effect caused by solvent molecules in n-decane diffusion in zeolites.[1] They found that the diffusion rate of n-decane into the zeolite with different solvents decreased as the molecular size of the solvent increased. In the diffusion of aromatic compounds in aluminas, surface blocking effect was not observed using cyclohexane, heptane and hexane as solvents by A. Chantong.[2] He explained that pore sizes in the aluminas were larger compared to the solvent molecular sizes, and therefore, steric hindrance of blocking caused by small changes in the solvent molecular size was not operative. As shown in Table 3, using dodecane as solvent, the effective diffusivity of tetraphenylporphine was reduced to one-fourth of that in cyclohexane solvent for alumina M. The molecular size of dodecane is about twice of that of cyclohexane. Thus, a steric hindrance or blocking effect may be obtained for larger size solvents. More experimental results will be required to confirm this.

Effective diffusivities (D_e) increased with temperature as expected, as seen in Table 3. (Results reported previously[3] for these runs are incorrect due to an error in calculation.) The increase is appreciably greater than predicted by the increase in bulk diffusivities for this temperature range (D_e (60°C)/D_e (25°C) = 10, D_b (60°C)/D_b (25°C) = 1.1). This difference indicates that pore diffusion is an activated process. The activation energy for diffusion of tetraphenylporphine into alumina M in dodecane solvent was 13 kcal/mole determined from an Arrhenius plot. Satterfield and Cheng[4] reported the effective diffusivity of mesitylene in NaY was 13 x 10^{-13} cm^2/s at 0°C, and increased to 60 x 10^{-13} cm^2/s at 30°C, the activation energy for diffusion being 9 kcal/mole.

Ratios of the effective diffusivities to the free-solution diffusivities of the same cross-sectional area ($D_{b\varepsilon}$) are also shown in Table 3. The ratios of $D_e/D_{b\varepsilon}$ were all less than 1 at elevated temperature, indicating that the mobility of the solutes in alumina is less than their mobility in free-solution of the same cross-sectional area.

Future Work

Additional diffusion runs of coronene and octaethylporphine in alumina M, C and L will be carried out at higher temperature.

References

1. J. Caro, M. Burlow and J. Karger, AIChE Journal, 26, 1044 (1980).
2. A. Chantong, Ph.D. Thesis, University of Utah, Salt Lake City, Utah, 1982.
3. W. Wiser and F.E. Massoth, DOE Contract No. DE-AC01-79ET14700, Quarterly Progress Report, Salt Lake City, Utah, April - June 1982.
4. C.N. Satterfield and C.S. Cheng, Chem. Eng. Prog. Symp. Ser., 67 (117), 43 (1972).

Table 1. Effect of He pressure on effective diffusivities of tetraphenylporphine in alumina M at room temperature.

	Pressure, atm		
	0.85[a]	2.9	69
$D_e \times 10^6$, cm^2/s[b]	0.69	0.69	0.72

[a] Ref 2.

[b] Cyclohexane solvent.

Table 2. Effect of H_2 pressure on effective diffusivities of coronene in alumina C and L at room temperature.

Alumina	C				L	
Solvent	decane		cyclohexane		cyclohexane	
Pressure, atm	2.9	69	0.85[a]	69	2.9	69
$D_e \times 10^6$, cm^2/s	4.9	4.7	4.4	4.3	3.8	3.7

[a] Ref 2.

Table 3. Effect of temperature on effective diffusivities of tetraphenylporphine in alumina M.

Temp, °C	Solvent	$D_e \times 10^6$ cm²/s	$D_b \times 10^{6}$ [a] cm²/s	$\frac{D_e}{D_b\varepsilon}$
25 [b]	cyclohexane	0.66	4.4	0.21
25	dodecane	0.15	4.0	0.05
40	dodecane	0.48	4.2	0.16
60	dodecane	1.5	4.5	0.47

[a] D_b is bulk diffusivity estimated from Wilke-Chang equation.

[b] Ref 2.

Task 13

Catalyst Research and Development

Faculty Advisor: F.V. Hanson
Graduate Student: C.S. Kim

Introduction

The objectives of this project are to develop a preparation technique for a Raney type catalyst (particularly Raney iron-manganese), to establish catalyst characterization techniques, and to determine the optimum process variables for the maximum production of gasoline boiling range hydrocarbons, low molecular weight olefins and BTX via hydrogenation of carbon monoxide. A detailed discussion of the objectives was presented in a previous report.[1]

An electric heating furnace was built to prepare the Al-Fe and Al-Fe-Mn alloys. Several samples of aluminum alloys were prepared and an optimum preparation technique was developed.

A stirred-tank reactor was fabricated to activate the alloys in an aqueous solution of sodium hydroxide at different activation conditions and is working satisfactorily.

A high pressure fixed-bed reactor system has been built to determine the catalyst composition and activation variables which will optimize the catalyst activity and selectivity. The same reactor will be used for the process variable investigation.

A series of exploratory runs were made to determine a proper range of process variables for a standard catalyst screening test. The catalysts were tested at the following conditions in the fixed-bed reactor: pressure, 200 psig; space velocity, 3.0 cc/g-cat-sec; H_2/CO, 2.0; temperature, 150 to 200°C.

The carbon mass balance of CO hydrogenation in the fixed-bed unit was satisfactory (> 95%), especially at low levels of CO conversion. The Raney catalysts were more active than the precipitated catalyst in terms of CO conversion. Among the Raney catalysts, high temperatures produced more active catalysts than low temperatures.

A thermogravimetric analysis technique was used to determine an optimum reduction temperature. The optimum temperature was 400°C for precipitated catalysts and 375°C for Raney catalysts. All the catalysts were reduced under a hydrogen gas stream at the optimum temperature for 5 hours, just prior to the activity test in the fixed-bed.

Other catalyst characterization work has been done such as BET surface area and X-ray diffraction.

Project Status

The standard activity tests of the catalysts were reported in the previous report. A duplication run for the Raney Fe-Mn (50°C, alloy addition) was made, since the activity test data indicated the catalyst activity did not reach a steady-state. Table 1 lists the results along with data of two other catalysts prepared at different temperatures for comparison.

The catalytic activity of Raney Fe-Mn, prepared at 90°C, was higher than the other two catalysts prepared at lower temperatures. The other two catalysts showed catalytic activity similar to each other.

The Raney Fe-Mn catalyst (50°C, alloy addition) was tested at a high space velocity and the results are shown in Table 2. When comparing the data in Tables 1 and 2 of Raney Fe-Mn catalyst (50°C), there was no significant change in product distributions, while the C_2-C_4 O/P ratio increased as the space velocity increased.

Another Raney Fe-Mn catalyst (50°C, caustic addition) was prepared from a different batch of alloy samples to check the reproducibility of the catalyst preparation technique and the alloy preparation technique. Figure 1 shows the aluminum % leaching curves of two catalysts prepared at the same conditions. The final aluminum % leaching data agreed well within experimental errors. Table 3 shows the results of the activity tests of the same catalysts. The catalytic acitvity, in terms of CO % conversion, also agreed, which again confirms the reproducibility of the catalyst preparation technique as well as catalyst testing procedures.

For iron catalysts, a first-order empirical Equation (1)[2] has been successfully used to determine kinetic parameters as follows:

$$-\ln (1-x) = \frac{A}{S} \exp (-E/RT) \qquad (1)$$

where A is the rate constant, E is the activation energy, x is CO conversion, and S is the space velocity. By rearranging Equation (1)

$$\ln (-\epsilon \ln(1-x) = \ln k = \ln A - E/RT \qquad (2)$$

The activity test data were used to determine the activation energy and the pre-exponential factor of each catalyst for CO hydrogenation using Equation (2). Figure 2 shows an Arrehnius plot for the Raney Fe-Mn catalyst (50°, alloy addition). The kinetic parameters of other catalysts were obtained and are listed in Table 2. Generally, the range of the activation energy agreed with the values of the iron catalysts reported in the literature.[2,3]

Since the activation energy of the catalysts were different from each other, the pre-exponential factor could be used as a sole criterion for comparing catalytic activity. A better comparison of catalytic activity can be made by comparing the turn-over number of each catalyst for CO hydrogenation. This can be obtained from selective chemisorption which gives the number of active sites on the catalyst surface.

The elemental composition of some catalysts was determined by Atomic Absorption technique. Table 5 lists the results. There is good agreement

between the values from AA and the measurement of aluminum % leaching during the activation of the alloys.

Future Work

The elemental analysis of catalysts will be completed using the same technique. The particle size of the catalyst srystallite will be determined using the X-ray line-broadening technique. The particle size data will be utilized in connection with the BET surface area to explain the differences in catalytic activity between different catalysts.

The Raney Fe-Mn catalyst (90°C, alloy addition) will be used for the process variable study. This work will be carried out by another graduate student for his master thesis. The chemisorption technique will be utilized to determine the turn-over frequency of each catalyst for CO hydrogenation as soon as the apparatus is available. The construction of the apparatus is underway.

References

1. W.H. Wiser, F.V. Hanson and C.S. Kim, DOE Contract No. DE-AC01-79ET 14700, Quarterly Progress Report, Salt Lake City, Utah, Oct-Dec 1979.

2. R.B. Anderson, "Catalysis," Vol. 4, Reinhold Publishing Co., New York, New York, 1961.

3. M.A. Vannice, J. Catal., 37, 449 (1975).

Table 1. Fixed-bed run of Raney Fe-Mn catalyst. Pressure, 200 psig; H_2/CO, 2.0; Space Velocity, 3.0 cc/g sec. Catalyst prepared at 50°C by alloy addition method.

Leaching Temp, °C	Reaction Temp, °C	CO Conv % (output)	Hydrocarbon Selectivity %				CO_2 %	C_2-C_4 O/P
			C_1	C_2-C_4	C_5^+	ROH		
50	150	0.6	42.9	41.5	15.7	0	10.6	1.93
	160	1.2	26.5	49.3	24.2	0	16.6	1.87
	170	2.7	24.6	49.0	26.1	0.4	24.6	1.85
	180	5.0	23.2	50.3	26.1	0.3	33.6	1.90
30	150	0.7	47.2	41.5	10.6	0.7	5.9	1.78
	160	1.4	39.7	41.9	17.6	0.9	7.7	1.68
	170	2.8	34.4	45.4	19.5	0.7	11.8	1.64
	180	4.6	31.7	48.0	19.9	0.4	17.2	1.69
	190	8.6	27.6	49.2	21.8	1.3	25.7	1.87
	200	12.9	25.5	50.6	22.8	1.0	33.2	2.14
90	150	1.2	33.7	34.3	32.0	0	7.6	2.39
	160	1.6	32.7	44.1	23.1	0	12.0	2.51
	170	2.9	28.2	49.0	22.5	0.4	19.5	2.58
	180	6.1	26.9	47.1	25.1	1.0	26.3	2.42
	190	13.0	23.2	49.1	26.7	0.9	35.4	2.17
	200	23.6	21.9	52.0	25.2	0.9	42.9	2.49

Table 2. Fixed-bed run of Raney Fe-Mn catalyst. Pressure, 200 psig; H_2/CO, 2.0. Catalyst prepared at 50°C by alloy addition.

Space Velocity (cc/g sec)	Reaction Temp, °C	CO Conv % (output)	Hydrocarbon Selectivity % C_1	C_2-C_4	C_5^+	ROH	CO_2%	C_2-C_4 O/P
9.8	170	0.9	27.5	51.0	21.0	0.45	16.7	2.03
	180	2.1	24.9	50.6	23.8	0.7	23.4	1.99
	190	3.7	24.0	51.3	24.1	0.48	30.3	1.97
	200	6.6	22.2	50.3	26.7	0.80	37.0	2.08
19.7	200	3.6	23.5	51.6	24.9	0.02	29.8	2.43

Table 3. Fixed-bed run of Raney Fe-Mn catalyst. Pressure, 200 psig; H_2/CO, 2.0; Space Velocity, 3.0 cc/g sec. Catalyst prepared at 50°C by caustic addition.

Reaction Temp, °C	CO Conv % (output)	Hydrocarbon Selectivity % C_1	C_2-C_4	C_5^+	ROH	CO_2%	C_2-C_4 O/P
150	0.9 (0.7)	30.8 (28.9)	50.8 (45.2)	17.4 (16.3)	0.94 (0.58)	5.5 (5.9)	1.83 (2.11)
160	1.9 (1.6)	28.2 (25.7)	49.8 (50.2)	21.2 (22.9)	0.74 (1.2)	6.7 (6.7)	1.72 (2.00)
170	3.8 (3.1)	27.7 (25.6)	50.2 (50.5)	21.6 (22.7)	0.52 (1.2)	10.1 (10.1)	1.69 (1.90)
180	6.5 (6.4)	26.2 (29.4)	49.6 (46.4)	20.9 (20.0)	3.2 (4.3)	14.0 (14.2)	1.75 (1.84)

( ) Numbers in parenthesis are from a catalyst prepared at the same conditions but made from a different batch of alloy samples.

Table 4. Kinetic Parameters.

Type	Catalyst Preparation Method, Temp (°C)	E_a (Kcal/mol) Activation Energy	A Pre-exponential Factor
Fe	Alloy Addition		
	25	27.8	8.1×10^{12}
	50	31.9	9.6×10^{14}
	90	27.4	5.9×10^{12}
	90[a]	23.5	7.0×10^{10}
	Caustic Addition		
	25	27.2	4.5×10^{12}
	50	29.6	7.8×10^{13}
	90	29.8	9.8×10^{13}
	10% solution 90[b]	24.7	1.2×10^{11}
	Precipitation	26.0	6.9×10^{11}
Fe-Mn	Alloy Addition		
	30	23.8	4.7×10^{10}
	50	28.0	5.3×10^{12}
	50[c]	27.7	4.5×10^{12}
	50[b]	30.7	9.1×10^{13}
	90	29.3	2.6×10^{13}
	Caustic Addition		
	50	26.1	8.0×10^{11}
	50	28.4	9.9×10^{12}
	90	26.8	1.9×10^{12}
	Coprecipitation	29.0	5.7×10^{12}

[a]Alloy from Alpha Products.

[b]10% NaOH solution used for preparation.

[c]From high space velocity run. (SV = 10, 20).

Table 5. Elemental Composition Analysis.

Sample Type	H_2 Evolution[a]			Atomic Absorption		
	Al	Fe	Mn	Al	Fe	Mn
Al-Fe-Mn Alloy (59/38/3 wt %)	--	--	--	59.2	37.7	3.1
Al-Fe-Mn Alloy[b] (59/38/3)	--	--	--	58.8	38.1	3.1
Coprecipitated Fe-Mn	--	--	--	--		
Raney Fe-Mn 90°C, Alloy Addition	0	92.7	7.3	2.8	92.5	4.7
Raney Fe-Mn 50°C, Alloy Addition	12.0	81.5	6.4	2.8	92.0	5.2
Raney Fe-Mn 30°C, Alloy Addition	26.8	67.8	5.4	29.9	66.0	4.1
Raney Fe-Mn 50°C, 10% Solution	38.3	57.2	4.5	34.1	61.7	4.2

[a]The elemental composition was estimated from aluminum % leaching, which was measured by H_2 evolution. It was assumed that Fe and Mn were not lost during activation.

[b]Alloy from Alpha Products.

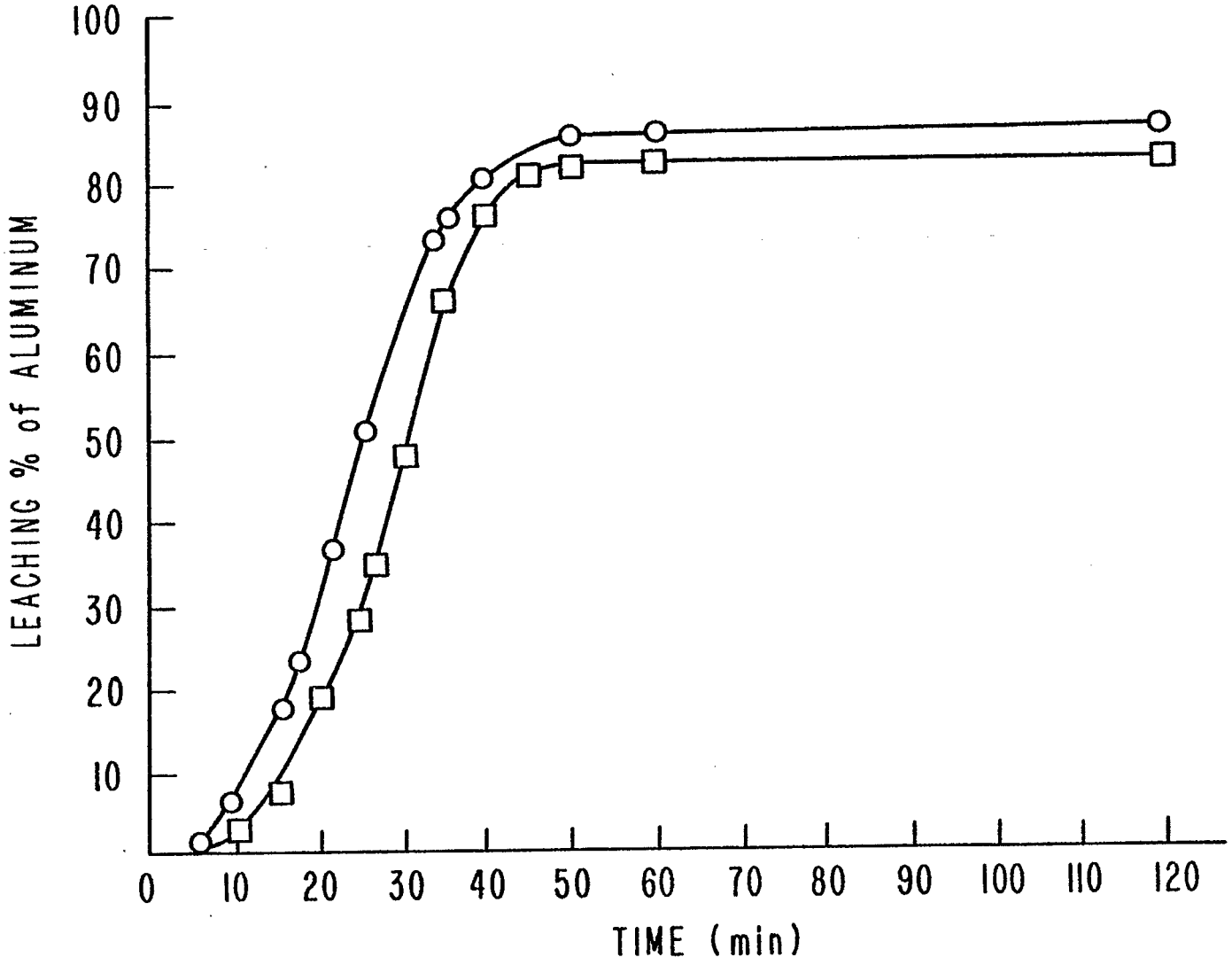

Figure 1. Leaching % Aluminum vs. Time. Catalyst prepared at 50°C by caustic addition.

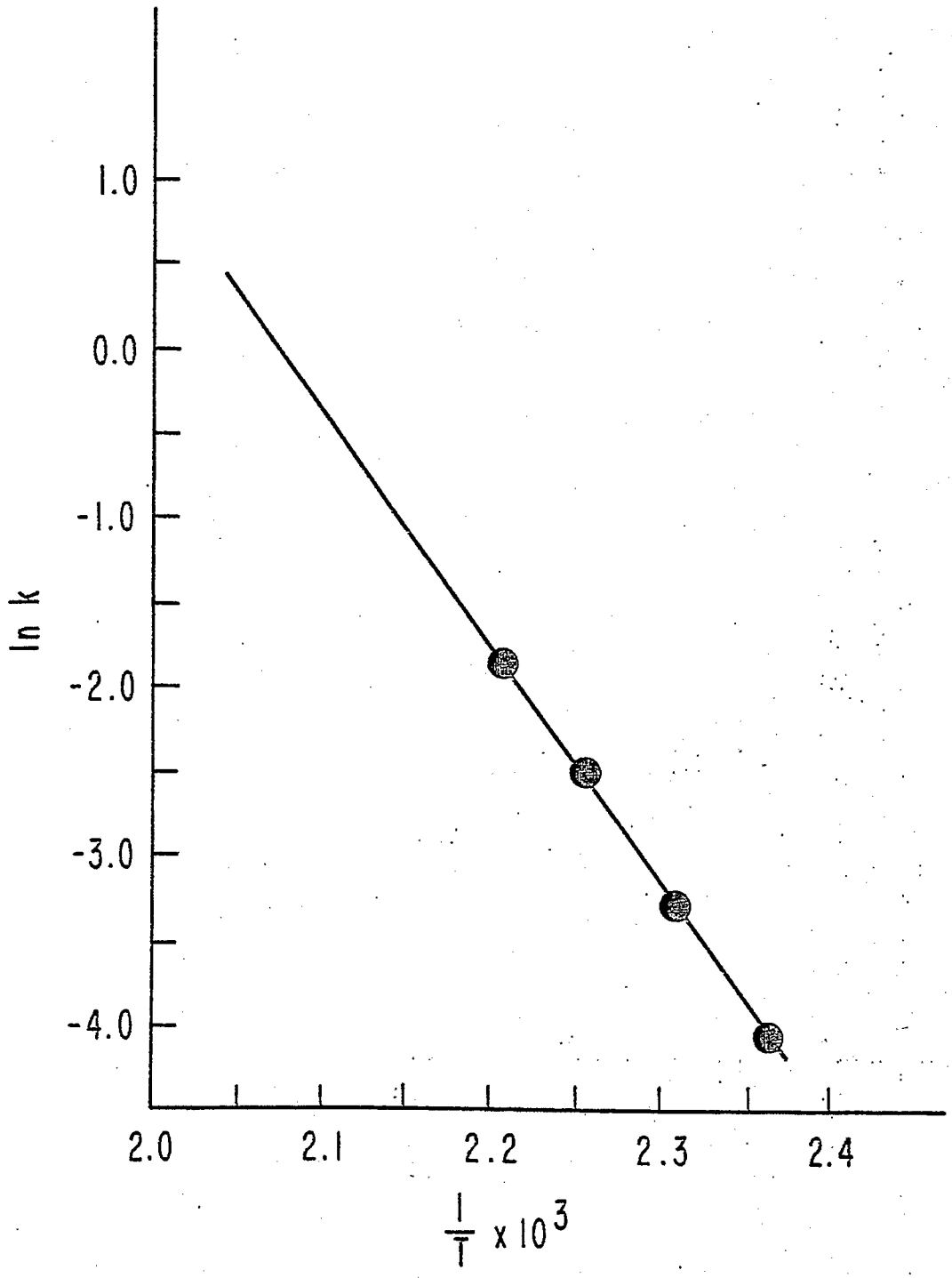

Figure 2. Arrehnius plot for a Raney Fe-Mn catalyst (50°C, alloy addition).

Task 14

Characterization of Catalysts and Mechanistic Studies

Carbon Monoxide Hydrogenation in Pseudo Slurry Reactor over Iron-Manganese Catalyst

Faculty Advisor: F.V. Hanson
F.E. Massoth
Graduate Student: Wei-Ping Tai

Introduction

The conventional fixed-bed reactor has been used in this department to test the catalytic activities of catalysts with different compositions. Because of the highly exothermic nature of the carbon monoxide hydrogenation reaction, conversion level in the fixed-bed reactor is always kept below 10 percent to guarantee reliable data. The "hot spot" occurring in the fixed-bed operation not only decreases the accuracy of kinetic data, but also accelerates undesired reactions, i.e., the Boudouard reaction (disproportionation of CO to CO_2 and carbon) with concomitant fouling of the catalyst and shifting of the selectivity in the direction of methane. The pseudo slurry reactor has been introduced to minimize the temperature rise in the reactor and thereby maintain the catalyst activity and selectivity. The objective of this investigation is to compare the performance of the traditional fixed-bed reactor with the pseudo slurry reactor.

Project Status

It has been reported in the previous report that temperature rise in a dense fixed-bed reactor is greater than that in a diluted fixed-bed reactor. A heat transfer media in a diluted fixed-bed reactor helps prevent a temperature rise inside the reactor. n-Hexadecane is a better heat transfer liquid than Mobil #1 base stock MCP 151 without any additives because the former produces more C_2-C_4 hydrocarbons and less carbon dioxide. In this investigation, the effect of process variables such as temperature, pressure, H_2/CO ratio and space velocity were tested in a diluted bed pseudo slurry reactor with n-hexadecane as the heat transfer liquid. Twenty grams of 20/32 mesh catalyst pellets were mixed with four volumes of Denstone 57 ceramic particles (20/32 mesh). The catalyst was pretreated in-situ with hydrogen at 673°K at ambient pressure for 20 hours. The catalyst was further stabilized by 1) reacting at 463°K at ambient pressure 16 hours with a H_2/CO = 2/1 and a space velocity of 0.4 cm^3/sec g-cat, 2) reacting at 473°K at the desired reaction pressure for four hours with a H_2/CO = 2/1 and a space velocity = 0.4 cm^3/sec g-cat and 3) reacting with the same conditions as in the previous step except that the heat transfer liquid was introduced at a rate of 0.103 cm^3/sec. The operation procedure has been explained in the previous report. n-Hexadecane circulating rate was kept at 0.103 cm^3/sec for all runs.

Figure 1 shows the effect of temperature on CO conversion in a diluted bed pseudo slurry reactor. Higher CO conversion occurs with an increase in reaction temperature. Total pressure also affects CO conversion as shown in

Figure1. Higher pressure means longer contact time and causes greater CO conversion. Temperature effect on carbon dioxide and C_2-C_4 hydrocarbon selectivities are shown in Figures 2 and 3. More carbon dioxide and less C_2-C_4 hydrocarbons are produced at higher reaction temperatures. At the same reaction temperature, lower pressure causes higher CO_2 selectivity and lower C_2-C_4 hydrocarbon production. The temperature effect on the olefin/paraffin ratio of C_2-C_4 hydrocarbons at different reaction pressures are shown Figures 4 to 8. The olefin/paraffin ratios of C_3, C_4 and C_2-C_4 hydrocarbons always increase as the temperature increases. The temperature effect on the olefin/paraffin ratio of C_2 hydrocarbons is not clear at low reaction pressures.

The effect of space velocity on CO conversion is shown in Figure 9. Higher space velocity means shorter contact time between reactant gas and catalyst, and it causes lower CO conversion. The pressure effect on CO conversion is also shown in Figure 9. Space velocity does have a significant effect on carbon dioxide selectivity. Figure 10 shows the carbon dioxide selectivity versus space velocity at different reaction pressures. Higher space velocity produces less carbon dioxide. The pressure effect on carbon dioxide selectivity is also observed in Figure 10. At the same reaction temperature and space velocity, less carbon dioxide is produced at higher pressure. Detailed product selectivities at different reaction pressures are shown in Figures 11 to 15. Generally speaking, as the space velocity increases, methane and C_2-C_4 hydrocarbon selectivities increase, but the increasing trend slows after the space velocity is higher than 1.5. Varying the space velocity between 0.5 to 2 has little effect on the combined C_2-C_4 olefin/paraffin ratiosat different reaction pressures as shown in Figures 16 to 20. There are some minor changes on the olefin/paraffin ratiosin C_2, C_3 and C_4 hydrocarbons as the space velocity changes. The effect of increasing space velocity above 2.0 has also been investigated. Figures 21 and 22 show the effect of space velocity on the activity and selectivity of carbon monoxide hydrogenation in the diluted bed pseudo slurry reactor. The trends of product selectivities and the olefin/paraffin ratio are similar.

Another important process variable for carbon monoxide hydrogenation is the H_2/CO ratio of the reactant gas. The reactant gas with a H_2/CO ratio from 0.5 to 4 has been investigated using a Union Carbide gas flowcontroller. Figure 23 shows the effect of the H_2/CO ratio on CO conversion at different reaction pressures. The CO conversion is proportional to the H_2CO ratio in the reactant gas. The effect of the H_2/CO ratio on the carbon dioxide selectivity is significant as shown in Figure 24. It shows that the carbon dioxide selectivity drops quickly as the reactant gas H_2/CO ratio increases from 0.5 to 2. For a H_2/CO ratio greater than 2, the carbon dioxide selectivity continues to drop at a slower rate. Figure 24 confirms that with other conditions constant, a higher carbon dioxide selectivity is achieved at a lower reaction pressure. Product selectivities of methane, carbon dioxide, and C_2-C_4 hydrocarbons versus a H_2/CO ratio at different reaction pressures are shown in Figures 25 to 29. Methane production increases linearly as the H_2/CO ratio of the reactant gas increases. Hydrocarbons in the C_2-C_4 range increase rapidly as the H_2/CO ratio increases from 0.5 to 2. For most runs the C_2-C_4 hydrocarbons selectivity reaches a maximum H_2/CO ratio of about three. The H_2/CO ratio of the reactant gas greatly effects the olefin/paraffin ratio of C_2-C_4 hydrocarbons especially at lower reaction pressures.

The olefin/paraffin ratios of C_2, C_3, C_4 and C_2-C_4 hydrocarbons drop unanimously when the H_2/CO ratio of the reactant increases from 0.5 to 4 as shown in Figures 30 to 34. The olefin/paraffin ratios of C_2 hydrocarbons are more sensitive to the H_2/CO ratio of the reactant than those of C_3 and C_4 hydrocarbons.

Future Work

The Ph.D. Dissertation of Mr. W.P. Tai is being written and a final copy will be submitted when completed.

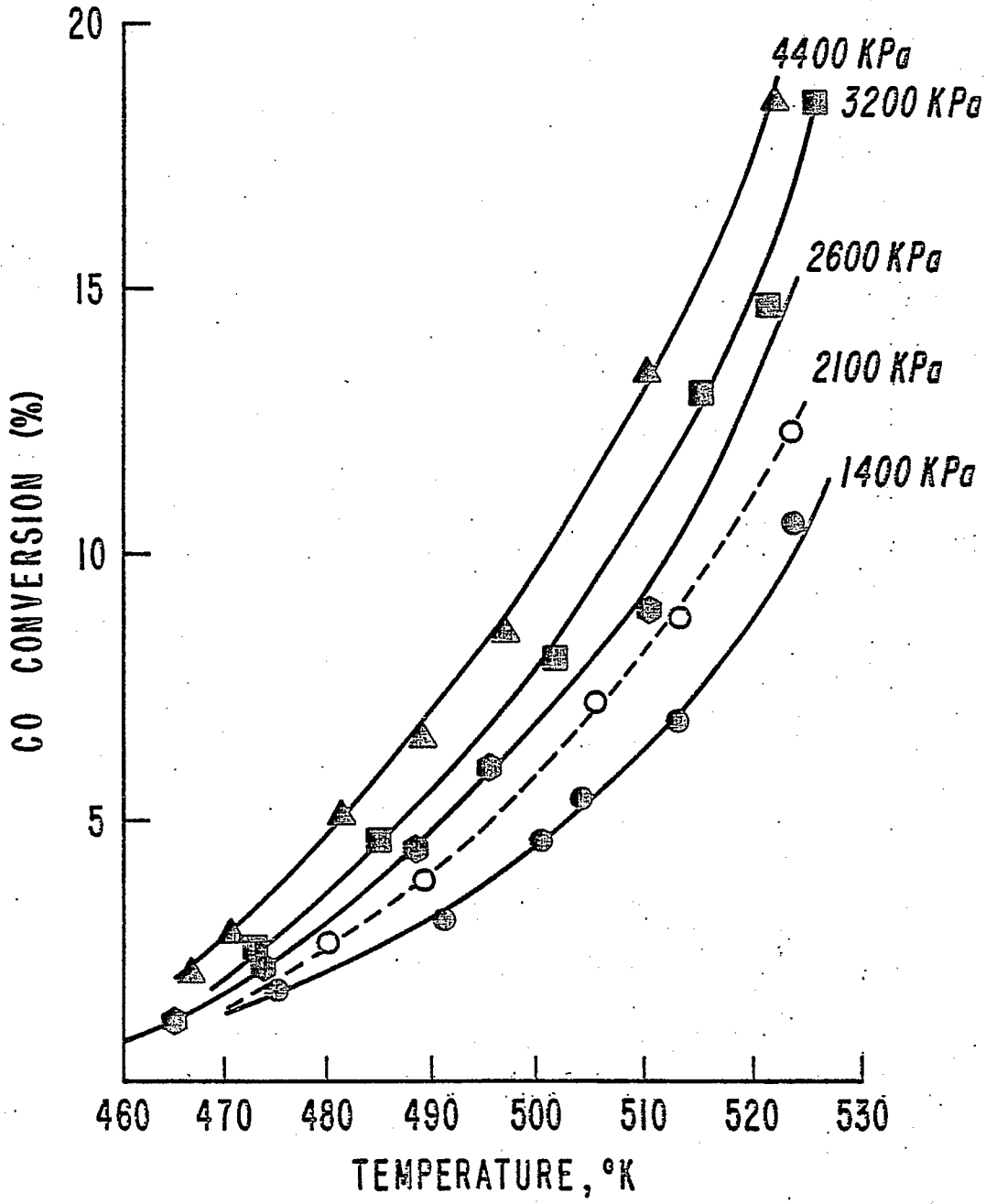

Figure 1. Effect of temperature on CO conversion in diluted bed pseudo slurry reactor. Pressure, 1400-4400 KPa; H_2/CO, 2/1; Space Velocity, 1 cm^3/sec g cat.

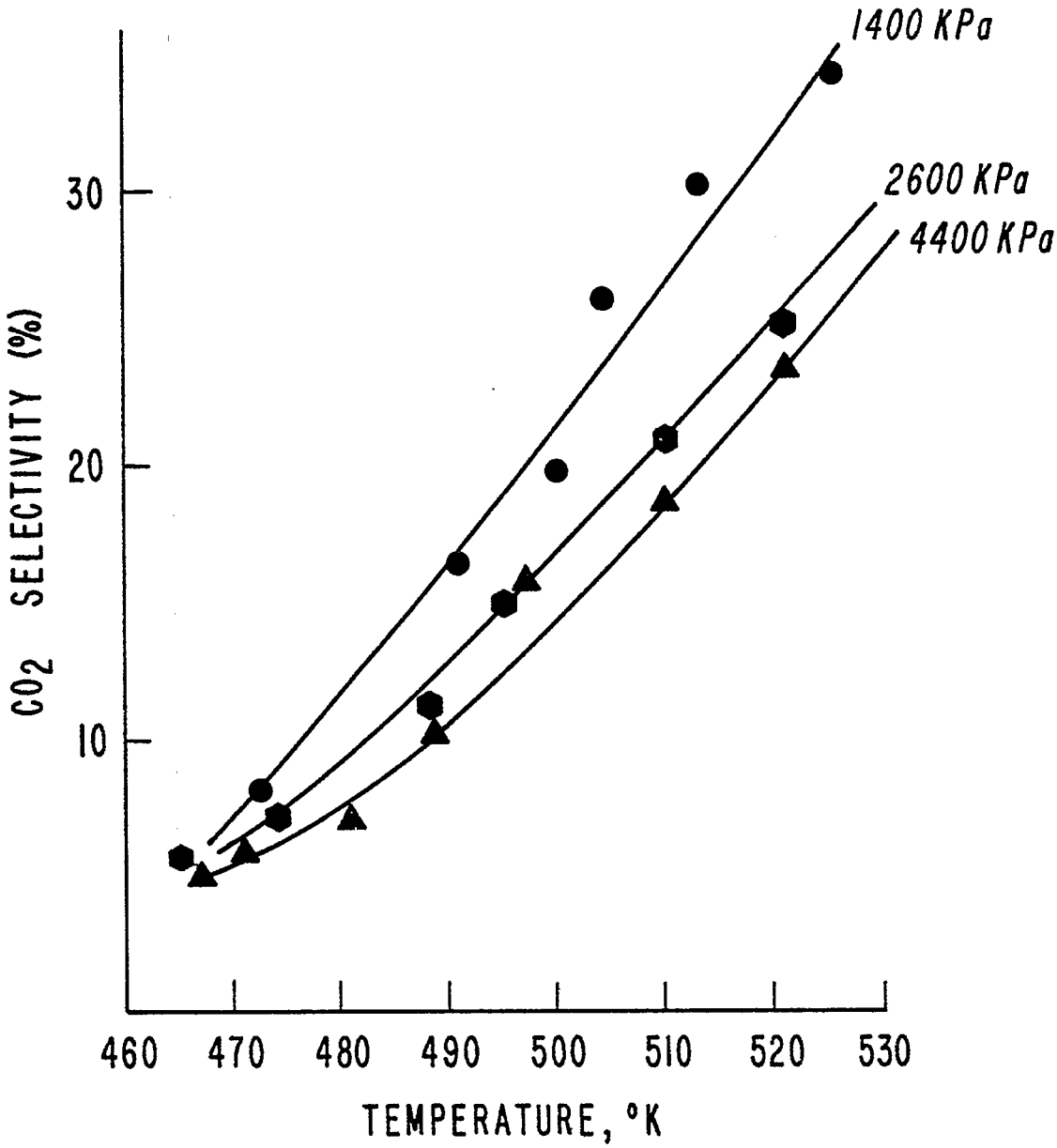

Figure 2. Effect of temperature on carbon dioxide selectivity of carbon monoxide hydrogenation in diluted bed pseudo slurry reactor. Pressure, 1400, 2600 and 4400 KPa; H_2/CO, 2: Space Velocity, 1 cm^3/sec g cat.

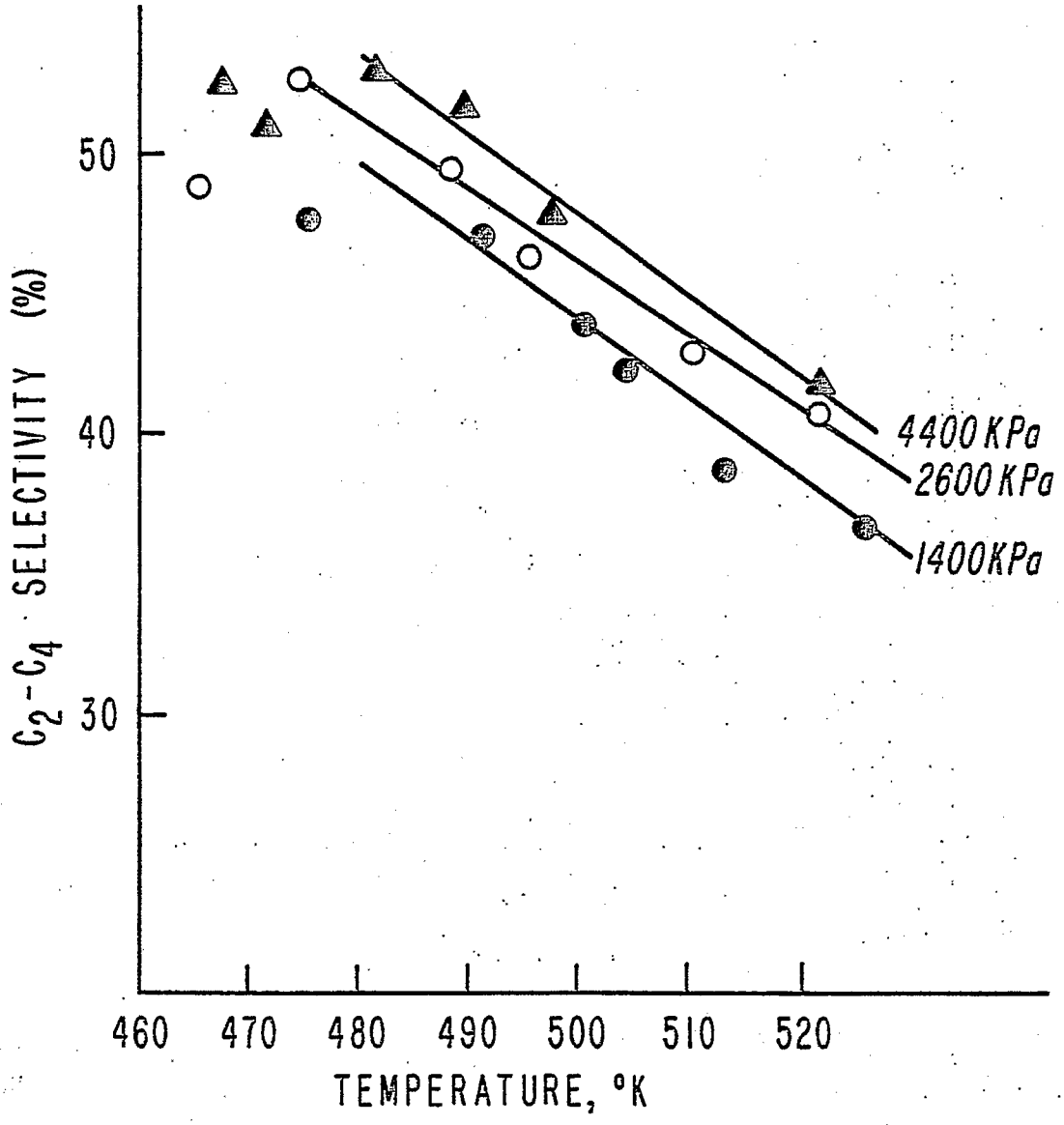

Figure 3. Effect of Temperature on C_2-C_4 hydrocarbons selectivity in diluted bed pseudo slurry reactor. Pressure, 1400, 2600 and 4400 KPa; H_2/CO, 2/1 and Space Velocity, 1 cm^3/sec g cat.

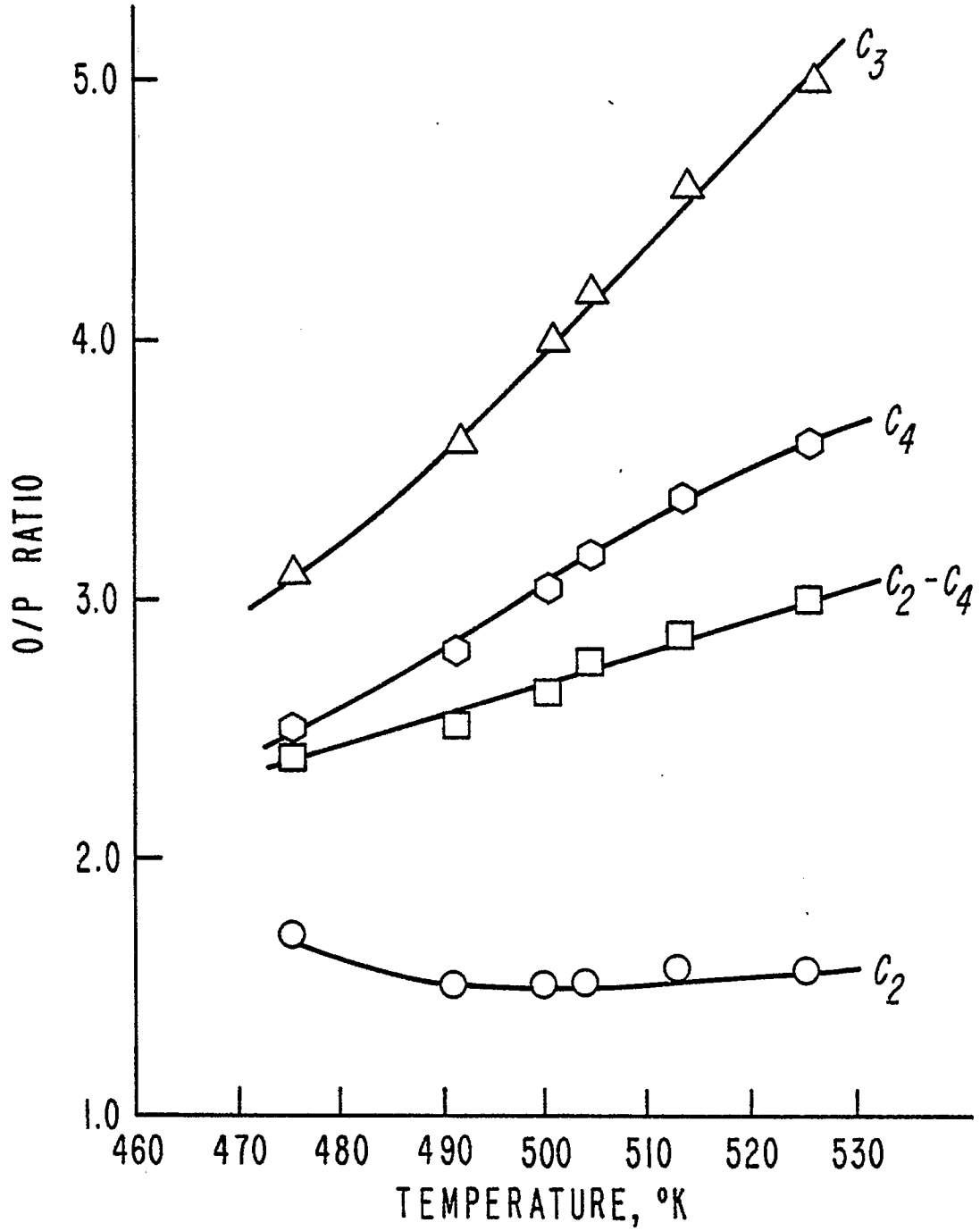

Figure 4. Effect of temperature on olefin/paraffin ratio of C_2-C_4 hydrocarbons in diluted bed pseudo slurry reactor. Pressure, 1400 KPa; H_2/CO, 2/1 and Space Velocity, 1 cm^3/sec g cat.

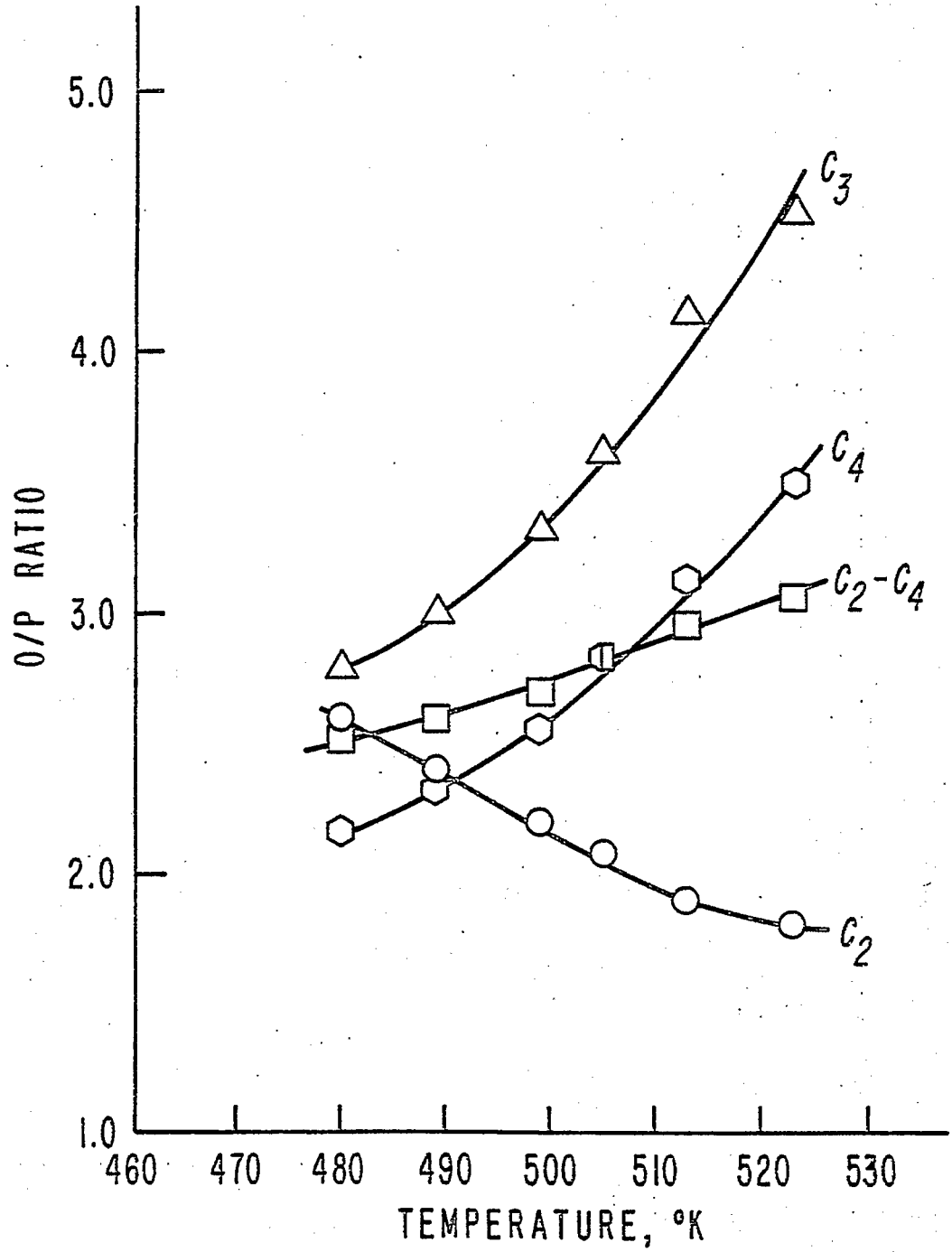

Figure 5. Effect of temperature on olefin/paraffin ratio of C_2-C_4 hydrocarbons in diluted bed pseudo slurry reactor. Pressure, 2000 KPa; H_2/CO, 2/1 and Space Velocity, 1 cm^3/sec g cat.

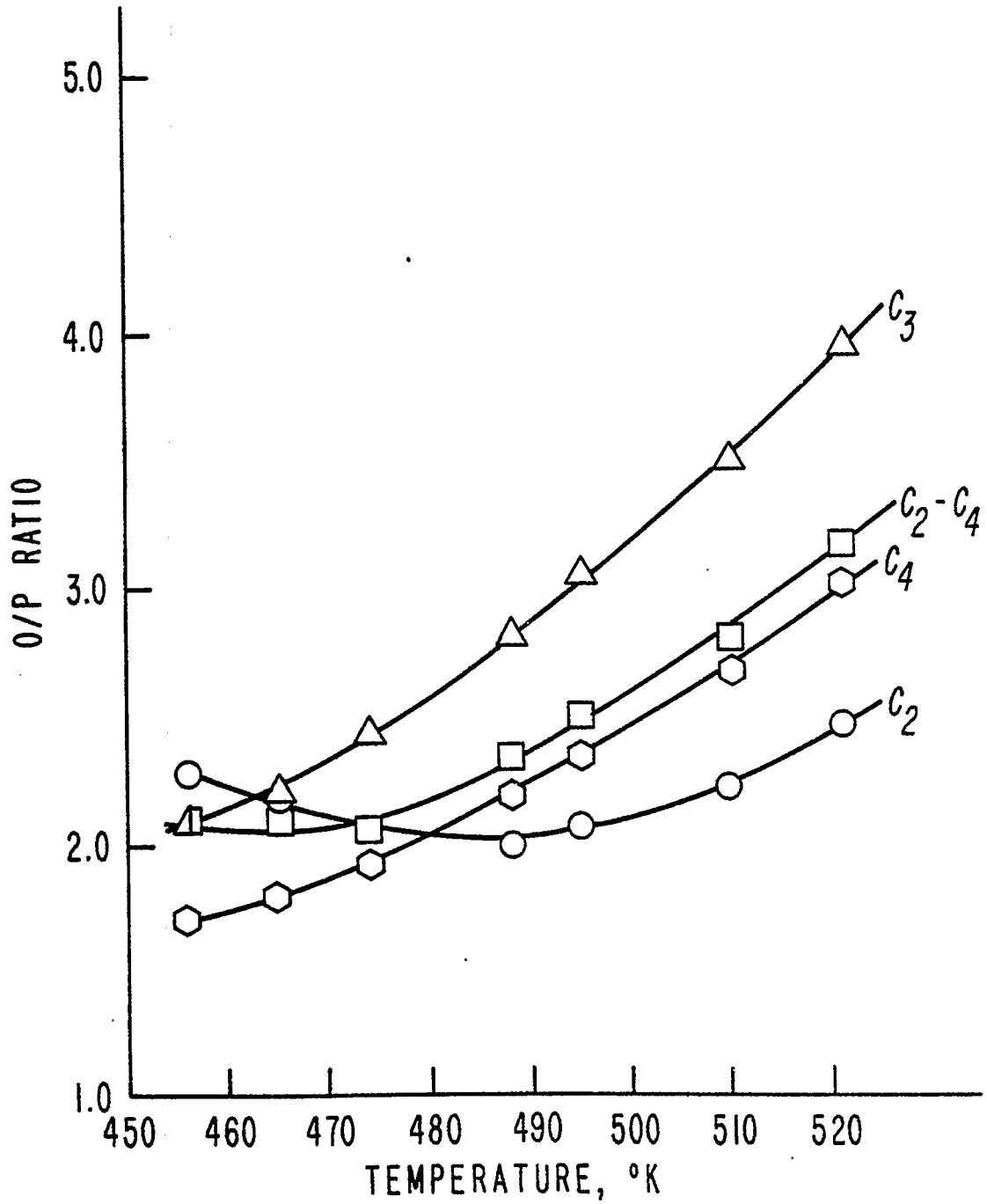

Figure 6. Effect of temperature on olefin/paraffin ratio of C_2-C_4 hydrocarbons in diluted bed pseudo slurry reactor. Pressure, 2600 KPa; H_2/CO, 2/1 and Space Velocity, 1 cm^3/sec g cat.

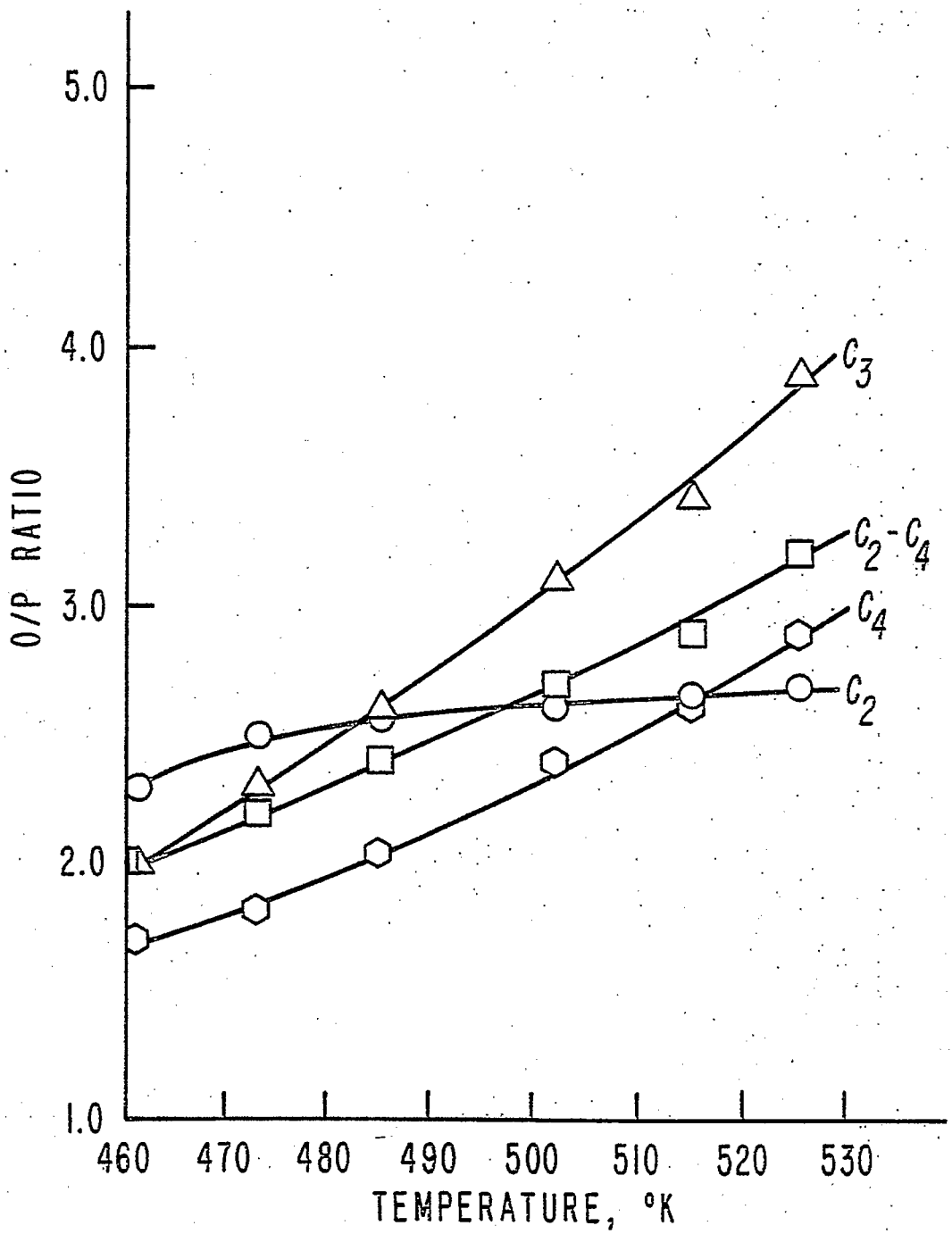

Figure 7. Effect of temperature on olefin/paraffin ratio of C_2-C_4 hydrocarbons in diluted bed pseudo slurry reactor. Pressure, 3200 KPa; H_2/CO, 2/1 and Space Velocity, 1 cm^3/sec g cat.

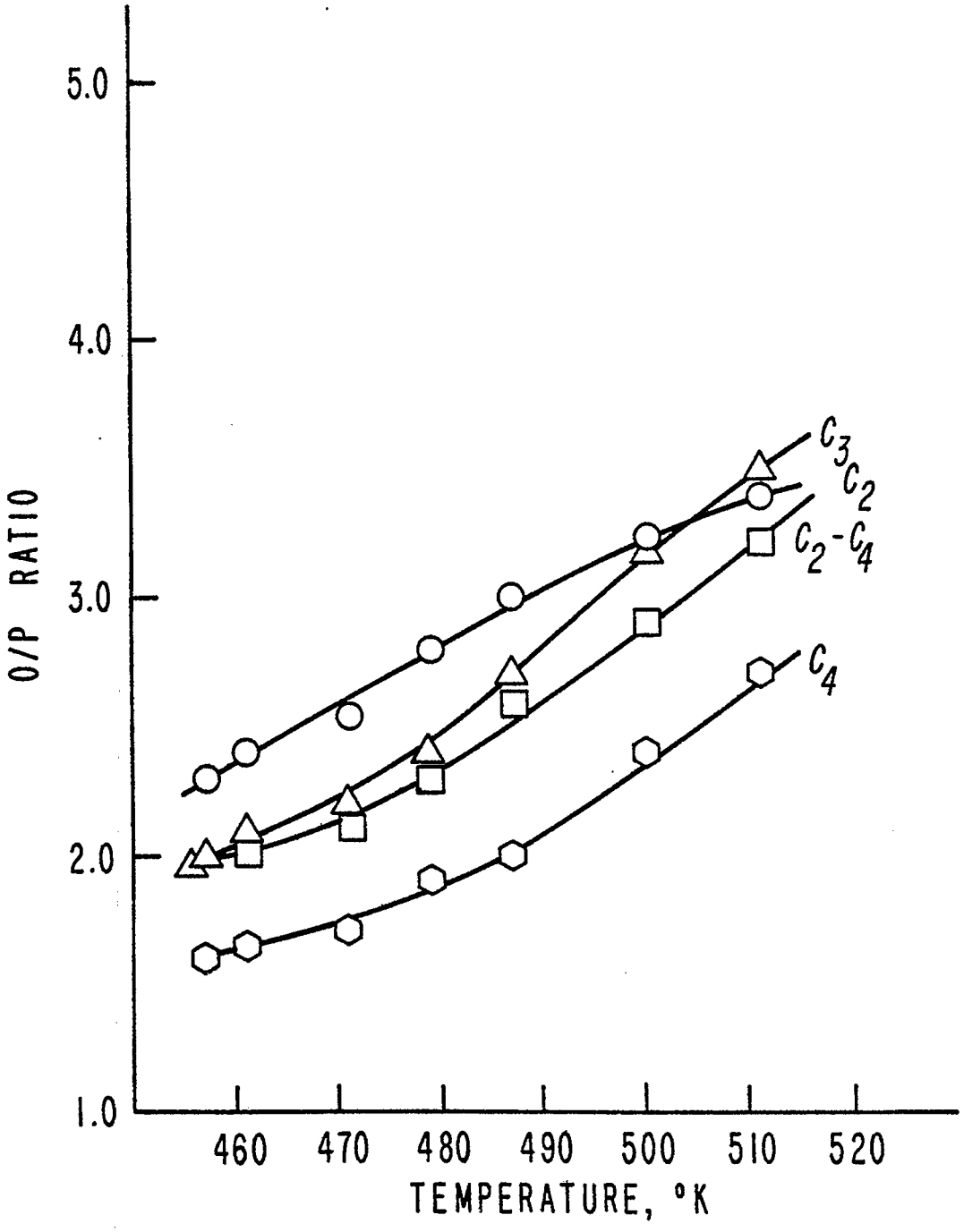

Figure 8. Effect of temperature on olefin/paraffin ratio of C_2-C_4 hydrocarbons in diluted bed pseudo slurry reactor. Pressure, 4400 KPa: H_2/CO, 2/1 and Space Velocity, 1 cm^3/sec g cat.

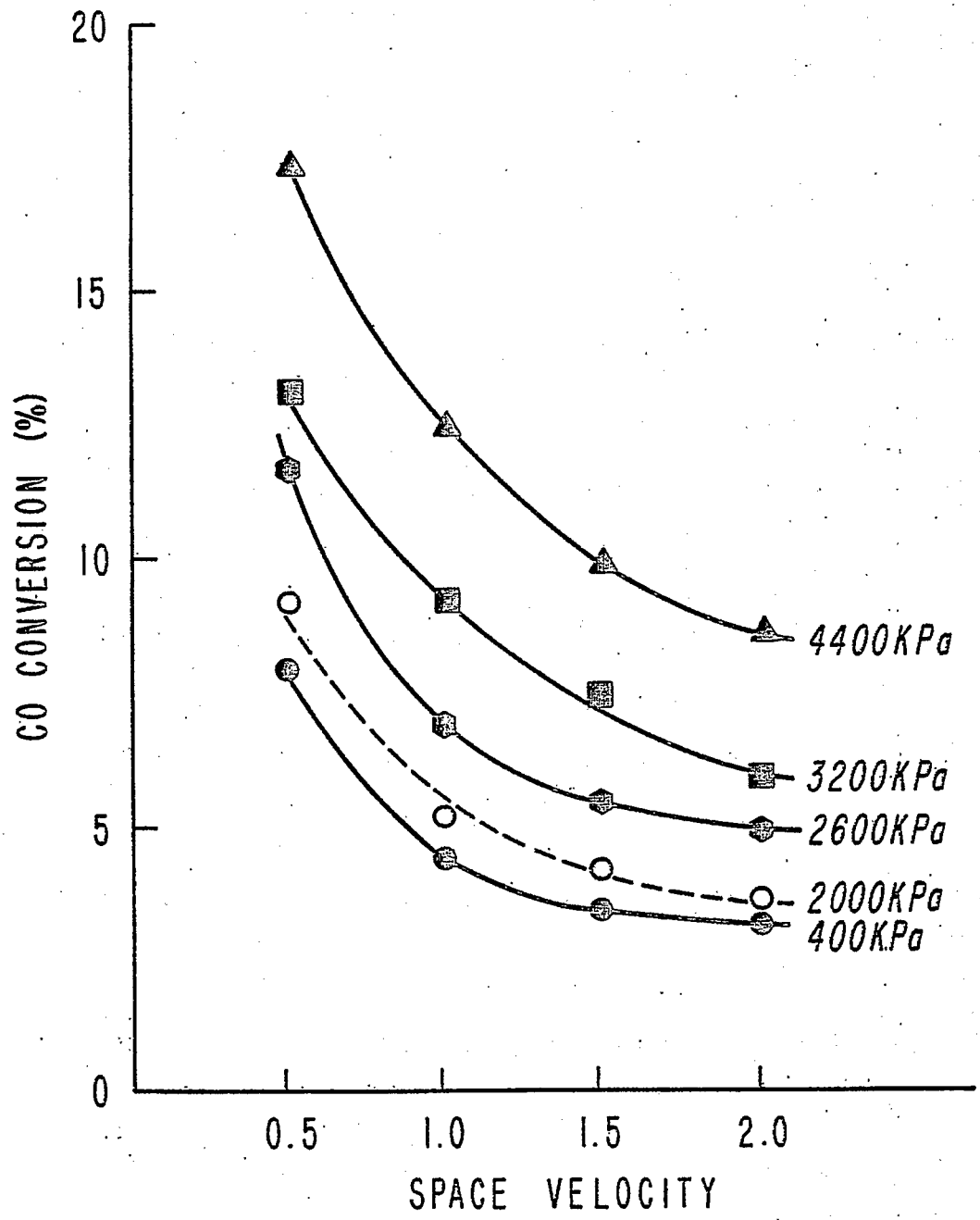

Figure 9. Effect of space velocity on CO conversion for carbon monoxide in diluted bed pseudo slurry reactor. Temperature, 503°K; Pressure, 1400-4400 KPa and H_2/CO, 2/1.

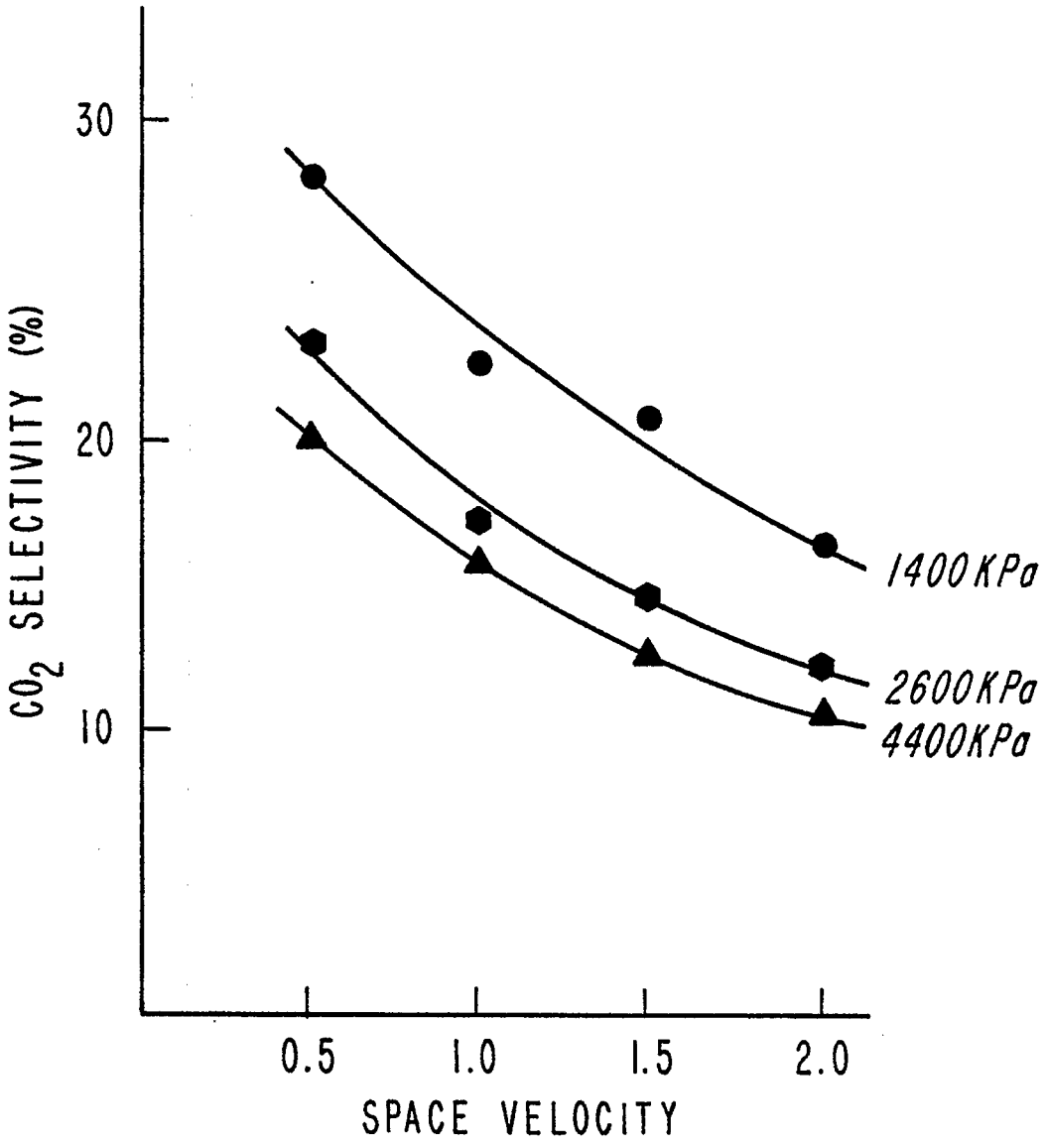

Figure 10. Effect of space velocity on CO_2 selectivity for carbon monoxide hydrogenation in diluted bed pseudo slurry reactor. Pressure, 1400, 2500 and 4400 KPa; H_2/CO, 2/1 and Temperature, 503°K.

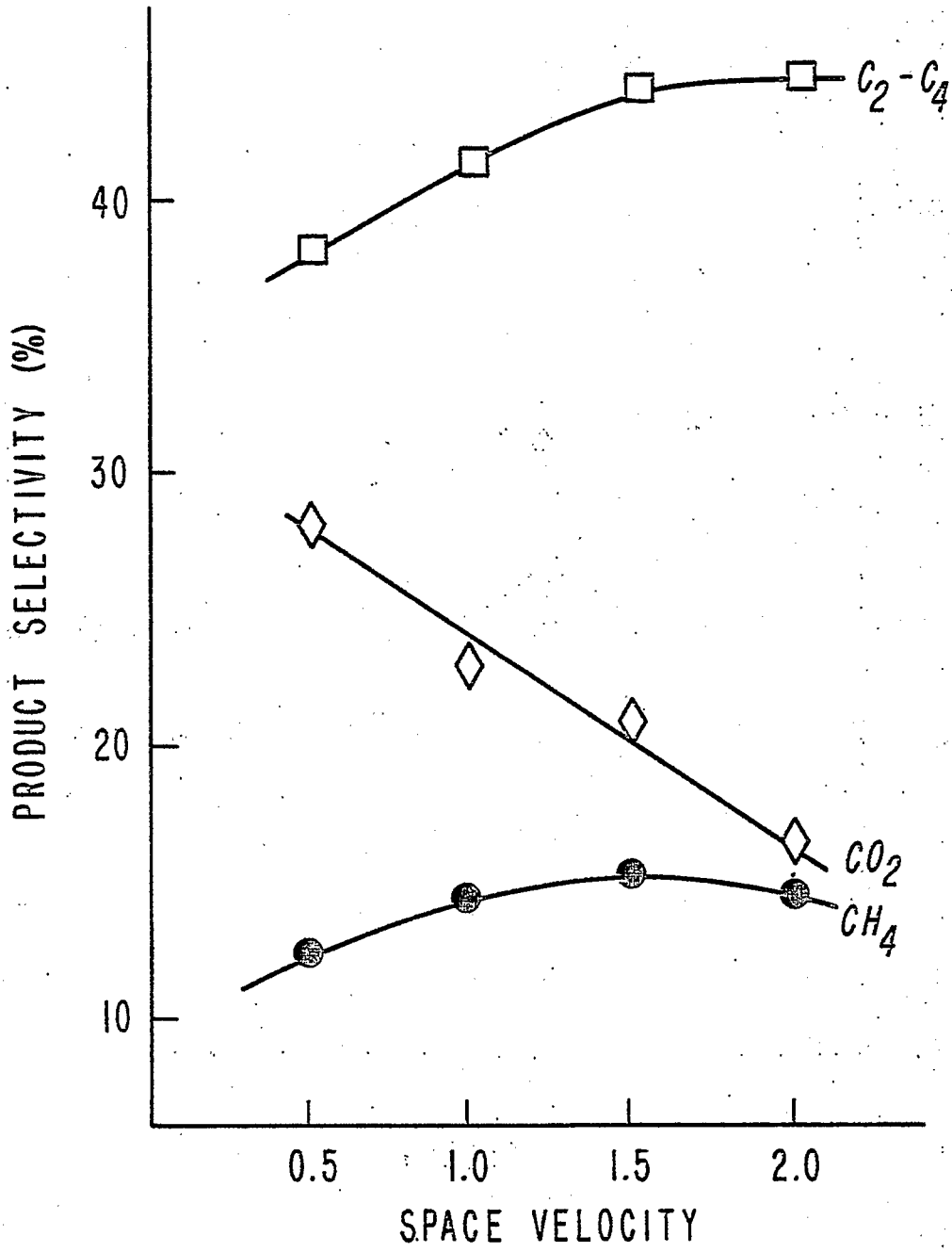

Figure 11. Effect of space velocity on product selectivities for carbon monoxide hydrogenation in diluted bed pseudo slurry reactor. Temperature, 503°K; Pressure, 1400 KPa and H_2/CO, 2/1.

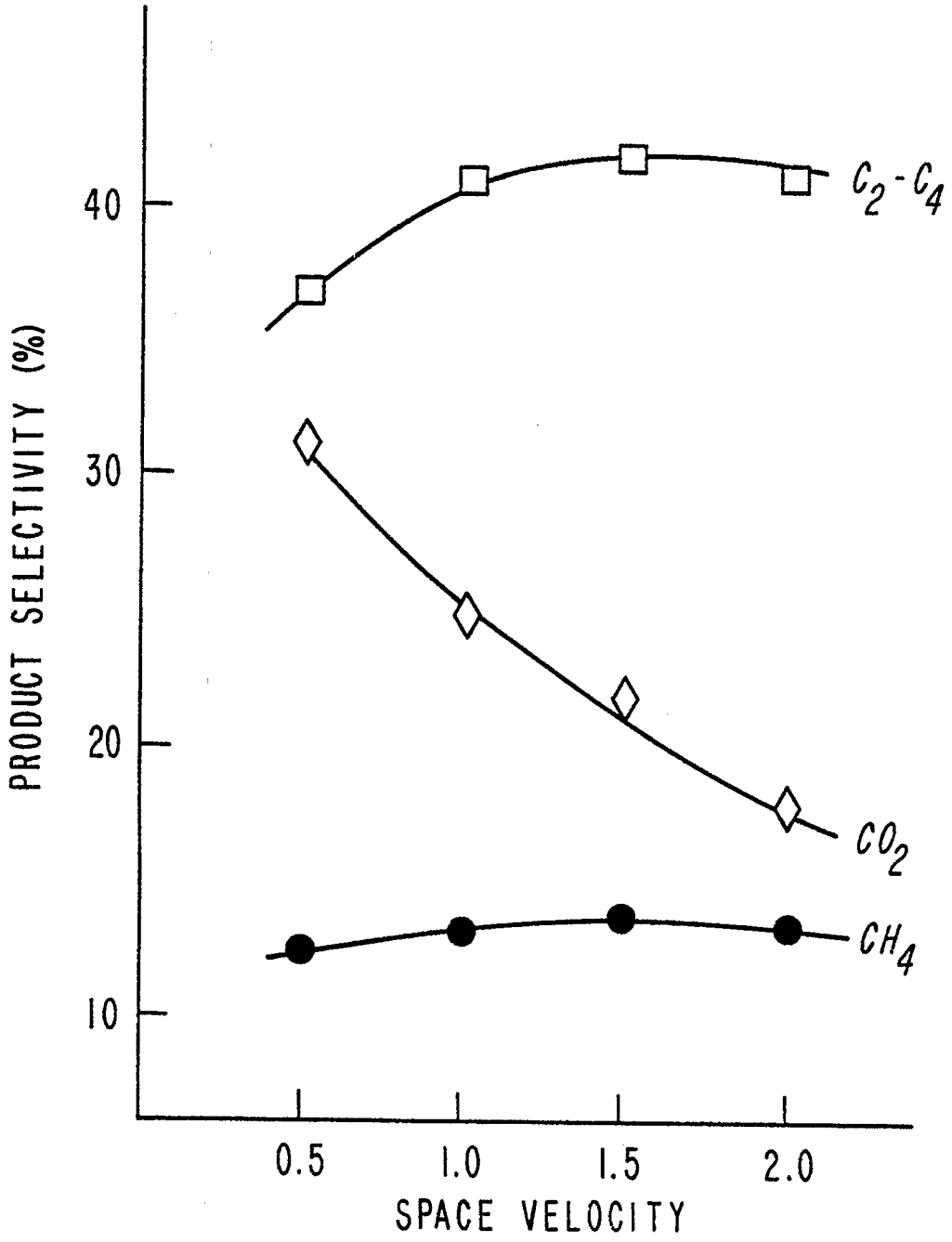

Figure 12. Effect of space velocity on product selecitivities for carbon monoxide hydrogenation in diluted bed pseudo slurry reactor. Temperature, 503°K; Pressure, 2000 KPa and H_2/CO, 2/1.

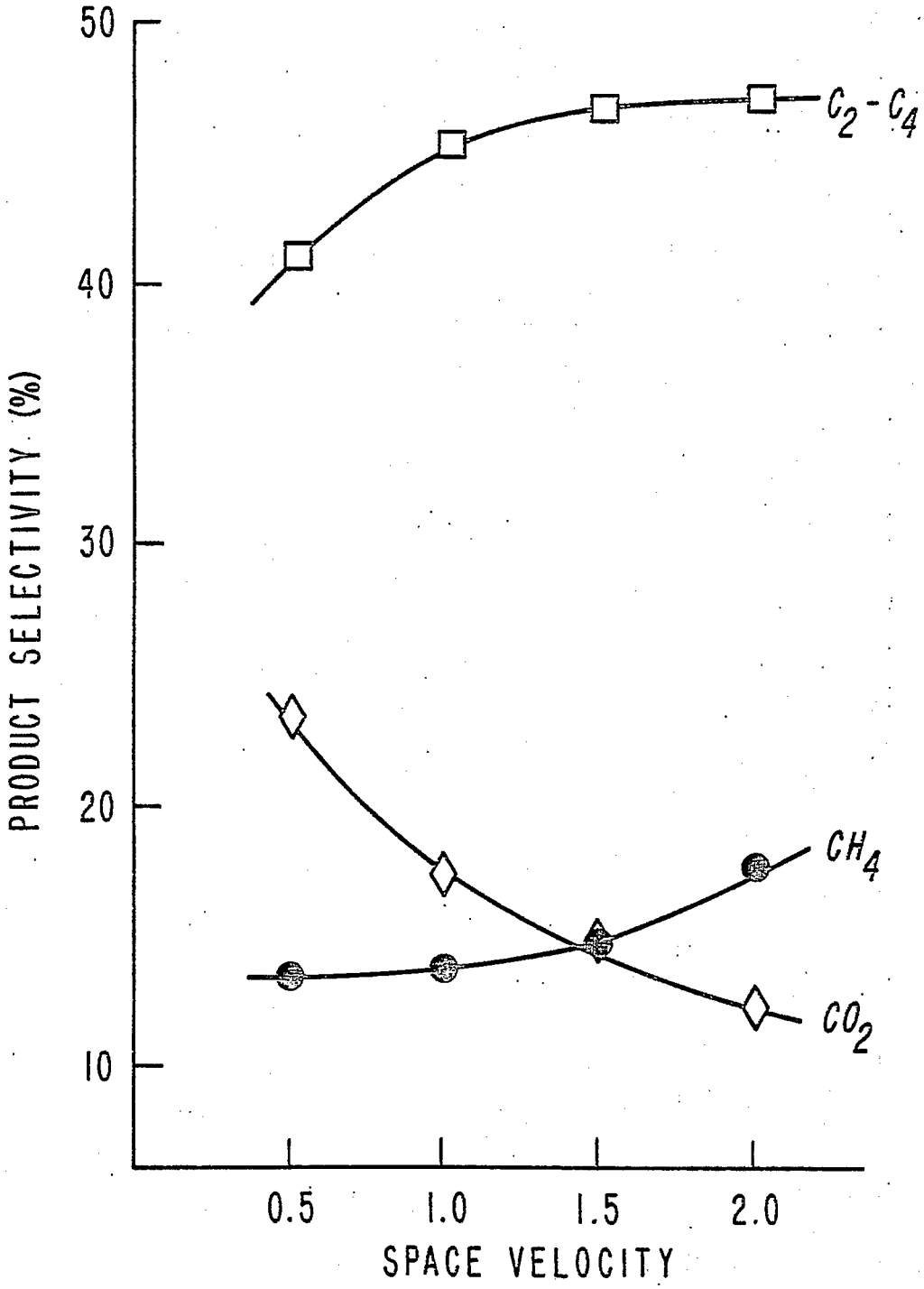

Figure 13. Effect of space velocity on product selectivities for carbon monoxide hydrogenation in diluted bed pseudo slurry reactor. Temperature, 503°K; Pressure, 2600 KPa and H_2/CO, 2/1.

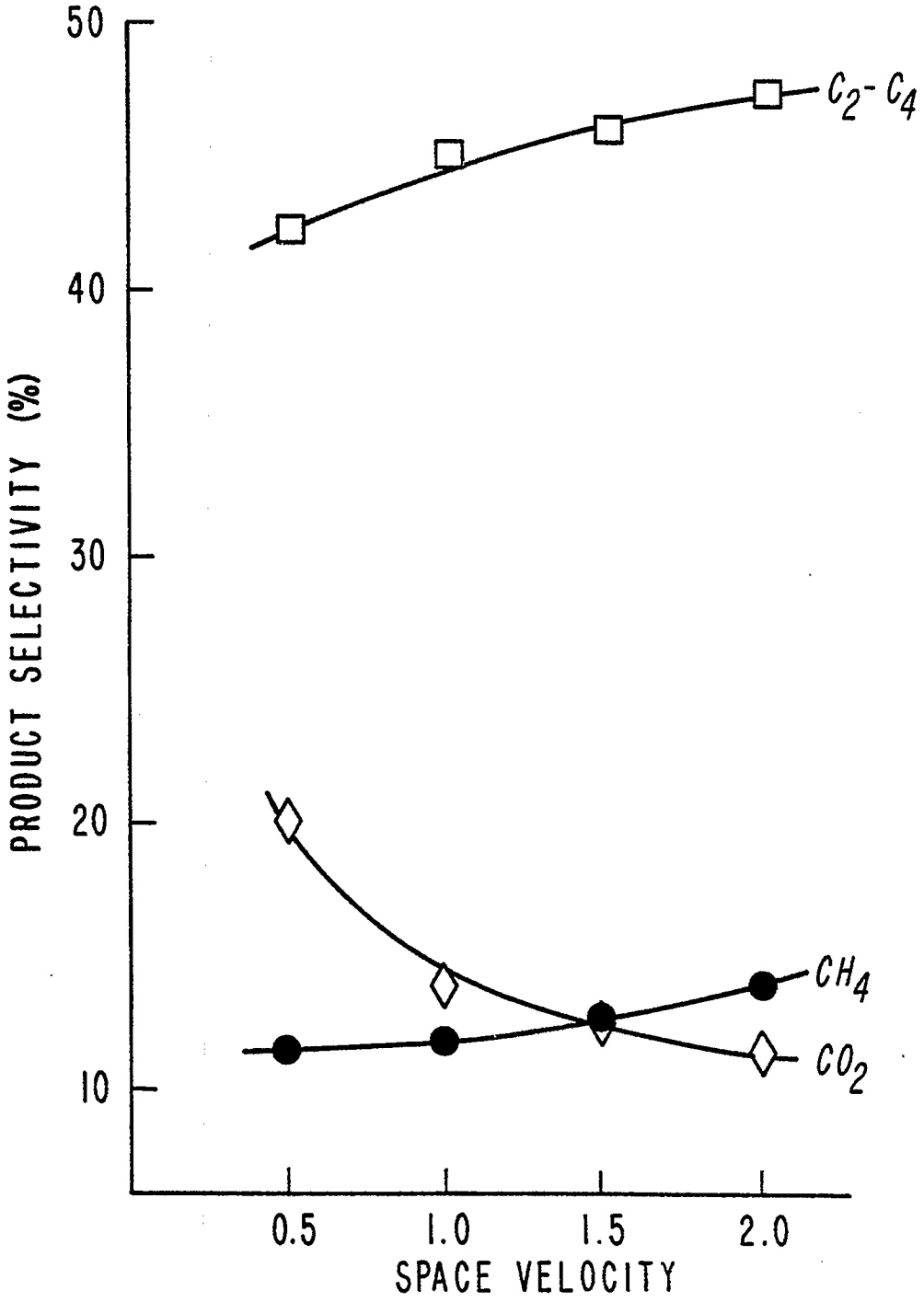

Figure 14. Effect of space velocity on product selectivities for carbon monoxide hydrogenation in diluted bed pseudo slurry reactor. Temperature, 503°K; Pressure 3200 KPa and H_2/CO, 2/1.

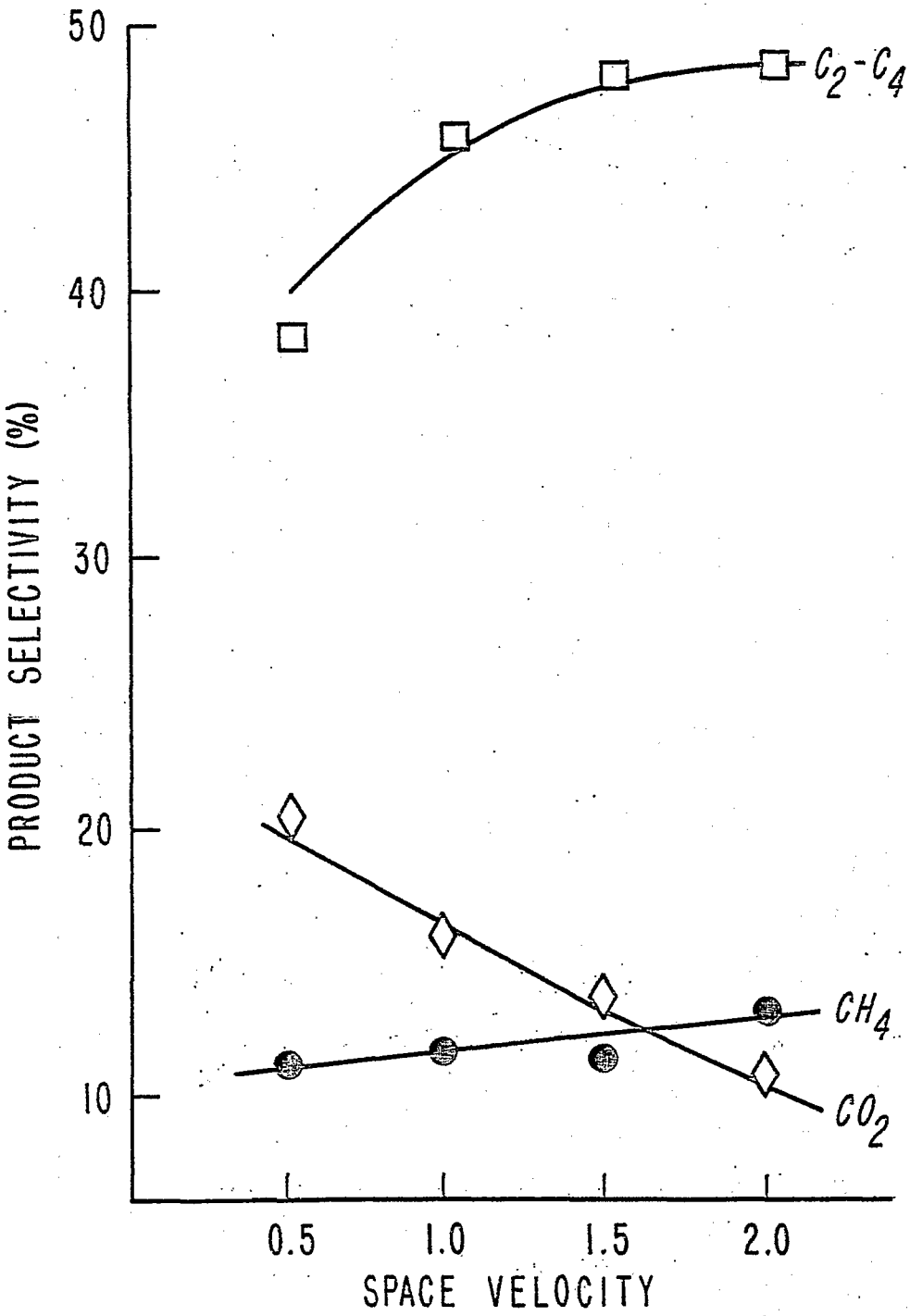

Figure 15. Effect of space velocity on product selectivities for carbon monoxide hydrogenation in diluted bed pseudo slurry reactor. Temperature, 503°K; Pressure, 4400 KPa and H_2/CO, 2/1.

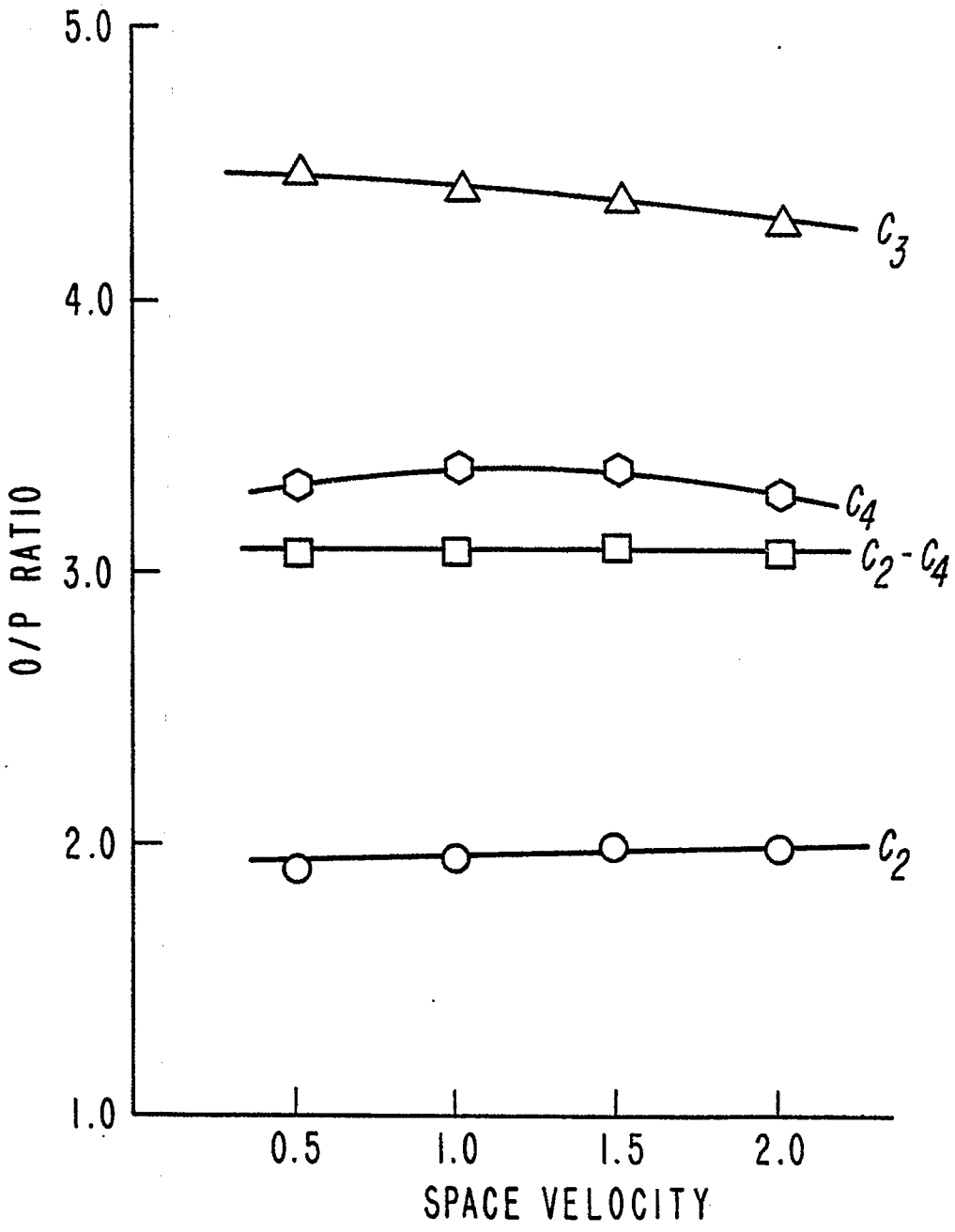

Figure 16. Effect of space velocity on olefin/paraffin ratio of C_2-C_4 hydrocarbons for carbon monoxide hydrogenation in diluted bed pseudo slurry reactor. Temperature, 503°K; Pressure, 1400 KPa and H_2/CO, 2/1.

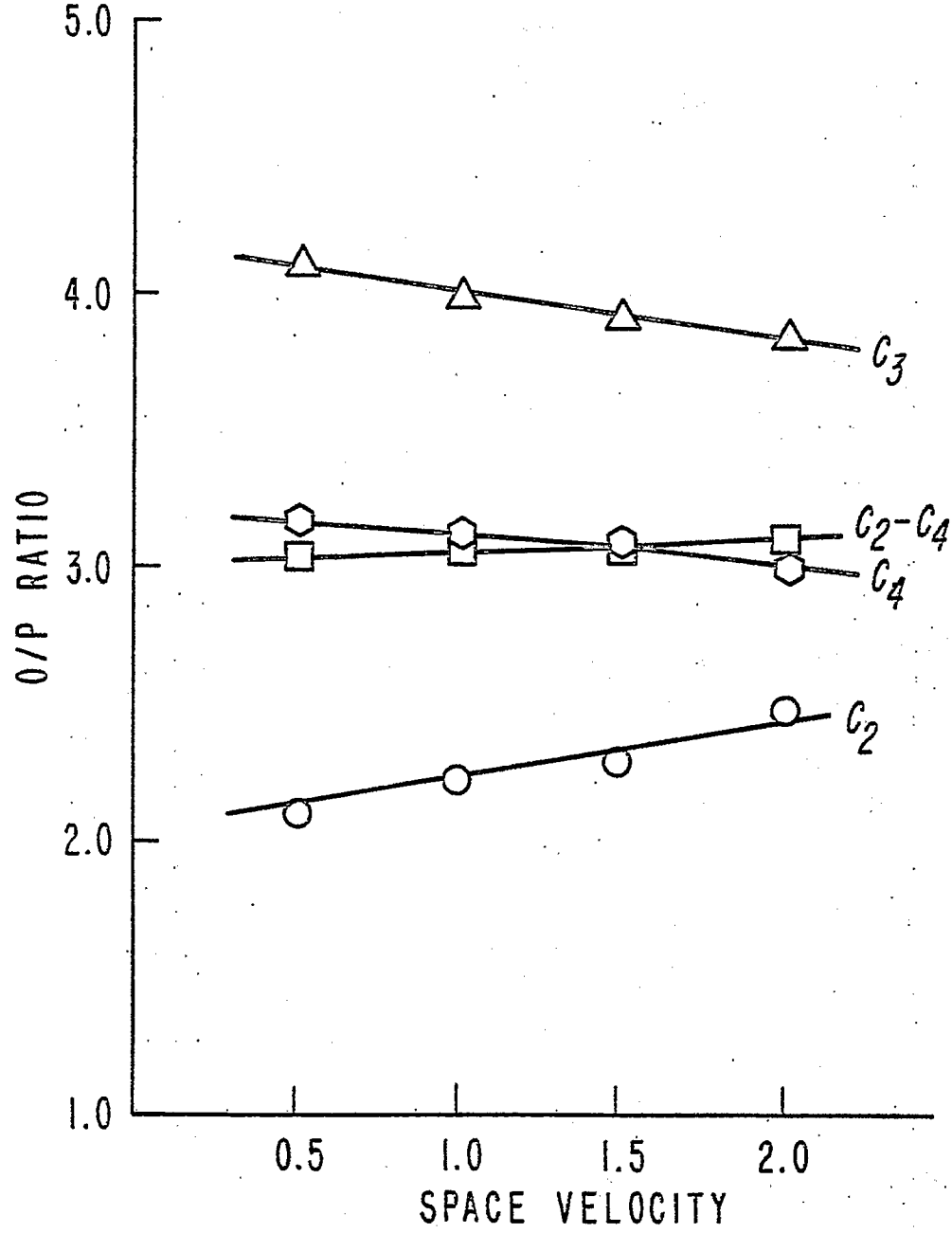

Figure 17. Effect of space velocity on olefin/paraffin ratio of C_2-C_4 hydrocarbons for carbon monoxide hydrogenation in diluted bed pseudo slurry reactor. Temperature, 503°K; Pressure, 2000 KPa and H_2/CO, 2/1.

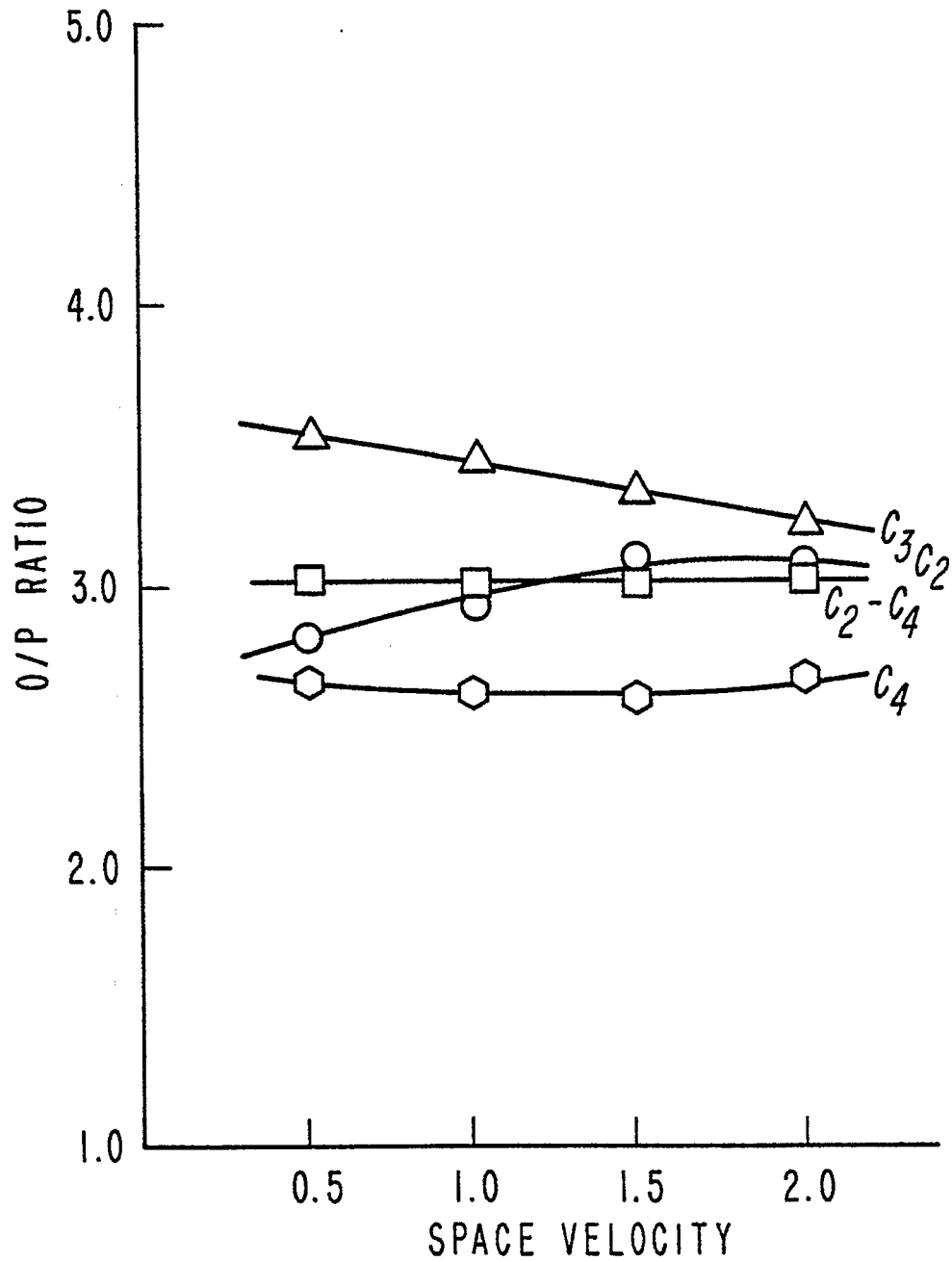

Figure 18. Effect of space velocity on olefin/paraffin ratio of C_2-C_4 hydrocarbons for carbon monoxide hydrogenation in diluted bed pseudo slurry reactor. Temperature, 503°K; Pressure, 2600 KPa and H_2/CO, 2/1.

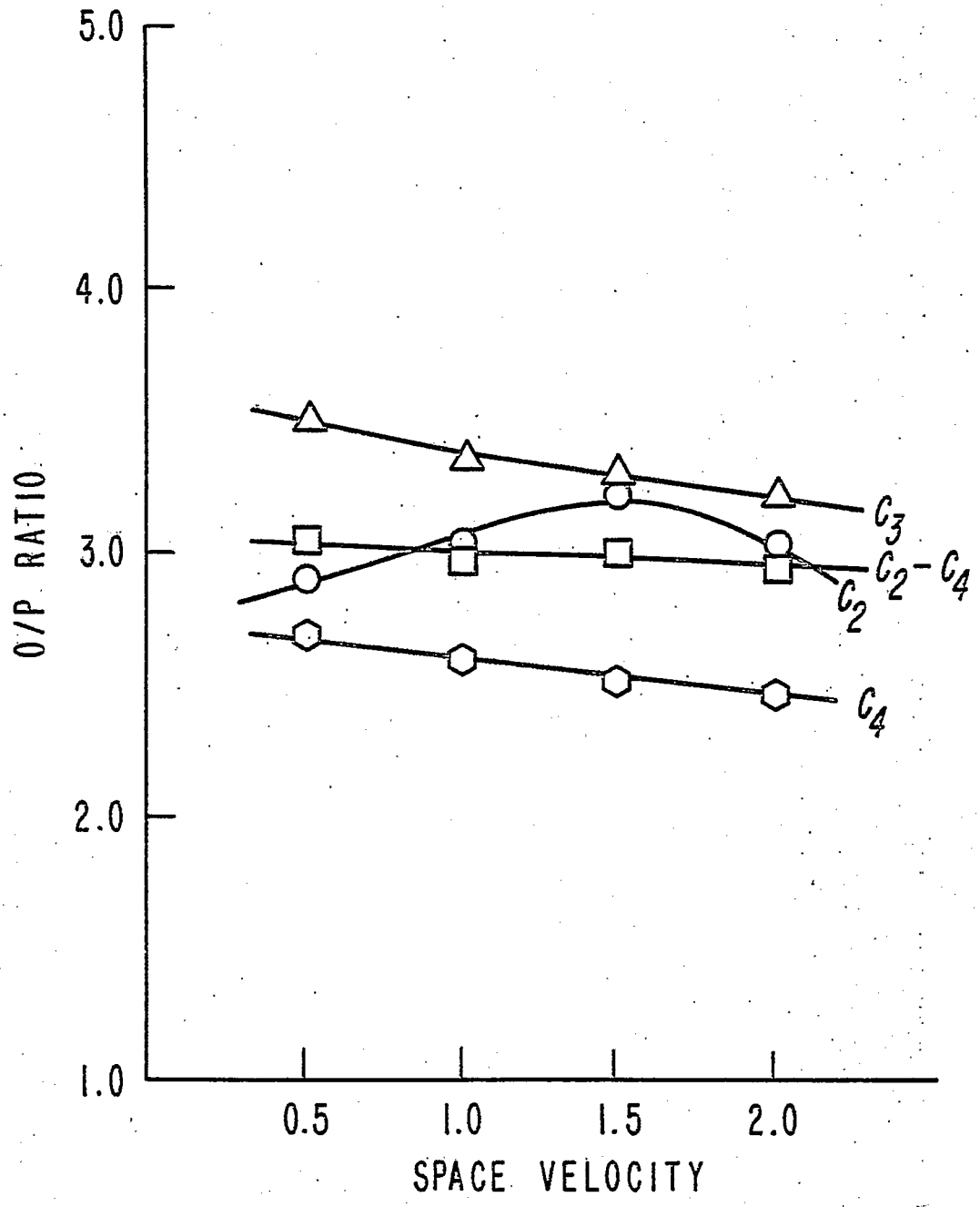

Figure 19. Effect of space velocity on olefin/paraffin ratio of C_2-C_4 hydrocarbons for carbon monoxide hydrogenation in diluted bed pseudo slurry reactor. Temperature, 503°K; Pressure 3200 KPa and H_2/CO, 2/1.

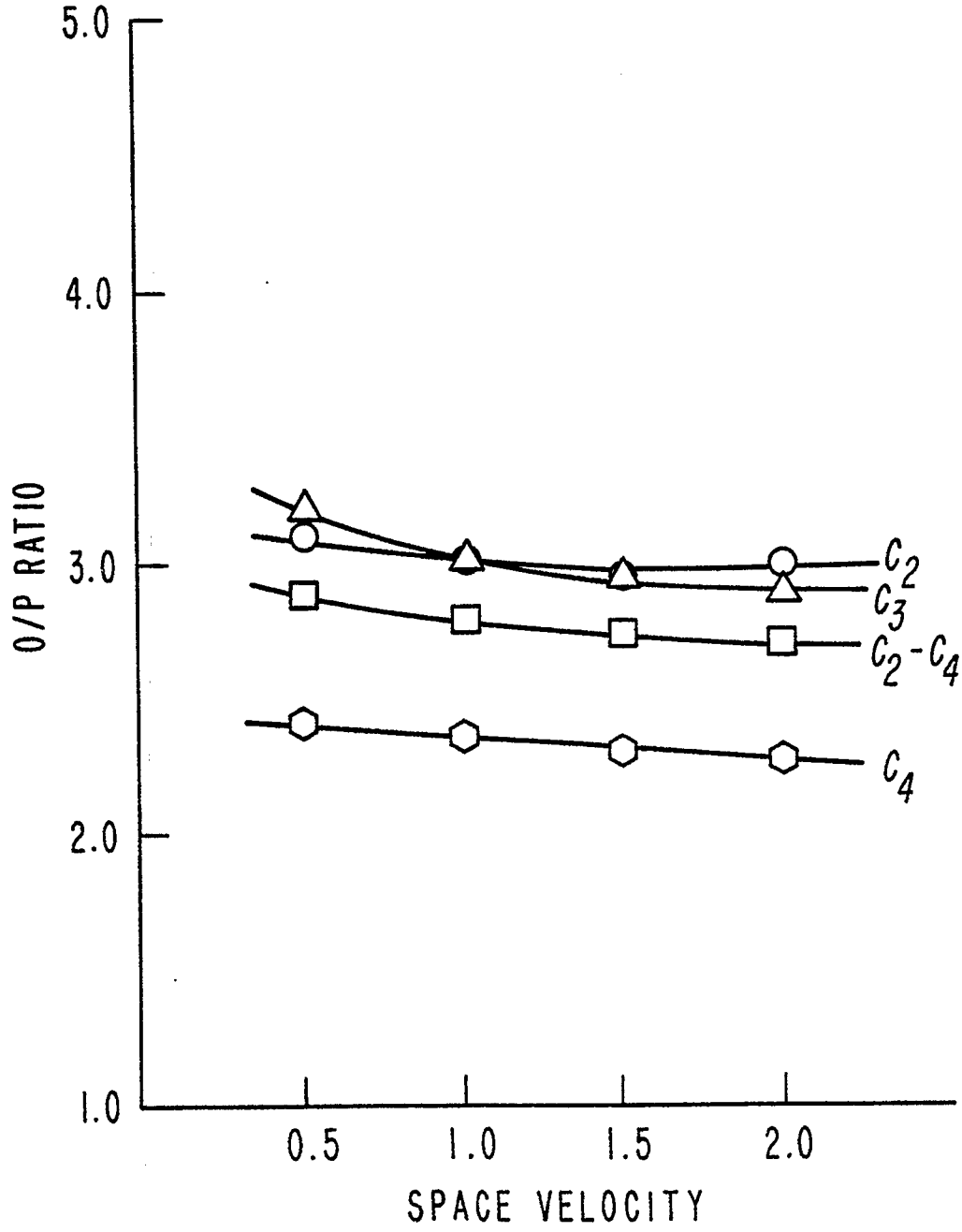

Figure 20. Effect of space velocity on olefin/paraffin ratio of C_2-C_4 hydrocarbons for carbon monoxide hydrogenation in diluted bed pseudo slurry reactor. Temperature, 303°K; Pressure, 4400 KPa and H_2/CO, 2/1.

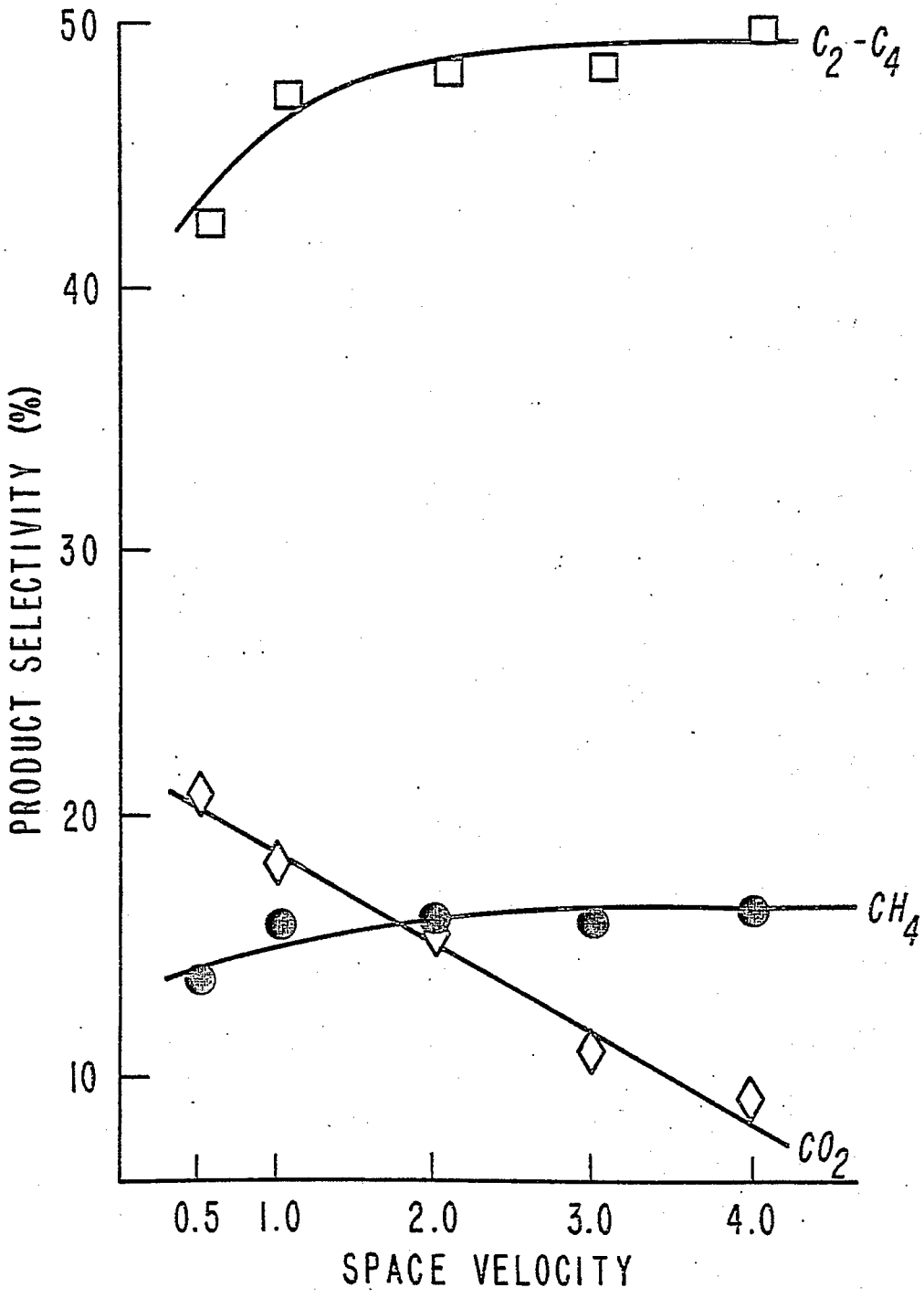

Figure 21. Effect of space velocity on product selectivities for carbon monoxide hydrogenation in diluted bed pseudo slurry reactor. Temperature, 493°K; Pressure, 2760 KPa and H_2/CO, 2/1.

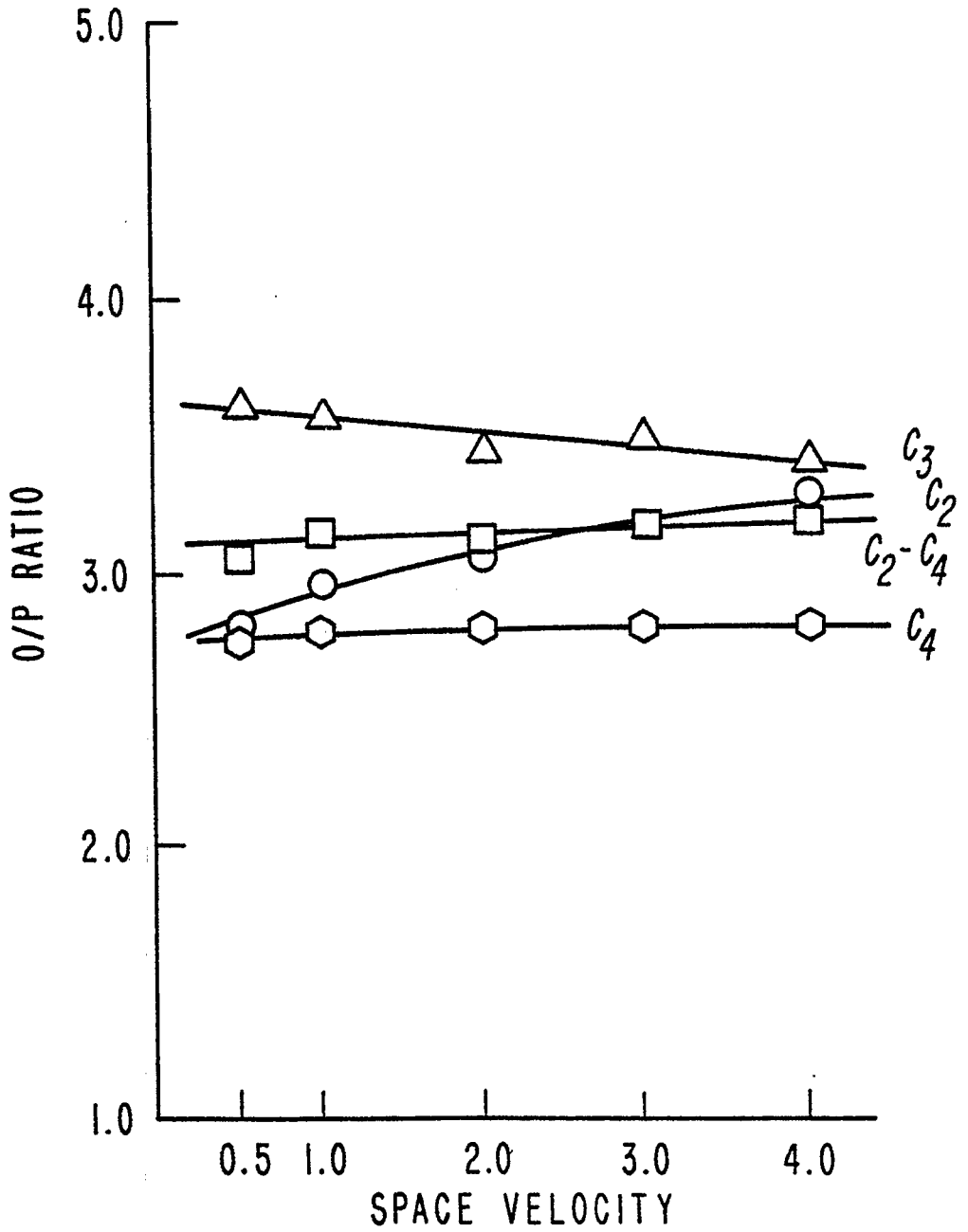

Figure 22. Effect of space velocity on olefin/paraffin ratio of C_2-C_4 hydrocarbons for carbon monoxide hydrogenation in diluted bed pseudo slurry reactor. Temperature, 493°K; Pressure, 2760 KPa and H_2/CO, 2/1.

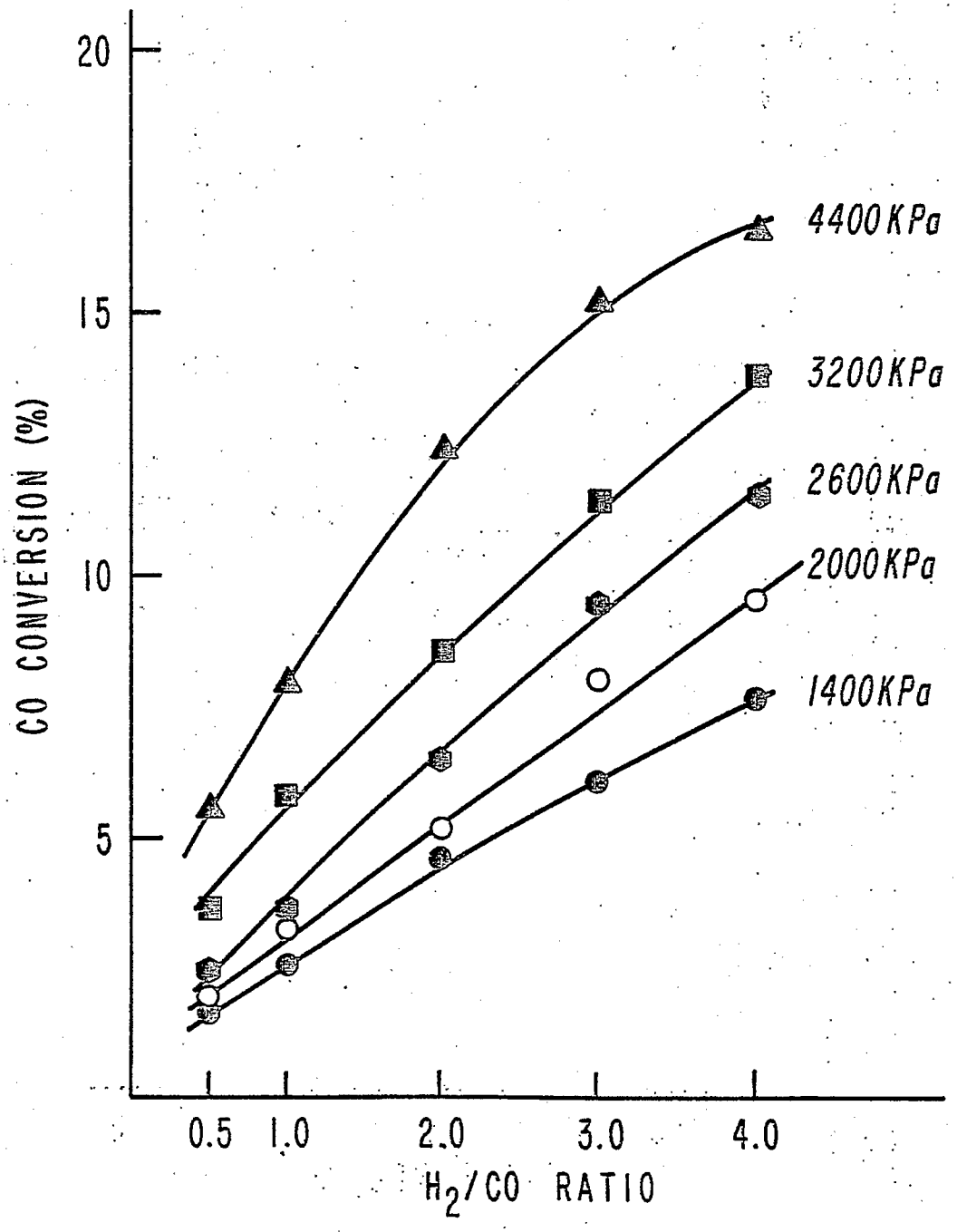

Figure 23. Effect of H_2/CO ratio on CO conversion for carbon monoxide hydrogenation in diluted bed pseudo slurry reactor. Temperature, 503°K; Pressure, 1400-4400 KPa and Space Velocity, 1 cm^3/sec g cat.

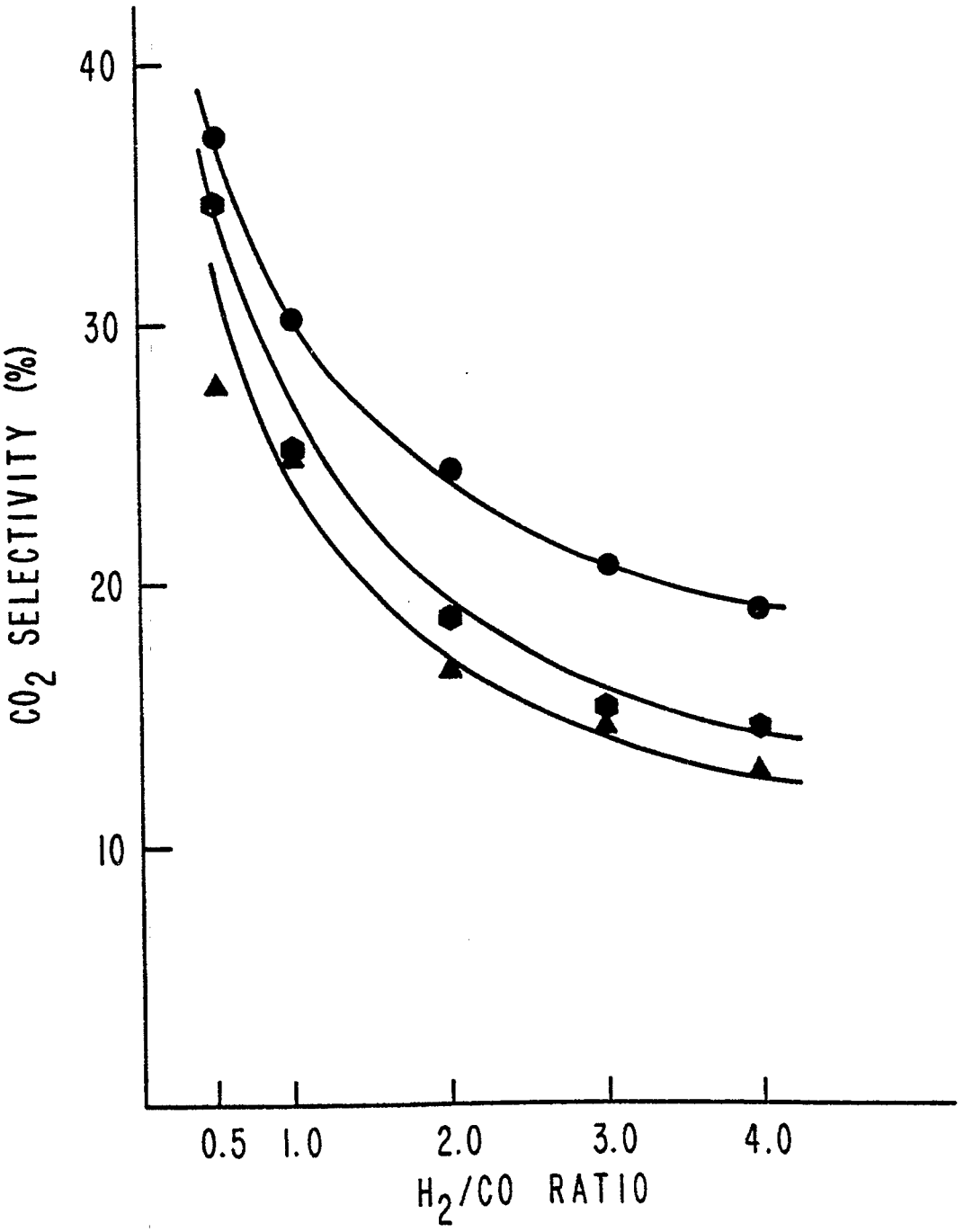

Figure 24. Effect of H_2/CO on CO_2 selectivity for carbon monoxide hydrogenation in diluted bed pseudo slurry reactor. Temperature, 503°K; Pressure, 1400, 2600 and 4400 KPa and Space Velocity, 1 cm^3/sec g cat.

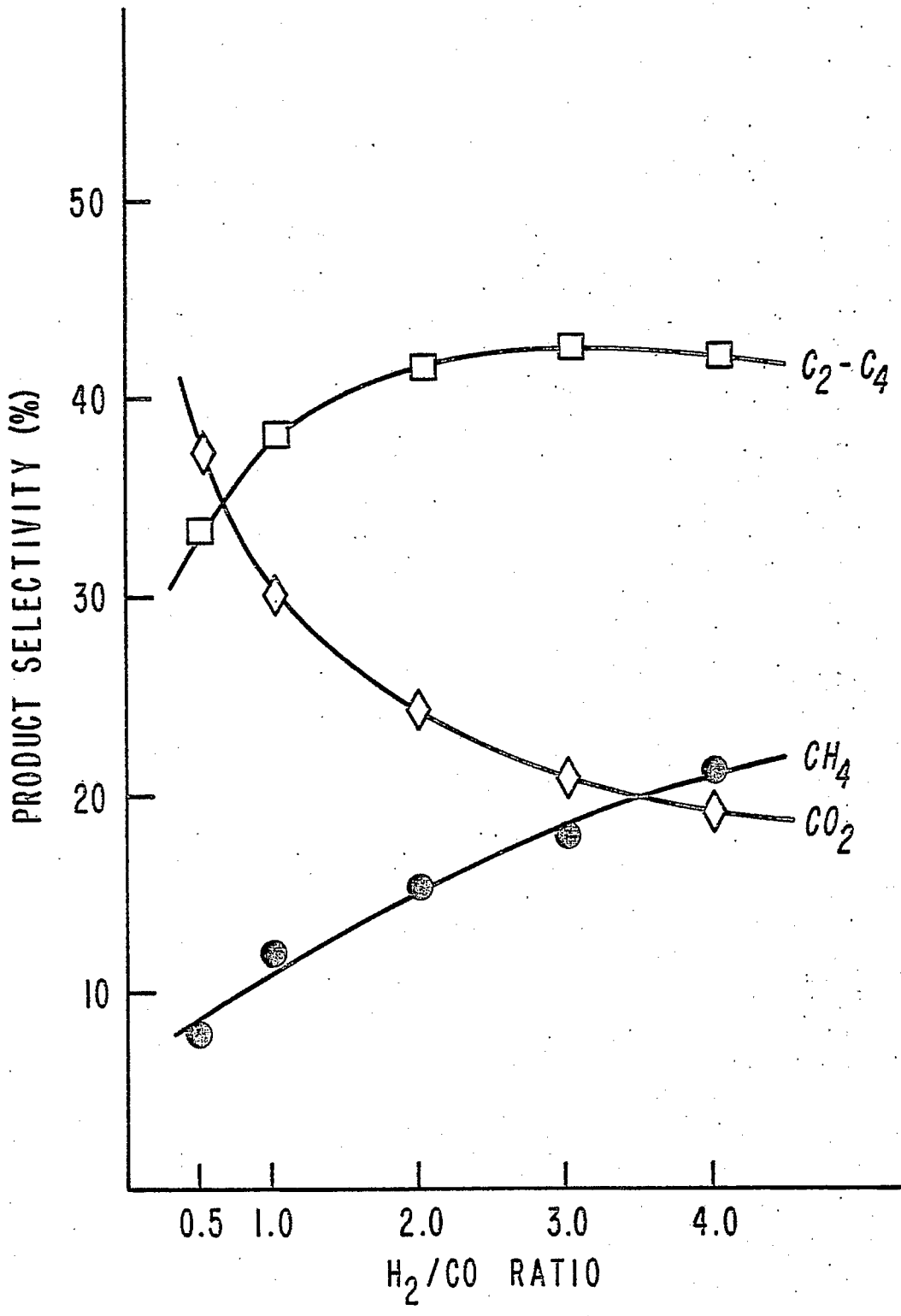

Figure 25. Effect of H_2/CO ratio on product selectivities for carbon monoxide hydrogenation in diluted bed pseudo slurry reactor. Temperature, 503°K; Pressure, 1400 KPa and Space Velocity, 1 cm^3/sec g cat.

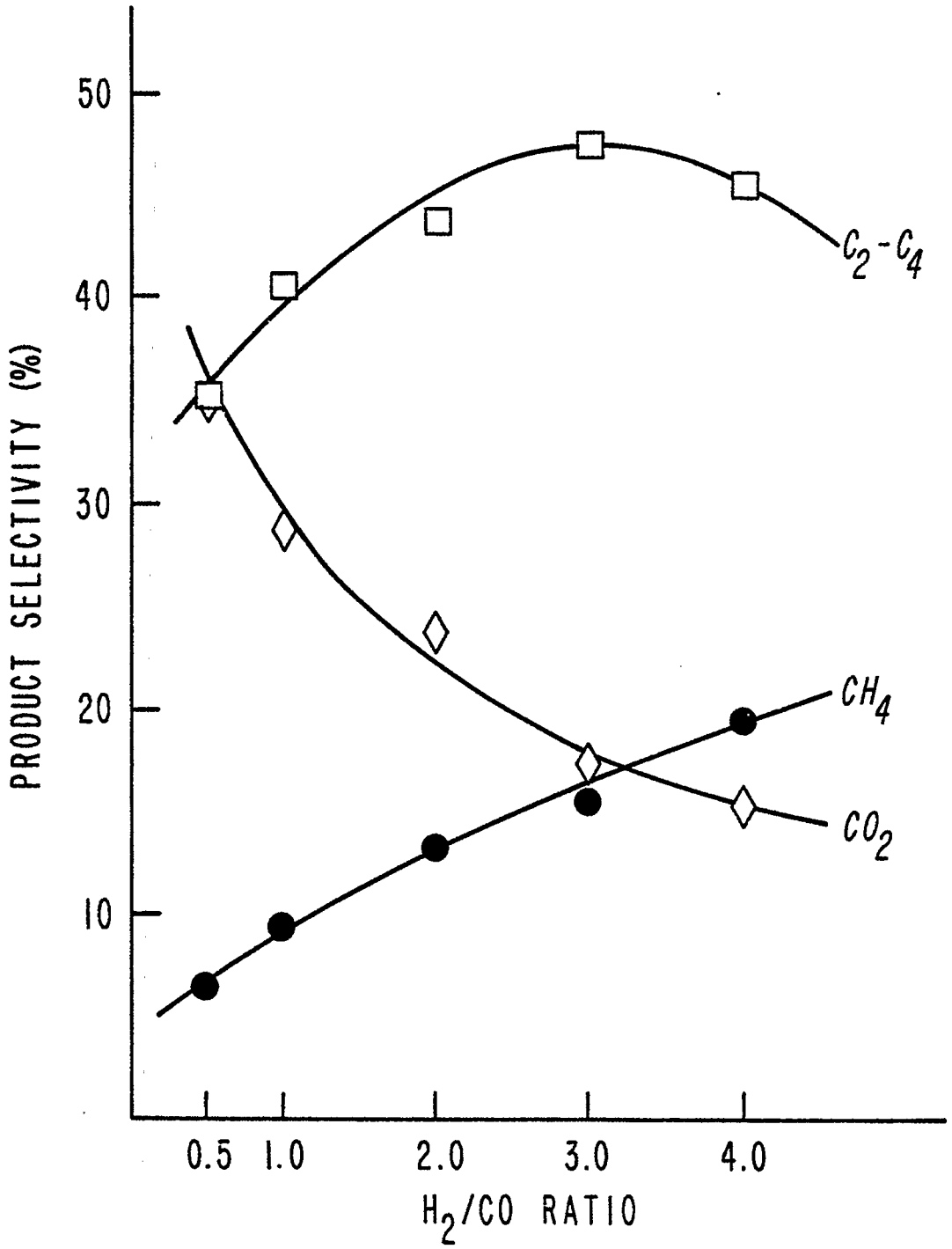

Figure 26. Effect of H_2/CO ratio on product selectivities for carbon monoxide hydrogenation in diluted bed pseudo slurry reactor. Temperature, 503°K; Pressure, 2000 KPa and Space Velocity, 1 cm^3/sec g cat.

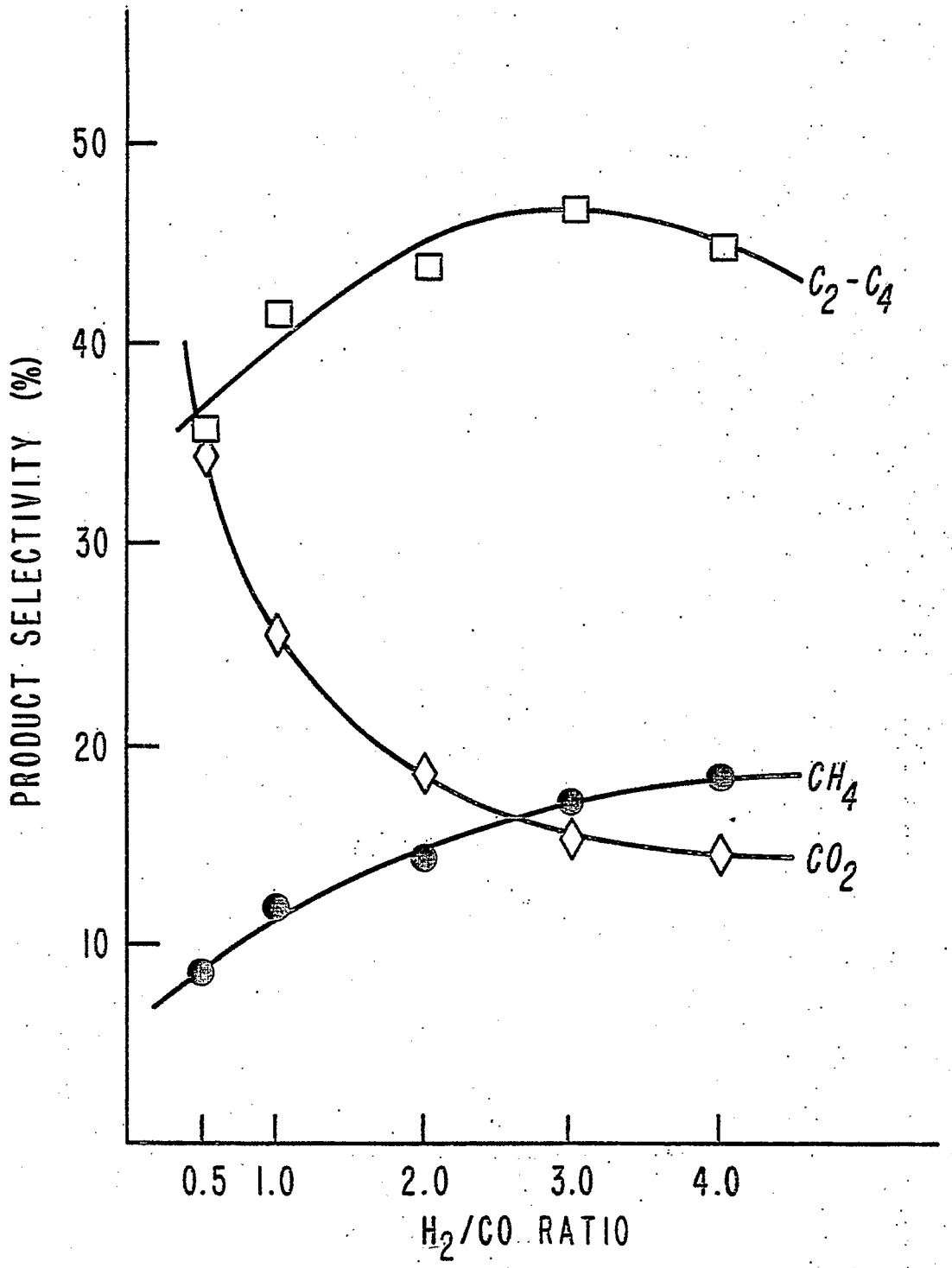

Figure 27. Effect of H_2/CO ratio on product selectivities for carbon monoxide hydrogenation in diluted bed pseudo slurry reactor. Temperature, 503°K; Pressure, 2600 KPa and Space Velocity, 1 cm^3/sec g cat.

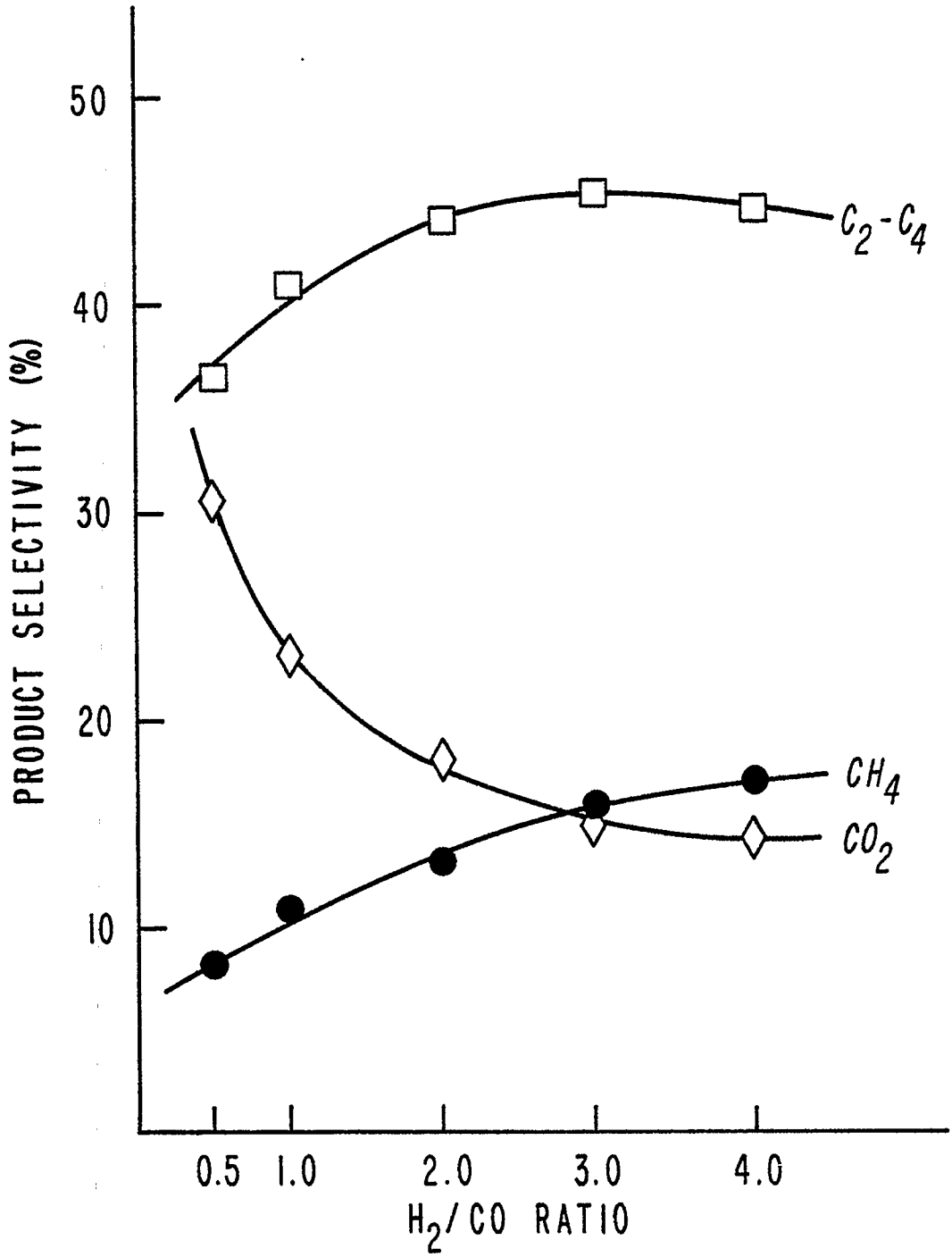

Figure 28. Effect of H_2/CO ratio on product selectivites for carbon monoxide hydrogenation in diluted bed pseudo slurry reactor. Temperature, 503°K; Pressure, 3200 KPa and Space Velocity, 1 cm^3/sec g cat.

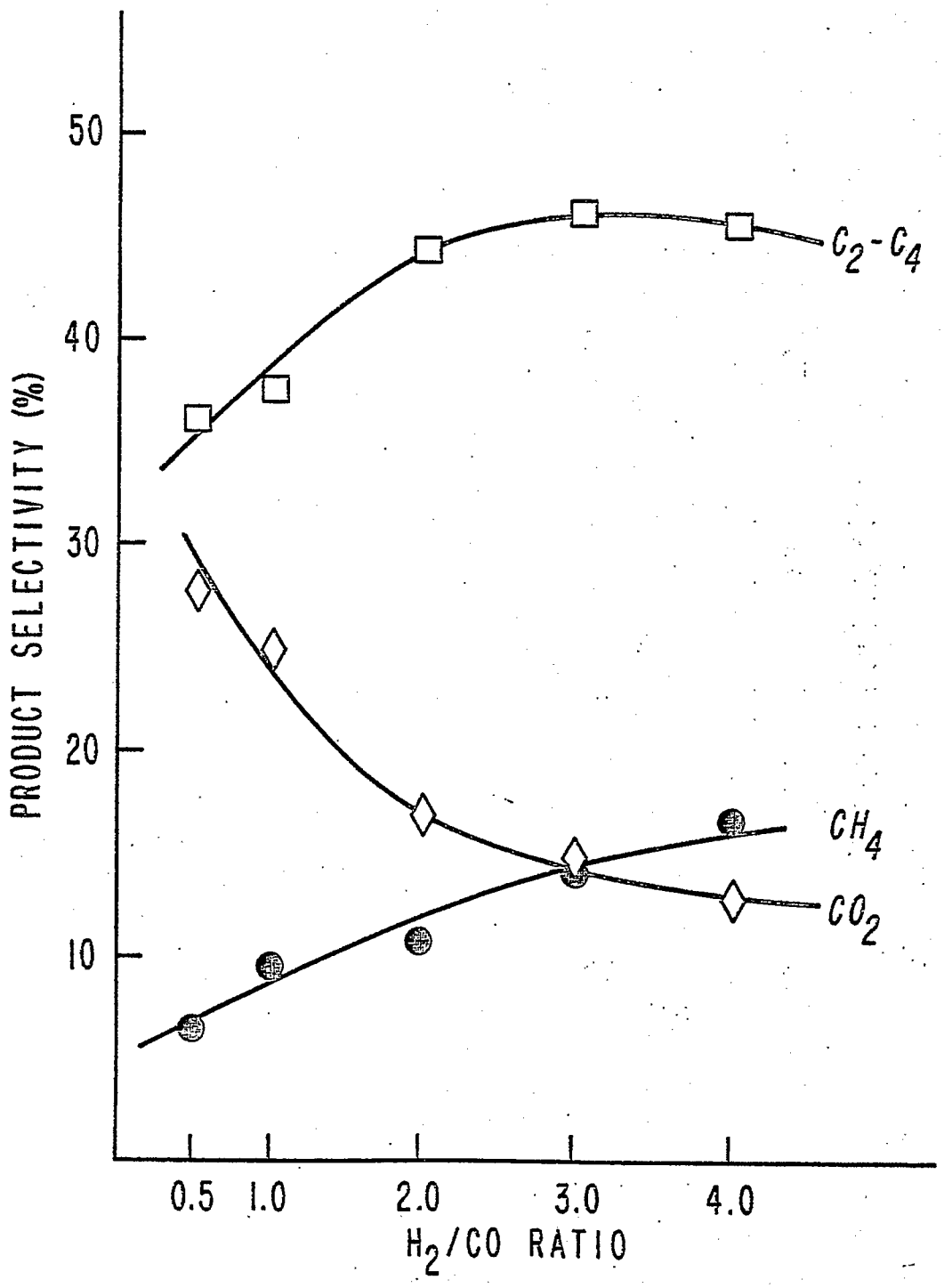

Figure 29. Effect of H_2/CO ratio on product selectivities for carbon monoxide hydrogenation in diluted bed pseudo slurry reactor. Temperature, 503°K; Pressure, 4400 KPa and Space Velocity, 1 cm^3/sec g cat.

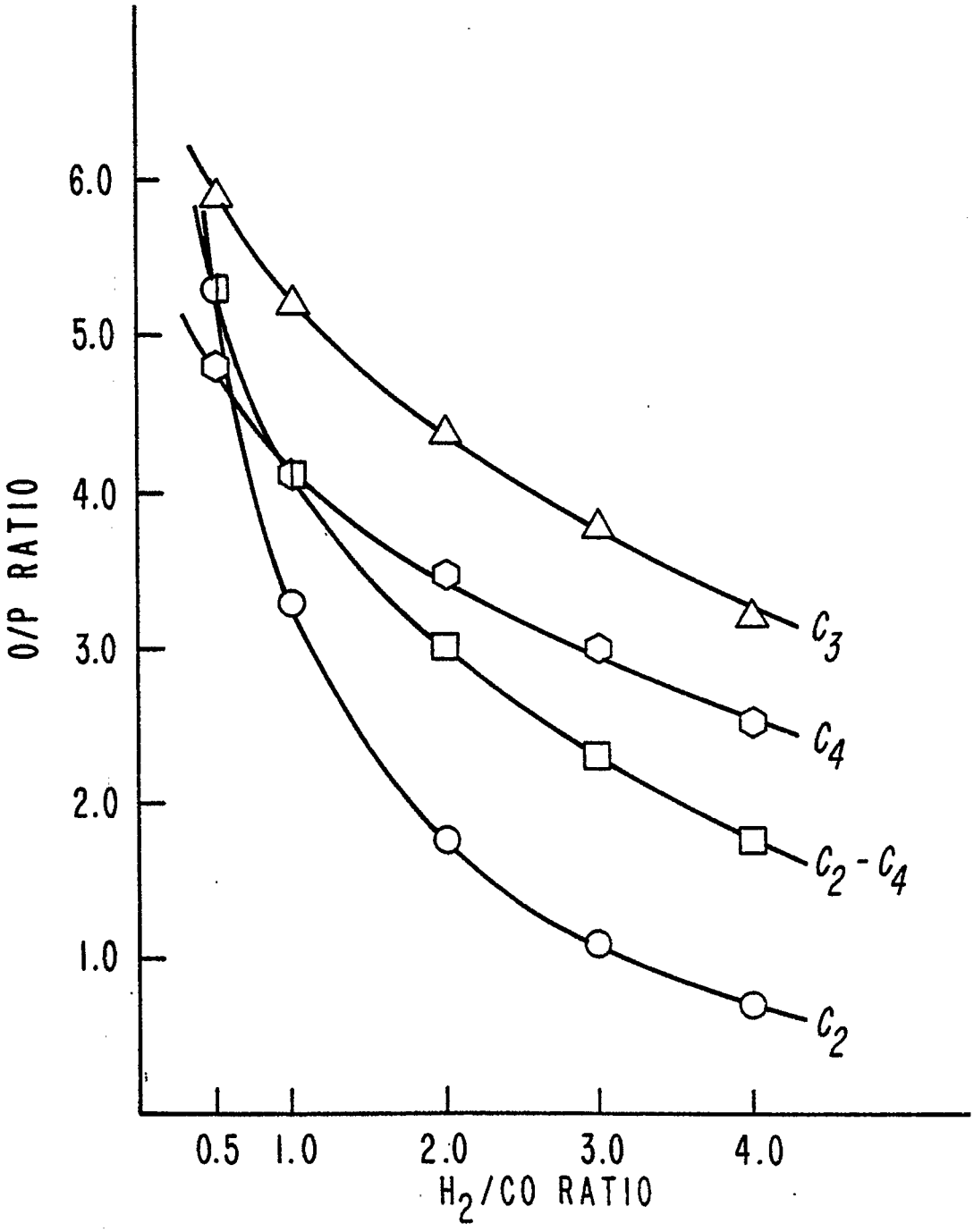

Figure 30. Effect of H_2/CO on olefin/paraffin ratio of C_2-C_4 hydrocarbons for carbon monoxide hydrogenation in diluted bed pseudo slurry reactor. Temperature, 503°K; Pressure, 1400 KPa and space velocity, 1 cm^3/sec g cat.

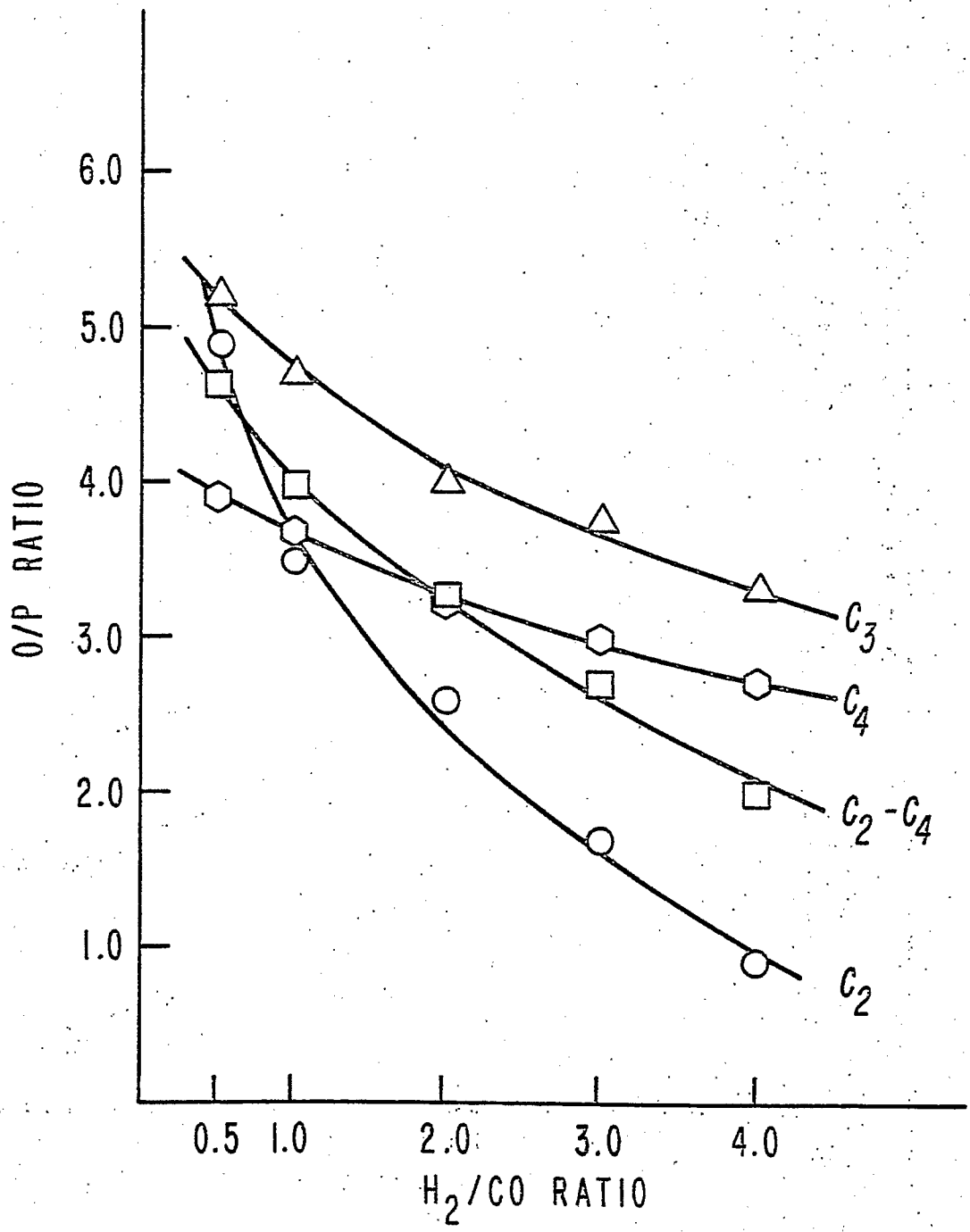

Figure 31. Effect of H_2/CO ratio on olefin/paraffin ratio of C_2-C_4 hydrocarbons for carbon monoxide hydrogenation in diluted bed pseudo slurry reactor. Temperature, 503°K. Pressure, 2000 KPa and Space Velocity, 1 cm^3/sec g cat.

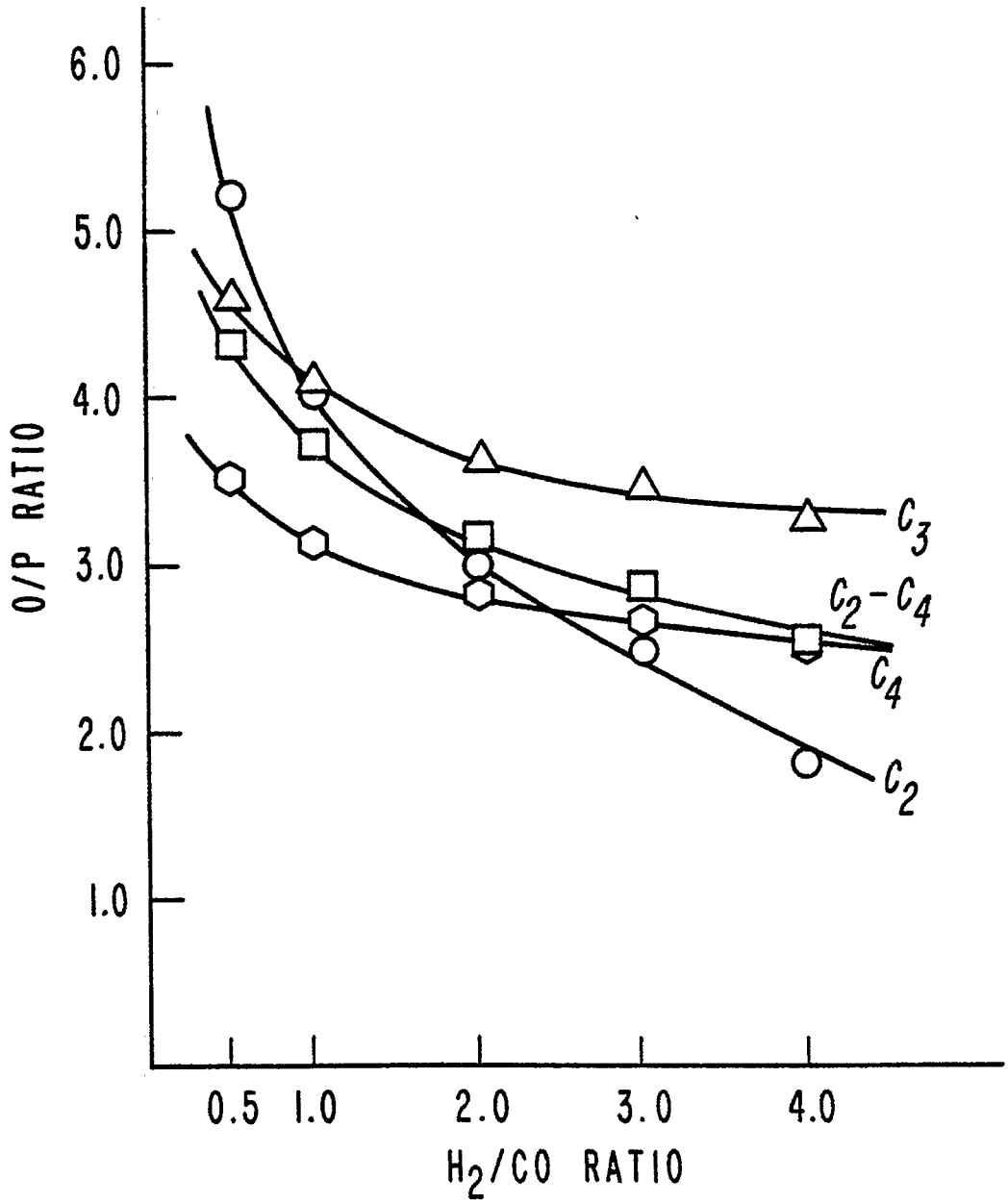

Figure 32. Effect of H_2/CO ratio on olefin/paraffin ratio of C_2-C_4 hydrocarbons for carbon monoxide hydrogenation in diluted bed pseudo slurry reactor, Temperature, 503°K; Pressure, 2600 KPa and Space Velocity, 1 cm^3/sec g cat.

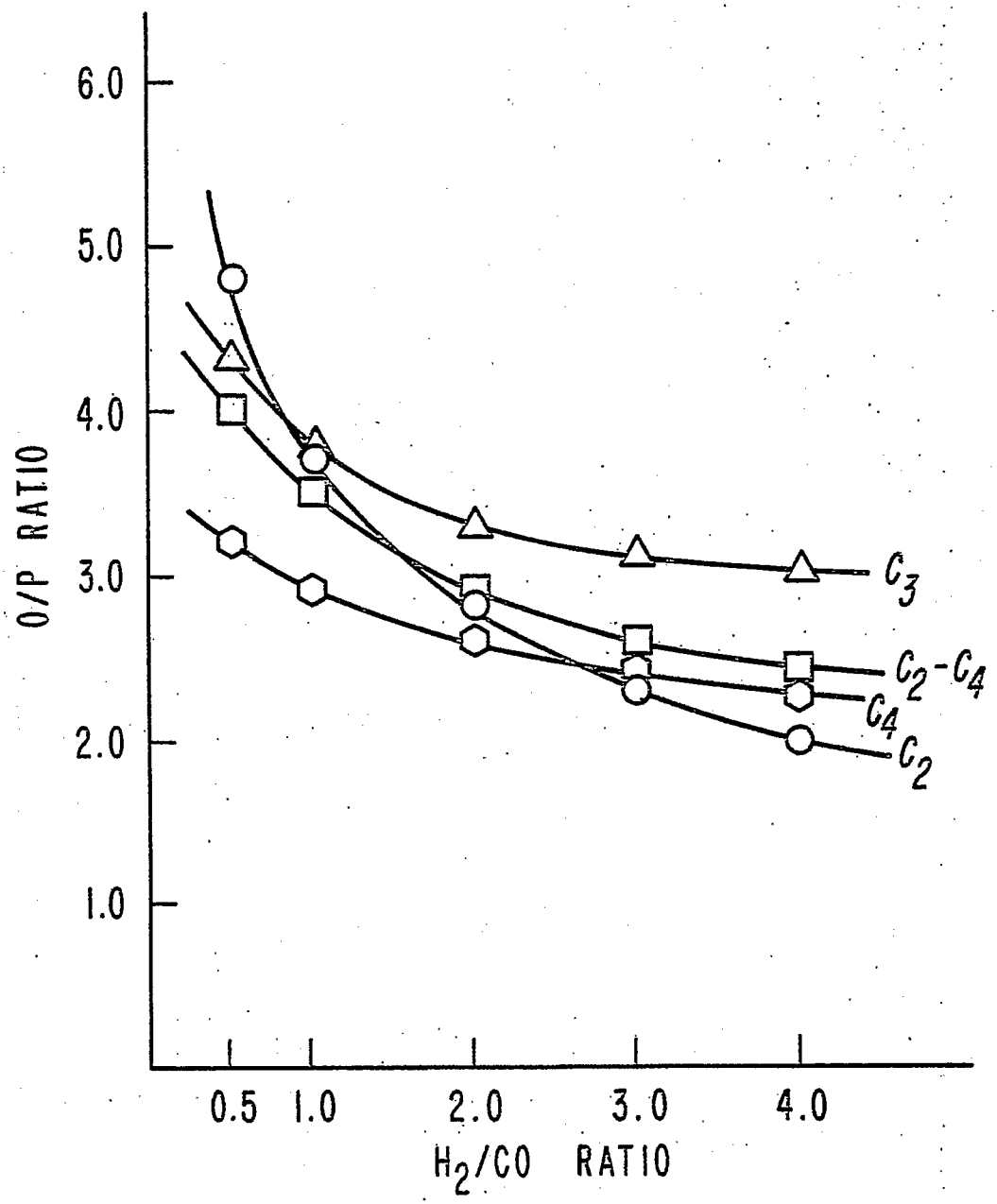

Figure 33. Effect of H_2/CO ratio on olefin/paraffin ratio of C_2-C_4 hydrocarbons for carbon monoxide hydrogenation in diluted bed pseudo slurry reactor, Temperature, 503°K; Pressure, 3200 KPa and Space Velocity, 1 cm^3/sec g cat.

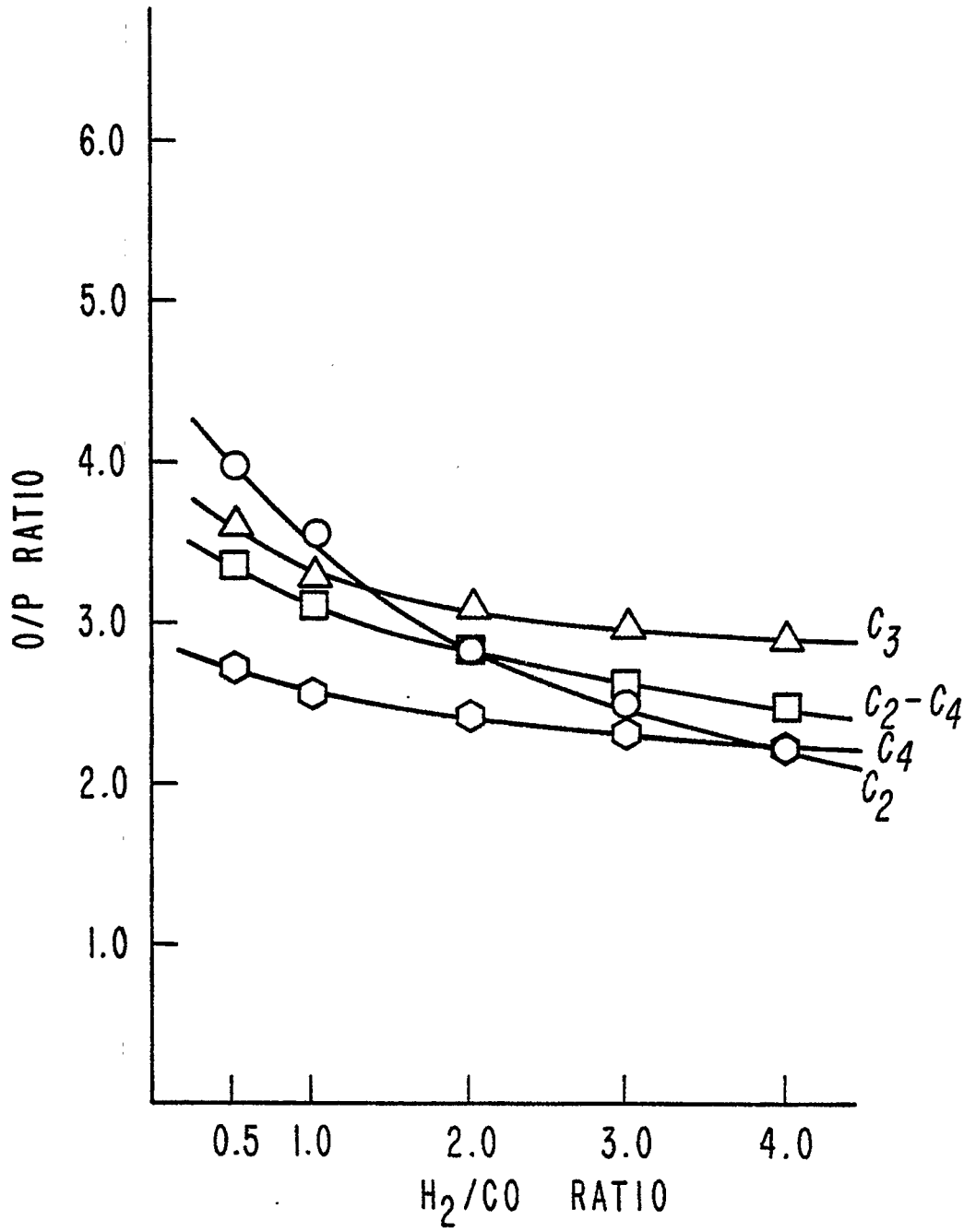

Figure 34. Effect of H_2/CO ratio on olefin/paraffin ratio of C_2-C_4 hydrocarbons for carbon monoxide hydrogenation in diluted bed pseudo slurry reactor. Temperature, 503°K; Pressure, 4400 KPa and Space Velocity, 1 cm^3/sec g cat.

V. Conclusions

Detailed conclusions are included in the reports for each task. Task 4 is no longer funded and has been discontinued. The report for Task 2 was not submitted. No work was done under Task 15.

☆U.S. GOVERNMENT PRINTING OFFICE: 1982-646-069/306